An interpretation of two-body hadron reactions*

G. L. Kane and A. Seidl

Physics Department, University of Michigan, Ann Arbor, Michigan 48104

This is a review and study of the absorption model approach to two-body hadron reactions. The basic view is that reactions proceed by Reggeized particle exchange, modified by (mainly) absorptive initial and final state interactions. Our approach is pedagogical in two respects. First, the conceptual basis of the approach is discussed in detail, and considerable emphasis is put on spin properties and relating amplitudes and observables. We attempt to explain the procedures in sufficient detail that the interested reader can apply them. Limitations and theoretical weaknesses of the approach are discussed. Second, by approaching the whole field of two-body hadron reactions from one viewpoint, we can give unified treatments of some areas, such as polarizations, and of many observables and regularities, and unified explanations of why the data behave as they do from the viewpoint of the model. Because our purpose is primarily pedagogical, we consider representative reactions and amplitudes rather than exhaustively discuss data. At least one example of every major kind of amplitude is discussed, so the extension to additional reactions is often qualitatively possible without further calculation.

CONTENTS

*Research supported in part by ERDA.

I. INTRODUCTION

If we have to rely on guidance from experiment in order to understand the structure of hadrons, for a number of reasons it would seem sensible to study two-body reactions. First, there exist more high quality data there than probably anywhere else in particle physics. Second, using polarization techniques, it is possible to study actual matrix elements experimentally as functions of their separate variables s and t (square of center of mass energy and four-momentum transfer, respectively), rather than risk losing dynamical information by averaging. Third, many different reactions with many different sets of quantum numbers can be studied over large ranges of s and t, so that dynamical ideas can be tested under different conditions, and symmetries can be studied.

A. Historical perspective

In the early 1960's, there was considerable interest in two-body reactions. New, basic ideas, particularly Regge behavior of amplitudes, were generating important new insights and results. It was realized by Gottfried and Jackson (1964) and by Durand and Chiu (1965) that initial and final state rescattering would be important because strongly interacting particles were involved, and that these rescattering corrections would be absorptive. Soon it was found that experimental data were more complicated than these theoretical structures seemed to allow. The understanding of the theory improved too; it was learned that the absorptive rescattering should be applied to the Regge pole amplitude (Arnold, 1967, and Cohen-Tannoudji *et al.*, 1967), and that inelastic intermediate states should be included in the calculation of the absorption correction.

By the end of the 1960's the situation was confused. There was strong disagreement among theorists about the form of the Regge pole amplitude, mainly about whether it had zeros. There was disagreement about how to calculate the absorption, particularly the inelastic intermediate state contribution. And experimental data appeared to be extremely complicated, with essentially every $d\sigma/dt$ being different in shape from every other one. On the other hand, some models had no difficulty in describing any differential cross sections, at least when considering only a few reactions at a time. There were some hints from polarizations that the situation with phases of amplitudes might not be straightforward.

In 1971, the polarization in $\pi^- p \to \pi^0 n$ was measured in the region $\frac{1}{3} < -t < 1$ GeV^2. The absence of a large negative polarization around the dip region immediately showed that phases were not as expected; essentially, for ρ exchange the models had given the real part of the amplitude a zero at a smaller t than the imaginary part of the amplitude, and the data was opposite.

Several approaches were taken to deal with this. The view which stuck to the traditional approach of the absorption model said that the basic physical ideas were good, but previously the phase of the absorptive rescattering had been ignored (essentially the Pomeron phase) and was likely to do the right thing if included. Fortunately, information constraining the Pomeron phase had by then come from elastic scattering, so it was not hard to find the modification needed. It has proved possible to pursue this approach, and so far there is not any serious disagreement with experiment that would require further basic modifications. A large number of reactions have been studied by Hartley and Kane (1973) and by Field and Sidhu (1974).

B. Other approaches and reviews

The purpose of this article is to review the traditional absorption model approach to hadron two-body reactions. Not much work has been done on other models since the comprehensive review of Fox and Quigg (1973). We will discuss approaches other than the traditional absorption one only occasionally, in the detailed context of reactions to which they have been applied. The lectures of Davier (1974) are a recent and useful guide, especially to analyses of the data. Analyses of experimental data with minimal reliance on models and ideas ("model-independent") have been repeatedly covered in detail by rapporteurs at meetings (Michael, 1972; Amaldi, 1973; Barger, 1974) as well as by Fox and Quigg (1973) and Davier (1974).

A number of other points of view and approaches, some closely related, were pursued by many workers. In addition to the path reviewed here there were first the original weak absorption models of Arnold (1967), Cohen-Tannoudji, Morel, and Navalet (1967), Gribov *et al.* (1965) [and the later Russian calculations of Kaidalov and Karnakov (1969) and Ter Martirosyan and collaborators (1973)], and the analysis of Dar, Watts, and Weisskopf (1969). Then a number of studies were done by Ringland, Roberts, Roy, and Tran Thanh Van (1972), Collins and Swetman (1972), and Martin and Stevens (1972, 1973); these and others making detailed remarks are reviewed by Fox and Quigg (1973).

C. Plan and summary of the review

In this section we will give a brief summary of the contents of the different sections and how they are intended to be used. We will indicate briefly where discussions of strengths and weaknesses of the model can be found and where various important experimental results are discussed. Since the review is long and it is often difficult to find things, we have tried to give a guide both in the contents and in this section.

The purpose of Sec. II is to show a reader with little previous interest in two-body hadron reactions why we feel absorption effects should be included if a reasonably accurate description of data is desired. By using examples and qualitative arguments, we can see the changes arising from absorption.

Section III is the essential one, stating in detail how to construct absorbed Reggeon exchange and elastic amplitudes for the present model. A reader who only wishes to calculate with the model or to see its present application to data can skip on to Secs. VII and VIII after Sec. III.

The rules of Sec. III have been arrived at by a mixture of methods, including intuition developed by a number of workers over about a decade, extensive data fitting to see what works, incorporation of theoretical constraints such as analyticity and crossing properties, singularity structure, and pole factorization. A major constraint on freedom was the requirement that the same Pomeron amplitude describe elastic scattering and give the right effects when used in absorption (the Pomeron does not give the full absorption amplitude, but it is the dominant contribution). Section IV discusses in detail the origin of the various parts of the rules.

For the Reggeon pole one must choose the form of the trajectory and residue, including the zero structure. We assume the residue has no zeros apart from kinematical ones, as has been traditional in the Michigan approach; all zeros originate from absorptive effects. That has a large impact on the way data are described. It gives very strong predictions: if ever a nonflip vector exchange contribution does not have an imaginary part with a zero near $-t = 0.25$ GeV^2, or a nonflip or double flip amplitude gives a dip near $-t = 0.5$ GeV^2, or a flip amplitude has a zero near $-t = 0.25$ GeV^2, etc., the model would be demonstrated to be wrong.

The Pomeron choice is based on a simple impact parameter picture, with the energy dependence and, therefore, the phase assumed to arise from a growing radius. A quantitative description of elastic data is deferred to Sec. VIII, but at this stage a qualitative description is given of the Pomeron behavior and how it accounts for different aspects of the data. The small t increase in slope, large t dip, medium t energy dependence, and the phase are discussed. The latter two were predictions of the model, and the data show some tendency to agree with the predictions, although clean tests are not yet possible.

For our Pomeron amplitude to be a useful description, several features of the data must behave in the right way

as s increases. The differential cross section must develop a bend at medium t, because of the small t shrinkage and large t antishrinkage. The dip must move slowly toward $t=0$. The secondary maximum height must slowly increase. The depth of the dip is a sensitive probe of the phase at energies above about 300 GeV/c where the Reggeon amplitude is gone; the dip is due to a zero in the imaginary part of the amplitude and is filled in by the real part. More discussion of these properties is given in Sec. VIII.

The Pomeron amplitude has several parameters, seven if one started from scratch. Four of them are fairly well constrained by geometrical arguments. Normally these parameters are fixed from elastic data. Then the Pomeron amplitude is fixed and is used in the absorption. For most reactions the elastic data do not give a unique set of parameters, so if one wants a very good χ^2 fit to data involving absorbed amplitudes one can combine the fits to both sets of data. Once the parameters have been determined they can be used by other workers studying elastic or absorbed reactions—they do not need to be newly obtained for each use. A serious practical problem with the model is that one does not yet know enough to get the parameters for different external particles from one another. Scaling R^2 and σ_T from one reaction to another gives a pretty good guess, but data are accurate enough so that is not sufficient. This problem is discussed further in Sec. VII.C.

A subject briefly discussed in Sec. IV is diffractive production, which is mainly of interest here because it is expected to be the most important contribution to the inelastic intermediate state sum (which contributes to the absorption, increasing it over the elastic contribution). The main feature of importance for us is the peripheral nature of this contribution in impact parameter, and that is qualitatively confirmed in the data by the dip or break structure in $d\sigma/dt$ at $-t=0.2$ GeV^2 in the low M^2 region.

The choice of the absorption prescription is the original Sopkovich one and we have nothing to add in insight. The content and interpretation of the absorbing S-matrix is discussed in detail. Phenomenologically it is necessary, given our Pomeron, that even signature Reggeons also enter in S; they affect particularly the phase of the absorbed Reggeon amplitudes, as well as the energy dependence.

Finally there is the question of which amplitudes should be absorbed. We believe that the s-channel helicity amplitudes show the simplest physical behavior and contain the most useful information. The main reasons for this are that their behavior as $t\to 0$ is just due to angular momentum conservation, and that the absorption mainly conserves s-channel helicities.

Basically, then, Sec. IV tries to present why the model has taken the form it has, with theoretical arguments given where they helped to push in a certain direction or improved our understanding. Considerable trial and error and unsuccessful phenomenology went into building up the model to the stage it is at now.

Section V is designed for readers who have not previously concerned themselves with the effects of absorption in any detail. Some elementary closed form calculations are shown, and such points as the introduction of zeros and the slopes in t adding inversely are noted. Some discussion is given of the history and role of the inelastic intermediate state contribution in this context, where its effects can be seen rather directly.

A good deal of the complexity of real data comes from the presence of several spin amplitudes in every observable. The absorption model treats amplitudes of different amounts of net helicity flip in characteristic ways, and these are discussed here. According to the present model, someone who understands the form of just four amplitudes (nonflip, single flip, double flip, and nonflip with a pole contribution vanishing at $t=0$) can put them together in appropriate mixtures determined by coupling strengths, and at least qualitatively understand the behavior of the data. These amplitudes and their zero structures are discussed here. An important and testable prediction of the absorption model is that all amplitudes with the same net helicity flip are absorbed the same way.

The purpose of Sec. V is to give the reader a qualitative understanding of the basic systematics of absorbed amplitudes. The differences between the amplitudes obtained from the procedure of Sec. III (the present form of the model, since 1973) and those described in Section V (essentially the form of the model of 1969-1972) are due mainly to the improved treatment of the Pomeron phase and energy dependence, and are studied in Sec. VI. We have proceeded in this way because the amplitudes at the stage of Section V are fairly easy to understand qualitatively, and the changes discussed in Section VI are perhaps best seen in relation to the simpler amplitudes, particularly for readers with some exposure to the earlier forms.

Although the procedure for calculating the full amplitudes given in Sec. III is fairly simple to state, the amplitudes can only be calculated numerically, and the resulting amplitudes behave in fairly complicated ways. Rather than just calculate and present results, in Sec. VI we try to explain physically how different aspects of the behavior come about. We consider separately the amplitude phases, shrinkage, fixed-t s-dependence, and fixed-s t- dependence. In some cases we can only separate out the behavior in question and illustrate it graphically, and in some we can give useful hand-waving arguments. The intent is that a study of Sec. VI should allow the reader to understand operationally why (within the context of the model) the amplitudes behave as they do, so that their relation to experiment will be as transparent as possible. All of the amplitude properties and behavior discussed in Sec. VI are consequences of the procedure stated in Sec. III, without modification.

The most important effects arise from the role of the energy dependence and associated phase of the absorbing S-matrix, S_{eff}. It has simultaneously a strong effect on the phases of absorbed amplitudes and on their shrinkage properties. Section VI.A illustrates how a vector meson exchange amplitude has a double zero in the real part rather than the single zero of the older model, how the order of zeros in real and imaginary parts is interchanged, and how the real part of a vector meson exchange amplitude, with net helicity flip zero but a pole

that vanishes at $t=0$, is suppressed near $t=0$. Results for tensor exchange are just rotated by $\pi/2$. Section VI.B shows how precisely the same aspect of the basic procedure, the energy dependence of S_{eff}, gives an absorbed amplitude with an energy dependence like that of the pole rather than the traditional form with half the shrinkage. These two parts of Sec. VI show how several well known problems connected with two-body reactions are dealt with in the present model. Parts C and D treat fixed-t s- dependence and fixed-s t- dependence, showing how different amplitudes behave. As individual amplitudes become available from analysis of experimental data in the future, testing the behavior shown here will provide a number of crucial tests of the model.

Section VI was to provide qualitative insight into the behavior of actual amplitudes. In Secs. VII and VIII we concentrate on applications. First, in Sec. VII, we take specific topics, such as "Polarizations," and show how the model allows a unified point of view about a number of reactions. Other topics considered are line-reversed reactions, the comparison of reactions with different external particles, the relation to various regularities considered in recent years by a number of workers (such as geometrical scaling, impact parameter universality, derivative relations among amplitudes), exchange degeneracy breaking, and duality. The intent in Sec. VII is to emphasize the features which many different reactions have in common; in Sec. VIII we treat the reactions separately.

We note here a few of the more important points of Sec. VII. Concerning polarizations an important prediction for the model is that the K^+p elastic polarization should show a single zero (due to the zero in the real part of the flip amplitude), while the pp polarization should show two zeros (the second one due to the nonflip amplitude) which separate as s increases. We expect that even at very high energies polarizations of a few percent will be seen. $P(\pi^-p\to\pi^0n)$, where the absorption model was wrong in the old days but is now satisfactory, is discussed. An important success for the absorption model is its ability to describe $P(np\to pn)$. This exotic channel has large polarization without structure, and is a serious problem for all other models so far.

The part on line-reversed reactions explains how our treatment differs from that of models where the pole terms are exchange degenerate. The prediction of the model which is probably most dramatic is discussed here: we require for a line-reversed pair with vector and tensor exchange, such as $K^+n\to K^0p$ ("real") and $K^-p\to\bar{K}^0n$ ("rotating"), that the real cross section be larger than the rotating one at energies in the 50–150 GeV/c range by a factor of about 1.5–2. All models with exchange degenerate poles, on the other hand, require that the ratio always get closer to unity as s increases, and it is already less than about 1.1 at about 10 GeV/c. To our knowledge this measurement, for any vector–tensor line-reversed pair, is the most clear experimental way to distinguish the present model from any of those with exchange degenerate poles. No data is yet available, although it could soon come from Fermilab or Serpukhov. If one takes the $K^-p\to\bar{K}^0n$ Serpukhov data, uses SU(3) and $\pi^-p\to\pi^0n$ and $\pi^-p\to\eta n$ to obtain $K^+n\to K^0p$, then the ratio does go our direction, being somewhat larger than 2 but with large errors; direct measurements will not be too far off.

Some detailed discussion is given about the model's present inability to relate reactions with different external particles. If an effective way to do that could be incorporated it would be of great practical value.

Energy dependence data, and the relation of phases to trajectories, allow us to determine fairly well a set of trajectories which are consistent with a wide range of data. The intercepts of the pole trajectories are $\alpha_\rho(0)=0.46$, $\alpha_\omega(0)=\alpha_{A2}(0)=0.3$, $\alpha_f(0)=0.39$. The last is not well determined because it is not easy to separate the Pomeron from the f. Remember that the effective trajectories of an absorbed amplitude lie about 0.1 above the pole trajectories at small t and in the 5–50 GeV/c region. It is possible that one could have a picture where all the pole trajectories are at 0.3 in a minimal theory, with the ρ raised up mainly by the effect of its width and the nearby 2π threshold (giving a large Imα) and the f by Pomeron–f mixing (Sec. VII.E).

An important limitation of the present model is that we do not understand very well how to extend it to low energies. As s decreases the number of open channels decreases and the absorption approximation gets less valid. At the same time, partial-wave amplitudes increasingly exceed their unitarity limits and are suppressed. Thus the structure of the model and the amplitudes probably should not change much as s decreases. In the present form this is poorly satisfied, for one reason because the pole term in our approximation has a $\ln s$ controlling the slope in t and at low energies $\ln s\to 0$. This results in some failures at low energies (normally below about 3 GeV/c). A major question related to these failures is the FESR behavior. It was first pointed out by Worden that the model, even with the best absorption procedure, did not have the low-energy structure required by FESR's. Subsequently Hartley pointed out that this could be corrected in practice by modifying the form of the Reggeon pole so that it has a steep slope at $t\approx 0$, and is probably largely unrelated to the absorption procedure. Consequently, while we can deal with this problem in practice, it is not really solved. Section VII.F is a discussion of this problem and of some of its implications.

In Sec. VII we consider various applications from the point of view of subject matter, cutting across different reactions and looking at what they have in common. In Sec. VIII we look at individual reactions, one or a few at a time, discussing a good deal of data in detail, showing some data fits, and providing a number of predictions for future experiments. First we discuss how we proceed. By requiring factorized Reggeon poles we can determine the Reggeon trajectories and residues in one place and then use them elsewhere. We have checked that one consistent set of Reggeon and Pomeron parameters can simultaneously describe many meson–baryon and baryon–baryon reactions approximately, over a large range of s and t. The quality of the fits is shown in the figures. They are by no means perfect, but given such effects as low-lying contributions not included,

normalization inconsistencies in experiments, and the attempt to go over an energy range of 3–1500 GeV/c, the general agreement with data seems to us to indicate that most physical effects are present in the model. Such detailed probes of phases as the ANL polarized beam data are analyzed in detail.

A few places should be watched for possible failures in the future. The recent $np \to np$ polarization from ANL is badly fitted at 3 GeV/c and below, although satisfactorily at 6 GeV/c. It may be that something is wrong, or only that an unusually large contribution is present at low energies but falls very rapidly with energy and is not included in high-energy models; measurements in the 6–12 GeV/c region may decide. The old question of the dip in $\pi^- p \to \eta n$ is not decided yet. The model predicts a shallow dip near $-t = 1$ GeV^2 (not at 0.6 GeV^2, as in the old form, because the tensor exchanges are more central than vector ones). This is not particularly observed (although it does appear to be present at one energy), but the errors are still at the stage where there is no inconsistency. Since the present model generally gives final amplitudes with a zero structure like that of poles with signature zeros, it is reasonable to expect this to work out, but it is not as yet apparent that it does.

The Reggeon and Pomeron parameters are summarized in Tables I–III. Where different reactions appeared to prefer slightly different values of some parameters we have given a weighted choice, which should be a good starting value for any future application. There appear to be a number of systematic regularities among different particles, indicating that many parameters could be eliminated by scaling rules, but we have not done so because of a lack of firm basis for the rules.

An Appendix is included to deal with spin problems, so the paper is basically self-contained for other applications. Using the information given in the Appendix it is possible to choose the independent helicity amplitudes, find the relations of other amplitudes to the independent ones, relate the amplitudes to the observables for a number of the most common reactions, including those treated in the paper, and relate the residues of the s-channel helicity amplitudes used in the paper to the coupling constants used in other contexts and in standard Lagrangians. One result of this analysis is a large set of coupling constants which are measured in a self-consistent way and can be useful in other applications.

II. HOW DO WE KNOW A SIMPLE EXCHANGE PICTURE IS INSUFFICIENT?

Many workers hoped in the early 1960's, and some have still continued to hope, that one could obtain a workable theory of hadron two-body reactions in terms of contributions, each given by a definite parity particle or Reggeon exchange contribution. Effects of unitarity were hopefully included by Reggeization.

In fact, there are reasons, both theoretical and phenomenological, why we should expect an unmodified exchange picture to be inadequate, and why we should expect physical effects like those associated with absorption to be important.

The present section is intended to give a qualitative and intuitive view of the situation, indicating to an uninitiated reader why more than simple exchange amplitudes are needed, and why the addition of absorption effects improves the picture. Several examples are discussed at a simple level, with more detailed treatment given later on.

The particles we are studying are hadrons. They interact strongly. Whenever they are near enough (i.e., within a certain impact parameter), they will scatter off one another in a variety of ways in addition to interacting via the quantum number exchange of interest. The dominant interaction will be absorptive elastic rescattering. These interactions will affect all aspects of what is observed.

It would be surprising if rescattering corrections to simple exchanges were not required to achieve an understanding of the data. The problem is to know how to calculate the corrections. Phenomenologically there is considerable evidence that a simple exchange picture is insufficient. Here we list a few qualitative and isolated cases that show both that the simple exchange is inadequate, and that the expected effects of absorption are in the right direction.

A. π-exchange reactions

Some years ago it was generally considered obvious that $\gamma p \to \pi^+ n$ and $np \to pn$ would have forward turnovers at high energies, because the π exchange contribution would be big and it flipped the nucleon helicity in the s-channel. In terms of our formalism (see appendix), pion exchange (Reggeized or not) contributions have $n + x = 2$ so the amplitudes vanish linearly in t as $t \to 0$. This is a necessary consequence of the exchange of a pseudoscalar pion.

The data, however, showed a sharp peak on a scale of order $m_\pi^2 = 0.02$ GeV^2; the "simple" expectation, that there should be a forward turnover, was wrong.

The explanation is generally thought to be as follows (see Sec. V). In one amplitude with $n = 0, x = 2$, the contribution associated with the pion does not have to vanish at $t = 0$ unless it has definite parity; then it is "evasive" (has a factor of t). Some other slowly varying contribution associated with the π exchange is present and interferes destructively with the pion pole, so that at $t = 0$ we see only the other contribution, while by $t \approx m_\pi^2$ the destructive interference has produced a large decrease in cross section because the pion pole term varies rapidly on that scale.

Without a theory, the other contribution could be anything, of course, but the regularities are such (seen in $\gamma N \to \pi N$, $pn \to np$, $\pi N \to \rho N$, and at different energies) that it is reasonable to say that it is something closely associated with π exchange. Such an effect is provided by s-channel unitarity corrections.

At high energies the absorption model is an attempt to approximate the effects of unitarity. If one begins with an amplitude which vanishes at $t = 0$, makes a partial-wave expansion, absorbs away essentially all the s wave, most of the p wave, some d wave, etc., then one finds after resumming that the delicate cancellation between partial waves that gave the zero is destroyed, and the amplitude no longer vanishes.

In different language, one can think of the absorption

as a rescattering effect. Then there are two exchanges, with relative angular momentum, and the exchanged state does not have definite parity. Then the amplitude does not vanish. We will illustrate this quantitatively in a definite absorption model below. However one thinks of it, for the present example the "other contribution" has the same quantum numbers as the π exchange apart from angular momentum and parity, a strength related to the π-exchange strength, and an s and t dependence different from the π pole but partially determined by it.

At low energies conventional unitarity corrections have exactly the same effect. Here a theorist would unitarize each partial wave, e.g., in an N/D calculation. The s wave would be modified most, etc. Again a peak appears. This is related to the "duality" of hadron amplitudes. This is best understood for charged pion photoproduction where the Born terms do give the correct answer for small t (Jackson and Quigg, 1969).

To summarize: the "simple" expectation is wrong because the π-exchange contribution peaks instead of vanishing at $t=0$. It is probably wrong because of s-channel unitarity corrections to the simple t-channel exchange contribution. Both are essential to an understanding of the data.

B. Polarization in $\pi^- p \to \pi^0 n$

At high energies only ρ exchange is allowed. Many workers expected that, because there was only one exchange, it would give both helicity amplitudes (the nucleon can flip helicity or not) the same phase. Then the polarization, proportional to $\mathrm{Im} M_{++} M_{+-}^*$, would vanish.

Experimentally the polarization was significant, at least 25% at some angles, and rather constant from 5 GeV/c to 11 GeV/c, so the "simple" exchange picture cannot be fully right.

Again, unitarity corrections in the absorption approximation do the right thing. The amplitude with $n=0$ is large in the forward direction and at small impact parameters, so it feels the absorption of low partial waves rather strongly, while the $n=1$ amplitude which vanishes at $t=0$ and at small impact parameters is less affected by the absorption. The real and imaginary parts in each amplitude are affected differently, since they contain different partial waves in general. Thus, the two amplitudes get different phases and polarization is generated. All models get the results correct at small t, and the experimental results at small t were predicted by Cohen-Tannoudji *et al.*, 1967. At larger t all predictions were wrong, and the experimental results helped lead to the present improvements in models. Again, both s- and t-channel effects must be considered.

C. Nonforward zeros of amplitudes

In the view of many theorists ρ or ω exchange amplitudes would be simple if they vanished whenever the trajectories passed through zero, α_ρ, or $\alpha_\omega = 0$. This occurs at $-t \approx \frac{1}{2}$ GeV^2.

This would imply, among other things, that in $\pi^\pm p$ or in $K^\pm p$ elastic scattering, where the ρ or the ω is a big contribution and changes sign, one should observe a zero in the differences of differential cross sections. This zero is observed, of course—it is the well-known crossover zero. But it occurs at $-t \sim 0.15$ to 0.2 GeV^2 rather than at 0.5 GeV^2. Physically that is a very big difference.

In addition, the zeros cannot just be associated with the exchanges, since they do not occur in nonelastic reactions where the same exchanges dominate. The ω exchange dominates $\gamma p \to \pi^0 p$, for example, in an amplitude with the same coupling at the nucleon vertex, and gives a maximum instead of a zero at $-t \approx 0.2$. *The simple exchange picture fails very badly where zeros are concerned.* Experiment completely excludes zero factorization.

Unitarity corrections again do the right thing. Whatever the detailed shape of the definite parity exchange contribution in t, when we remove mainly low partial waves the t distribution gets sharper and a zero is introduced or moves toward $t=0$ in $n=0$ amplitudes where the absorption is strong. For amplitudes with $n>0$, as in $\gamma p \to \pi^0 p$, the zeros will occur further out in $-t$.

Similarly it would have been simpler if in a given amplitude the zero would be at the same t value for both real and imaginary parts. But for the $n=0$ ρ exchange in πN scattering this is not so (Ringland and Roy, 1971; Halzen and Michael, 1971), and probably it is not so for the vector and tensor K^* exchanges (Barger and Martin, 1972; Worden, 1974). For the vector exchanges in πN and KN the zero in ImM is near $-t = 0.2$ GeV^2, but the zero in the real part is further out in $-t$ (around 0.4 GeV^2) if it occurs at all. Although the absorption model will separate the zeros of the real and imaginary parts because their partial-wave structure is different, the traditional versions of the model give less of an effect than is observed, and have the zero in ReM closer to $t=0$ than that in ImM. We will see below how the observed zero structure arises.

D. Both s and t channels needed

A final example of a view we have to give up is the possibility that one could understand experimental data by only specifying quantum numbers in the s channel (as proposed by the old naive strong absorption model) or in the t channel (as required by any model with only poles exchanged), but not both.

That the t-channel quantum numbers do not suffice is clear from $\pi^- p \to \pi^0 n$, where there is t-channel ρ exchange but the data shows a completely different zero structure in the amplitudes with s-channel net helicity flip $n=0$ or $n=1$. That the s-channel quantum numbers are not sufficient is not completely established experimentally but is probably the case, with tensor exchanges f, A_2, K^{**} having zeros at different t values than vector exchanges ω, ρ, K^* in the same amplitudes (Phillips, 1971; Barger and Martin, 1972; Worden, 1974).

Thus any model which will help us understand the data must simultaneously depend on s- and t-channel quantum numbers for each reaction.

III. GENERAL PROCEDURE FOR CONSTRUCTING ABSORBED AMPLITUDES

In this section we give the procedure for constructing the full amplitudes. In the following sections we study the consequences for the behavior of amplitudes as functions of s,t; we compare the predictions with data, etc. Most of the general questions concerning spin are dealt with in the appendix, while spin-dependent differences in the behavior of amplitudes (which are crucial for understanding data) are discussed in Sec. V.

To give the general procedure for constructing a given amplitude, we must first give the form of the Reggeon pole exchange as a function of s,t. Then we must tell how to take account of absorption effects. The latter requires giving both the procedure to follow and the functional dependence of the complex rescattering amplitude on s,t. First we state the rules, then we discuss their origin, and then examine their consequences. The following rules incorporate those of Hartley and Kane (1973, hereafter referred to as HK) and what has been learned since then:

The absorption model rules

(1) For any two-body reaction

$$a+b\to c+d \tag{3.1}$$

define helicity flip quantum numbers

$$\begin{aligned} &m_a=\lambda_c-\lambda_a,\quad m_b=\lambda_d-\lambda_b\,,\\ &n=|m_b-m_a|\,,\quad n+x=|m_b|+|m_a|\,. \end{aligned} \tag{3.2}$$

(2) For each definite parity Reggeon pole, r with nonvacuum quantum numbers that can be exchanged, the amplitude is

$$R^r_{\lambda_c\lambda_d;\lambda_a\lambda_b}(s,t)=\pm(-t)^{(n+x)/2}\gamma_{rca}(t)\gamma_{rdb}(t)\Gamma\left(\frac{J-\alpha_r(t)}{2}\right)\times\left(\frac{s}{s_0}\right)^{\alpha_r(t)}\exp\left(\frac{-i\pi[\alpha_r(t)-J]}{2}\right), \tag{3.3}$$

where $\alpha_r(t)$ is the Reggeon trajectory, J the spin of the lowest physical particle on the trajectory (0 for π, 1 for ρ, 2 for A_2, $\frac{1}{2}$ for N, etc.), and $\gamma_{rca},\gamma_{rdb}$ are factorized pole residues. The residues can be obtained from our measured values given below, or from the reader's favorite theory, etc.

We parametrize the residues as

$$\gamma_{rxy}(t)=g_{rxy}\exp\{[c_{rxy}(\overline{m}^2-t)^{1/2}-\overline{m}]\}\,. \tag{3.4}$$

Then g_{rxy} is the rxy coupling constant, measured at $t=0$, for s-channel helicity amplitude vertices. Numerical values for g's and relations to Lagrangian definitions are given in the Tables. The energy scale s_0 is fixed at $s_0=1$ GeV^2. The mass $\overline{m}$ is given by the lowest threshold in the t channel allowed by quantum numbers (e.g., $\overline{m}=2m_\pi$ for ρ,f; $\overline{m}=3m_\pi$ for ω,A_2; $\overline{m}=m_K+m_\pi$ for K^*, etc.). This presumably reproduces a reasonable impact parameter distribution and introduces reasonable theoretical structure.

The trajectory is parametrized by

$$\alpha_r(t)=J'+\alpha_{1r}(t-m^2)/[1+\alpha_{2r}(m^2-t)^{1/2}]\,. \tag{3.5}$$

Here J' is the spin J of the lowest physical state on the trajectory as above, plus any correction to the real part of the trajectory due to the dispersion integral over the width (this correction is probably only important for the ρ, where we estimate $J'\simeq 1.1$; see Sec. VII.E).

(3) For the vacuum quantum number exchange, diffractive, elastic amplitude (called the "Pomeron") we use

$$P(s,t)=-is[R_c^2A_ce^{B_ct}J_1(R_c\sqrt{-t})/R_c\sqrt{-t}+R_e^2A_ee^{B_et}J_0(R_e\sqrt{-t})]\,, \tag{3.6}$$

$$R_c^2=R_{c0}^2+R_c'^2(\ln s-i\pi/2)\,, \tag{3.7}$$

$$R_e^2=R_{e0}^2+R_e'^2(\ln s-i\pi/2)\,, \tag{3.8}$$

with an energy scale of 1 GeV^2 for s.

The parameters R_c,R_e,B_c,B_e correspond to the radii and thicknesses of central and edge regions and are strongly constrained by geometrical ideas.

(4) For vacuum quantum number, diffractive processes where mass changes and/or helicity flips we use only the peripheral part of the above amplitude

$$D_n(s,t)=-is(R_e'^2+K)A_e'e^{B_e't}J_n\{R_{e0}'[-t(\ln s-i\pi/2)]^{1/2}\} \tag{3.9}$$

where n is the net helicity flip and $R_e'^2=R_{e0}'^2(\ln s-i\pi/2)$. These will describe the s-channel helicity amplitudes for low-mass diffraction dissociation, and the Pomeron helicity flip amplitudes at high energies. The energy scale where helicity and mass changes are important will presumably differ from elastic ones, so we allow a constant added to R^2 in front.

(5) The Hankel transforms, to calculate the impact parameter (b) distributions for each t distribution, are defined as

$$R_{\lambda_c\lambda_d;\lambda_a\lambda_b}(s,b)=\frac{1}{2q^2}\int_0^\infty\sqrt{-t}\,d\sqrt{-t}\,R_{\lambda_c\lambda_d;\lambda_a\lambda_b}(s,t)J_n(b\sqrt{-t})\,, \tag{3.10}$$

$$R_{\lambda_c\lambda_d;\lambda_a\lambda_b}(s,t)=2q^2\int_0^\infty bdbR_{\lambda_c\lambda_d;\lambda_a\lambda_b}(s,b)J_n(b\sqrt{-t})\,, \tag{3.11}$$

where n is the net helicity flip. A similar transform pair exists for each amplitude.

(6) An elastic rescattering amplitude is defined as

$$M_{\rm eff}(s,t)=P(s,t)+(2q/W)M_f(s,t)+\Sigma(s,t)\,. \tag{3.12}$$

Here P is the Pomeron amplitude from elastic scattering and is determined from elastic data, and M_f is the f Reggeon exchange in elastic scattering. It has been suggested by Collins and collaborators (see Collins and Fitton, 1974, and references there) that f should be included in $M_{\rm eff}$, and we will see below why it is indeed necessary. Σ represents the contribution to the absorption from the sum over all nonelastic intermediate states. All we know for certain about Σ is that it is peripheral in impact parameter, since most contributions to it are peripheral. Thus we parametrize Σ as

$$\Sigma(s,t)=-isde^{Dt}(R''^2+K)J_0\{R_0''[-t(\ln s-i\pi/2)]^{1/2}\}\,. \tag{3.13}$$

R'' and D must correspond to the behavior of a peripheral object of size about a fermi, with R'' expected to be somewhat greater than $1f$, since the long-range π-exchange tail will contribute. The size is set by d and the energy scale by K. One value of d should hold for all NN reactions, etc. Independent estimates of d are only valid to about a factor of 3, so they are not very useful; at medium energies Σ and the edge of the Pomeron should be comparable in size.

(7) The absorption is described by an effective S matrix for elastic scattering

$$S_{\text{eff}}(s,b) = 1 - i(2q^2)\, M_{\text{eff}}(s,b)/4\pi s \tag{3.14}$$

where $M_{\text{eff}}(s,b)$ is calculated from Eq. (3.12) with Eqs. (3.10), using Σ from Eq. (3.13), P from Eq. (3.6), and M_f is an absorbed Reggeon.

(8) The full absorbed amplitudes are now

$$M_{\lambda_c\lambda_d;\,\lambda_a\lambda_b}(s,b) = R_{\lambda_c\lambda_d;\,\lambda_a\lambda_b}(s,b) S_{\text{eff}}(s,b) \tag{3.15}$$

$$M_{\lambda_c\lambda_d;\,\lambda_a\lambda_b}(s,t) = 2q^2 \int_0^\infty b\,db\, M_{\lambda_c\lambda_d;\,\lambda_a\lambda_b}(s,b)\, J_n(\sqrt{-t})\,. \tag{3.16}$$

With these, one constructs the observables, as in the Appendix, for any two-body reaction.

These rules, rather simple to state, give a general prescription for describing two-body reactions. We will discuss the implications of this prescription and compare it with experiment below. The amplitudes depend on some parameters, essentially the Reggeon trajectories and residues which have not yet been calculable, and on the geometrical quantities in the Pomeron. Although there are considerably fewer parameters than the number of reactions, there would still be too many to meaningfully describe a single reaction. However, we have determined ("measured") the parameters by simultaneously describing a large number of reactions, which tightly constrains them and appears to give a fairly well determined set. In the future, analyses of other reactions can be done with few or "no" parameters by using our measured values.

In this section we have learned how to write down each complete absorbed s-channel helicity amplitude. To summarize: if the Pomeron contributes simply use Eq. (3.6). For each Reggeon write the pole term from Eq. (3.3) and transform it to impact parameter with Eq. (3.10). Construct the elastic amplitude $M_{\text{eff}}(s,b)$ by adding the Pomeron from Eq. (3.6) transformed to impact parameter, the inelastic intermediate state contribution from Eq. (3.13) transformed to impact parameter, and the f contribution (see Sec. IV.D for complete details). Now we have $R(s,b)$ and $M_{\text{eff}}(s,b)$ for each Reggeon contributing to the helicity amplitude. Multiply these as in Eq. (3.15) and transform back as in Eq. (3.16) to obtain the absorbed Reggeon contribution to each helicity amplitude. Add all the Reggeons which contribute and you have the full amplitude. The spin structure for various reactions is discussed in the Appendix, to help determine which amplitudes are present. Numerical values for all necessary quantities are given in tables in the appropriate part of the text. The Appendix shows how to construct $d\sigma/dt$ and experimental observables.

IV. DISCUSSION OF THE GENERAL PROCEDURE

In this section we give theoretical and phenomenological arguments to explain the physical origin of the rules postulated in the previous section. If something has been discussed in detail in HK or in Ross *et al.* (1970) we will be brief here.

In general, it will be clear that the theoretical situation could be worse, but could also be much better. Unfortunately, the worst gaps are in places where unitarity effects matter, so it may be some time before better theory is available.

A. The form of the Reggeon pole

The pole has the standard power law behavior $s^{\alpha(t)}$, and therefore must have the phase which is required by crossing and analyticity, $\exp[-i\pi\alpha(t)/2]$ time 1 or i for signature. Theoretically, essentially nothing is known about the form of the trajectory $\alpha(t)$ or the residue $\beta(t)$. There should be a pole of the amplitude at every other integer value of the trajectory, which we have included via $\Gamma([J-\alpha(t)]/2)$, which introduces no other poles.

The trajectories are suggested by phenomenology to be approximately linear near $t=0$. At large $-t$ their behavior is a significant fundamental question. For example, if hadrons were composed of a few point constituents the trajectories would approach a negative integer for large $-t$. For a world with a finite number of infinitely composite hadrons with no point structure, probably $\alpha(t) \sim (-t)^\gamma$, where γ is a fractional power like $\frac{1}{4}$ or $\frac{1}{2}$. In a theory with infinitely many hadrons and constituents, the trajectories would continue linearly. We have chosen to use $\alpha(t) \sim \sqrt{-t}$ at large t, as shown in Eq. (3.5).

In studying high-energy data for $-t \leq 2$ GeV^2 only the linear behavior of α at small t matters in practice. We have considered the larger t behavior because it may be possible, eventually, given a trajectory which is known to describe small t data, to discriminate between qualitatively different large t behaviors even with a limited amount of data. Figure 1 shows the pole trajectories we have used.

The residue t dependence must also be chosen with limited guidance from theory. We have tried to use a form which is likely to closely resemble one from a good theoretical treatment. Probably choosing $\alpha \sim \sqrt{-t}$ will imply $\beta(t) \sim e^{-\rho\sqrt{-t}}$ at large $-t$. The residue will show some effect of the t-channel thresholds, especially for the ρ pole which should have a strong 2π branch point. Both of these features are included in our choice, Eq. (3.4). Since we work with data in the scattering region we define couplings g_{rxy} for Reggeon r and external particles x and y, measured at $t=0$.

The slope of the residue at $t=0$ is important for extending the range of applicability of the model to low energies. For high-energy data ($P_L \gtrsim 5$ GeV/c), the t dependence is essentially determined by the absorption. As the energy decreases the absorption strength grows (see Sec. VII.B, F) and the results are sensitive to the

impact parameter distribution of the pole, especially how much is concentrated near $b=0$. The steeper the pole in t the more spread out it is in b, so the pole slope near $t=0$ matters.

One other feature of the pole term needs discussion, its zero structure. For a number of years there has been a controversy. Historically, the so-called "Michigan" approach has been to argue that (1) all known zeros in high-energy amplitudes were naturally introduced by absorption, (2) some known zeros (crossover zeros, the zero in $n=1$ π exchange near $-t=0.5$ GeV^2) were *only* introduced by absorption, and (3) no compelling theoretical argument required zeros in the pole terms at the nonsense, wrong-signature points. Consequently, the Michigan approach was to assume no zeros were present in the pole terms until such a time as experiment should require them.

The alternative view was that exchange degeneracy requirements forced zeros in pole terms (Finkelstein, 1969). For a general exposition of this point of view, see Jackson (1970).

Our approach here is the Michigan one, without zeros. The dip structure of many reactions is given in a satisfactory way by absorption zeros, and we have not found any place where a zero is needed in a pole. This is a fairly strong statement, since absorption zeros follow a very clear systematics, correlated with helicity flip. For example, a zero near $-t=0.5$ GeV^2 in any $n=0$ or $n=2$ amplitude for the ρ or ω exchange contribution to any reaction, where the nonsense wrong-signature zeros are expected, would have ruled out the absorption approach. There is also evidence against the pole zeros in some reactions (Ross *et al.*, 1969; Kelly *et al.*, 1970). In addition, many workers have studied ways to get adequate descriptions of data with zeros in the poles and have generally been unable to do so. We are aware of only one published statement that it is not normally possible to describe data with zeros in the pole, by Collins and Swetman (1972). One approach, by Ringland, Roberts, Roy, and Tran Thanh Van (1972) has adequately described the πN reactions but has not been applied (to our knowledge) to the more stringent tests of $np \to pn$, $\gamma p \to \pi^+ n$, and related reactions. These questions are discussed in detail by Fox and Quigg (1973).

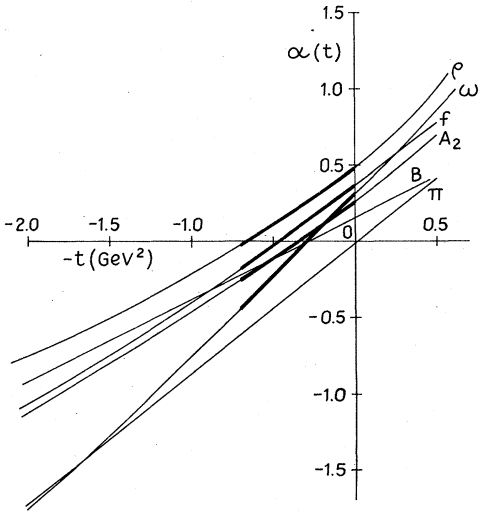

FIG. 1. This shows the actual trajectories we use. Only the region $0 > t > -\frac{1}{2}$ GeV^2 is determined by the data. For a discussion of the exchange degeneracy breaking see Sec. VII.E, and for a discussion of the shape, Sec. IV.A. The ρ, ω, A_2, and π are rather well determined, the f moderately well, and the B poorly determined.

The above arguments have all been phenomenological. We do not have a new theoretical argument as to why we think the zeros are not in the pole term. We suspect that two points are relevant. First, exchange degeneracy is a property of data, which are described by full amplitudes, not poles. We suspect Finkelstein's arguments should be applied to the full amplitude, qualitatively, in which case the zeros are present and our attitude is consistent with Finkelstein's. Second, the following argument may suggest what happens in a full dual theory (which includes the Finkelstein argument as a special case when no loops are included). In a full dual theory the leading Reggeon pole has higher-order contributions which break exchange degeneracy by containing all double spectral functions. These are shown, for example, by Schwarz (1974) or Halpern, Klein, and Shapiro (1969). Such pieces will shift the zeros in exchange degenerate poles. We can very crudely estimate how important the exchange degeneracy breaking is, by noting that both it and the Reggeon–Pomeron cut in such theories are of the same order in the relevant coupling. We know the RP cut is of order 50% of the amplitude at $t \sim 0$, and more important at larger t. Thus the exchange degeneracy breaking term which shifts the zero in the pole away from the point $\alpha=0$ could be quite large for the actual leading Reggeon poles, which are what is relevant for comparison with experiment.

Similar older arguments that the zeros were not in the pole terms have been given (Henyey *et al.*, 1969). Essentially, the argument was that the same physics which gave large absorption effects also breaks exchange degeneracy and gives amplitudes without the zeros. These arguments are as valid now as when they were given; the interested reader can pursue them.

Whether the theoretical situation is clear or not, it appears rather definite that, in an approach to two-body reactions which is generally applicable and which is based on definite parity Reggeon exchanges modified by external hadron interactions, the pole terms will not be taken to have exchange degenerate zeros. Any model with the zeros will be significantly different in its basic structure, although certainly a hybrid version could be constructed.

B. The effective Pomeron

In this section we will discuss the "effective" Pomeron amplitude which we have written in Eq. (3.6). By "Pomeron" we do *not* mean a simple t-channel pole, but merely the amplitude corresponding to diffractive elastic scattering, whatever its origin or J-plane properties. Our amplitude will be an "effective" one because it will take into account the important effects, and have reasonable behavior at least for s large and for $t<0$ and

$-t \ll s$. Whether it also behaves reasonably in other regions (e.g., small s, positive t, the J plane) has not been looked at very much and will only be mentioned briefly below.

The basic view that motivates our Pomeron is an s-channel one—elastic scattering is the shadow of all inelastic processes, via unitarity. The interacting particles are hadrons which interact more or less as strongly as possible, rather than by an exchange of a fundamental t-channel singularity with small modifications.

With this basic view in mind, then, we assume that one can think of two hadrons interacting in terms of two components, a central core plus an edge. The central piece is something like a black disc of radius somewhat less than 1 F, say $R_c \lesssim \frac{2}{3}$ F. The edge is peaked at around $R_e \gtrsim 1$ F.

With the transform Eq. (3.11), if the central part were given by a pure black disc

$$M_c(b) = \theta(R_c - b)\,, \tag{4.1}$$

then

$$M_c(t) = R_c^2 J_1(R_c\sqrt{-t})/R_c\sqrt{-t}\,. \tag{4.2}$$

Similarly, if the edge were a dimensionless delta function

$$M_e(b) = R_e\delta(R_e - b)\,, \tag{4.3}$$

then

$$M_e(t) = R_e^2 J_0(R_e\sqrt{-t})\,. \tag{4.4}$$

In reality the disc cannot have a sharp boundary and the edge contribution cannot be sharply peaked but must be spread out. Depending on how the spreading is done the result can take many forms; the simplest is to multiply the Bessel functions by monotonic functions such as exponentials. The slopes of the exponentials are a measure of the spreading out; as the slopes approach zero the sharp edges are obtained. One would expect values corresponding to about $\frac{1}{2}$ F to be reasonable.

What about energy dependence? It is attractive to try the hypothesis that we can allow the radius to change with energy and need introduce no other s-dependence (Kane, 1972a; see also Sec. VII.D.1). The fact that shrinkage is observed over a wide range of energies suggests that the size of hadrons increases slowly with s, diffraction peaks getting sharper.

Precisely how the radius grows with energy is unclear. Three arguments suggest, crudely, that we assume the edge radius $R_e^2 \sim \ln s$. The first is that an important contribution to the elastic amplitude may arise from Reggeon exchanges via unitarity, in which case $M \sim e^{(\alpha' \ln s)t} \sim e^{R^2 t}$ so $R^2 \sim \ln s$. A second argument, presented by Stodolsky (1969) for hadrons, comes from the observation that the multiplicity grows with s. Then at a higher energy there are more virtual particles around colliding hadrons and a given collision probability occurs at a larger radius than at a lower energy. If $\langle n\rangle \sim \ln s$ and $\sigma_T \sim R^2$, then $R^2 \sim \ln s$.

Third, elastic absorption applied to a power law amplitude reduces the growth to $\sigma_T \sim \ln^2 s$ (Finkelstein and Zachariasen, 1971; Cheng and Wu, 1971) or $R \sim \ln s$, and additional final state multiparticle absorption presumably reduces it more (Blankenbecler *et al.*, 1973; Ciafioloni and Marcheseni, 1974), so $R \sim (\ln s)^\gamma$ with $\gamma < 1$. All of these arguments should apply to the edge part of the Pomeron, where very strong unitarity effects do not yet operate and presumably a multiperipheral kind of dynamics is relevant. Thus with some justification we have used $R_e^2 \sim \ln s$.

For the central region, presumably a different dynamics operates at present energies. The data show less shrinkage and a faster growth in multiplicity than could be expected from multiperipheral types of models (Henyey, 1973). The data also suggest a slow increase of the central region in size. Consequently, we put $R_c^2 = R_{c0}^2 + r_c^2 \ln s$, where we expect $r_c^2 \ln s$ to be a small part of R_c^2 at ISR energies.

We want to guarantee that the Pomeron amplitude has even signature. Then absorbed amplitudes will have correct crossing properties to leading order in s as well. To do that, it is sufficient to relate the phase and the energy dependence by using the quantity $se^{-i\pi/2}$ as a variable.

Putting all this together, we have

$$P(s,t) = -is[A_c e^{B_c t} R_c^2 J_1(R_c\sqrt{-t})/R_c\sqrt{-t} + A_e e^{B_e t} R_e^2 J_0(R_e\sqrt{-t})]\,, \tag{4.5}$$

with

$$R_c^2 = R_{c0}^2 + r_c^2(\ln s - i\pi/2) \text{ and } R_e^2 = R_{e0}^2(\ln s - i\pi/2)\,. \tag{4.6}$$

In this amplitude the parameters are constrained by geometrical ideas. R_c should be $\frac{1}{2}$–$\frac{2}{3}$ F, $R_e \sim 1$–1.3 F; for B_c, B_e, which measure the "rounding of the edges," note that if only an exponential e^{Bt} were present, it could give a range in b of $4B$, so $B = 4$ corresponds approximately to $\frac{4}{5}$ F, while $B = 1.55$ corresponds to $\frac{1}{2}$ F. The sum of $A_c R_c^2/2 + A_e R_e^2$ just gives σ_T. The ratio A_c/A_e is constrained by the contribution of the peripheral part of the elastic amplitude, which is given partially by the long-range 2π cut and partially by the contribution of peripheral diffractive processes to unitarity.

In practice we fix these parameters by describing elastic data, which determines them well. They all have values consistent with those expected. In addition, the role of the Pomeron in absorption is very sensitive to its details and the same Pomeron is used both in describing elastic data and in absorbing.

In addition to its role in our picture of two-body reactions the above Pomeron amplitude is of great pedagogical value. All of the properties of high-energy elastic scattering are nicely summarized in a clear way in its properties. We briefly describe here how each important feature of the data is easily understandable.

1. Small t slope

We can estimate the small t slope by calculating the logarithmic derivative as $t \to 0$. This is

$$\frac{[dM(t)/dt]_{t=0}}{M(0)} = \frac{A_c R_c^2 (B_c + R_c^2/8)/2 + A_e R_e^2 (B_e + R_e^2/4)}{A_c R_c^2/2 + A_e R_e^2}\,. \tag{4.7}$$

If $M(t)=ae^{bt/2}$ so $d\sigma/dt \sim e^{bt}$ this derivative would be $b/2$. To see numerically what this is we assume

$$B_c = B_e = 2 \text{ GeV}^{-2},$$
$$R_c = \tfrac{2}{3} \text{ F} = \tfrac{10}{3} \text{ GeV}^{-1},$$
$$R_e = 1.2 \text{ F} = 6 \text{ GeV}^{-1}.$$

Then as the edge contribution varies from $\frac{1}{3}$ to $\frac{1}{2}$ of $M(0)$ the slope of $d\sigma/dt$ would vary from 12 to 14.4 GeV^{-2}. The result is very sensitive to the size and radius of the edge term, which dominates the slope. This range contains the experimental values.

At a lower energy the radii are smaller and the slope will be smaller. The edge contribution is large at $t=0$ because of the radius, and even steeper away from $t=0$ because it is quickly going to zero; the first zero of J_0 is around $-t=0.2$ GeV^2 for $R \simeq 1$ F. At small t this effective Pomeron will show shrinkage (approximately ln$s$) indefinitely with increasing energy because R grows indefinitely. But as soon as $-t \gtrsim 0.15$ GeV^2 the situation changes because of the interferences.

2. Medium t energy dependence

Away from small t the energy dependence is more subtle, though still easy to understand. Basically, in the region from $-t=0.2$ to $-t \sim 1.0$ GeV^2 the following picture holds, as in Fig. 2. We show the result for K^+p since that is relevant to new data, but the same picture holds for Pomeron contribution to any reaction.

The central contribution varies very slowly with energy compared to the edge. At the t value ($-t=0.56$ GeV^2 here) where the two contributions cross (this will always occur because of shrinkage) the amplitude itself is not changing with energy so the shrinkage rate has gone approximately to zero. This will happen at a t value which varies slowly with energy but is beyond $-t=0.2$ GeV^2; as s increases the crossing t-value moves slowly toward $t=0$ so the data will develop an inward bend, as shown in Fig. 2(b).

In two reactions that we know of the data are behaving this way, perhaps because of this mechanism. These are $\gamma p \to \varphi p$ at SLAC, from a few GeV/c to 16 GeV/c, and the ISR elastic pp scattering. Both are consistent with no shrinkage near $-t=\frac{1}{2}$ GeV^2 and with small t shrinkage. Preliminary data from FNAL shows similar behavior (Akerlof *et al.*, 1975).

3. Large t dip

Consider the zero structure of our effective Pomeron. The zeros of $J_1(x)$ are at $x=3.83$ and 7.0, etc. and those of $J_0(x)$ at $x=2.4, 5.5, 8, 65$, etc. Thus we will get a dip in $d\sigma/dt$ near $-t=1.4$ GeV^2; the *exact* position depends sensitively on *both* radii, since the zero must be near the zero of the J_1 but can be shifted by the J_0 (outward). A second dip may appear at about $-t=4.2$ GeV^2 according to these systematics, although by that large a t it would be somewhat fortuitous to actually see it because of the real part of the amplitude. From this point of view the zero at $-t=1.4$ GeV^2 is due to the structure and size of the central region. The depth of the dip in $d\sigma/dt$ depends on the real part of $M(s,t)$, which could always turn a dip into a break; we will discuss the real parts below. At energies below a few hundred GeV/c the Reggeons will not be negligible in dip regions, and they

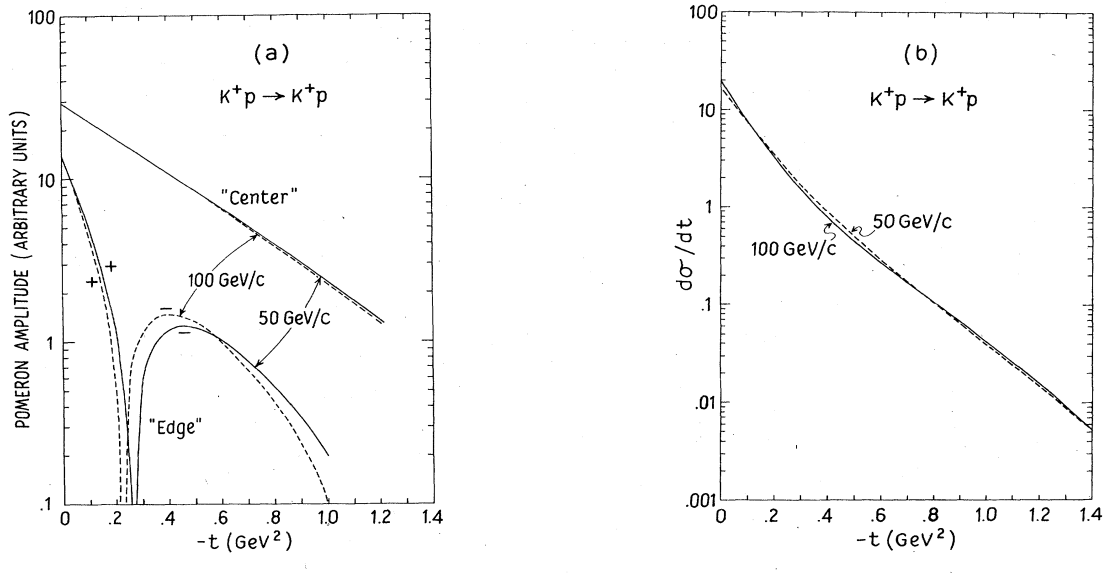

FIG. 2. Shows at two energies the t dependence of the imaginary part of the Pomeron amplitude, separated into the central and edge contributions, for K^+p as a typical example. The central contribution varies very slowly with energy, the edge contribution varies noticeably. Because of the shrinkage in t of the edge (expansion in size), at some t value near 0.5 GeV^2 no shrinkage will occur in the full amplitude. At a smaller t there will be shrinkage, at a larger t antishrinkage (hidden in pp because of the approaching zero). This gives a cross section which bends inward with increasing energy, as shown in 2(b) (only the Pomeron part of $d\sigma/dt$ is shown). Such behavior will appear whenever data is dominated by the Pomeron, e.g., all reactions above about 100 GeV/c, K^+p at even lower energies, and perhaps $\gamma p \to \varphi p$ at SLAC energies.

will fill in the dip by 100 GeV/c.

A similar discussion can be given for πN and KN, with radius scaled by $\sqrt{\sigma_T}$. At high energies we find $\mathrm{Im}M_{\pi N}=0$ near $-t=2.1$ GeV^2 and $\mathrm{Im}M_{KN}=0$ near $-t=2.5$ GeV^2. Above low NAL energies the dips are not filled in by Reggeons and should be observed.

4. Phase–Re$M(s,t)$ at all t

The phase of the Pomeron is one of its most interesting and important aspects; it is not often studied. Independent of any model, if the even-signature elastic amplitude changes with energy at any t value then it will have a nonzero real part at that t value. This can be seen intuitively by our method of using $se^{-i\pi/2}$ as a variable; then with any s dependence goes a phase. In particular, if the amplitude depends on $\ln s$ it will really depend on $\ln s - i\pi/2$.

The general result is given by the very useful formula

$$\mathrm{Re}T(s,t)=\tan\left[\frac{\pi}{2}\frac{d}{d\ln s}\,\mathrm{Im}T(s,t)\right] \tag{4.8}$$

where $T(s,t)=M(s,t)/s$ (Bronzan, Kane, and Sukhatme, 1974). The tan is defined by its power series expansion. This form holds for any *even-signature* scattering amplitude.

Since ImT is slowly varying, only the first term in the expansion is needed,

$$\mathrm{Re}T(s,t)\approx\frac{\pi}{2}\frac{d}{d\ln s}\,\mathrm{Im}T(s,t)\,. \tag{4.9}$$

To see the phase that goes with the effective Pomeron we could directly compute the Bessel functions of complex argument. To see qualitatively we can just make an expansion in $(\pi/2)/\ln s$, so

$$iJ_0\{R[-t(\ln s-i\pi/2)]^{1/2}\}$$
$$\approx iJ_0[R(-t\ln s)^{1/2}]-\frac{\pi R}{4\ln s}(-t\ln s)^{1/2}J_1[R(-t\ln s)^{1/2}], \tag{4.10}$$

$$\frac{iJ_1\{R[-t(\ln s-i\pi/2)]^{1/2}\}}{R[-t(\ln s-i\pi/2)]^{1/2}}$$
$$\approx\frac{iJ_1\{[R(-t\ln s)^{1/2}]\}}{R(-t\ln s)^{1/2}}-\frac{\pi}{4\ln s}J_2[R(-t\ln s)^{1/2}], \tag{4.11}$$

i.e., the real part of iJ_0 is approximately $-J_1$ and the real part of $iJ_1(x)/x$ is approximately $-J_2$; both J_1 and J_2 vanish at $t=0$. In addition there is the factor in front $iR^2\sim i(\ln s-i\pi/2)=\pi/2+i\ln s$, so if σ_T rises one has for the even-signature amplitude at $t=0$ ReM/Im$M=\pi/2\ln s$. Thus we expect that we should find the Pomeron phase as in Fig. 3.

Note that over most of the range in t the ratio ReM/ImM is negative. At lower energies the Reggeon contributions enter here as well and are negative at small t, so the ratio is entirely negative; that is very important for understanding the effects of absorption. Analysis of the data using Eq. (4.9) confirms this picture (Bronzan *et al.*, 1974).

C. Diffractive production

From the point of view of our analysis, low-mass diffractive production is relevant in two ways. First, the view of hadron reactions we are studying suggests rather clearly that low-mass diffractive production will occur peripherally in impact parameter, with the central region being suppressed by unitarity and by absorption. It suggests that changes in mass and in spin may give comparable amplitudes. From these suggestions (Ross *et al.*, 1969; Cohen–Tannoudji, Quigg, and Kane, 1972; Kane 1972b) one can construct a model for diffractive production which predicts or is consistent with many features of experiment, including the slope-mass correlation, the dip structure in the t dependence, and the helicity structure. To do so it is necessary to have further physical arguments for the relative amount of production of states of different J or M^2, and so far no compelling arguments have been given. There is too much freedom to consider most features as confirmed or even tested. Whatever the final form, the peripheral nature of low-mass diffractive production, which is what is most important for us, is confirmed qualitatively by the presence of a dip or break at $-t\approx0.2$ GeV^2 in the cross sections.

Second, thinking of absorption as an s-channel rescattering effect and picturing it as in the box diagrams of Fig. 4, we expect diffractive inelastic states to enter in an important way in the sum over all inelastic intermediate states. Presumably at high energies they are the most significant inelastic contribution.

D. The absorption prescription

We use the absorption prescription of Eq. (3.15). It is the physically obvious choice, originated by Sopkovich

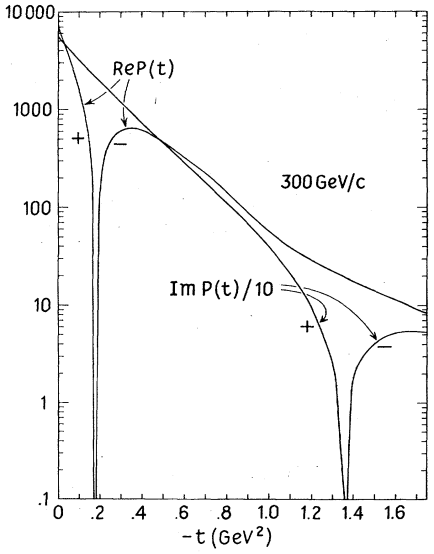

FIG. 3. The predicted Pomeron real and imaginary parts vs t at a typical ISR energy. The energy dependence of ISR data suggests that the prediction is qualitatively correct (Bronzan *et al.*, 1974). Both real and imaginary parts shrink slowly, with zero and maxima moving toward $t=0$.

(1962) and shown to be relevant to particle physics by Gottfried and Jackson (1964) and by Durand and Chui (1965).

It is an attempt to take unitarity effects into account in an approximate way, so it is unlikely that a full derivation will be feasible, because of the complexity of the unitarity effects. Rather, we assume that the basic prescription is so obvious as not to be in question. But the real physics question is the interpretation of $S_{\rm eff}$. What processes significantly affect the hadronic scattering, and precisely how do they enter in $S_{\rm eff}$?

Certainly $M_{\rm eff}$ will contain the Pomeron part of the elastic amplitude, and this will be the largest single contribution. One could argue that the full elastic amplitude at a given energy should be used. Collins and Swetman (1972; see also Collins and Fitton, 1974) have proposed that the f should be included. Probably it is sensible to retain the f contribution and not others, so the crossing properties and quantum numbers of the absorbed amplitude are not changed from those of the pole. One might hope that various cancellations make the other contributions small, but there are no compelling arguments.

Phenomenologically, there is a very convincing argument that for us the f is present. As shown in the section on the effect of the Pomeron phase on absorption (Sec. VI.A), it is necessary that over most of the t range one has $\mathrm{Re}M_{\rm eff}/\mathrm{Im}M_{\rm eff}$ negative. For our Pomeron if σ_T were constant this would be automatically true. But, with σ_T rising, one has $\mathrm{Re}P/\mathrm{Im}P$ positive at $t=0$ and for small t, at all s. The phase of the elastic amplitude which has the correct effect on Reggeon phases via absorption is the phase of actual elastic scattering, not the Pomeron part. Thus from the phase properties it is clear that the f (which is the main Reggeon contribution) should be included. Before the knowledge of the rising σ_T it was not possible to decide this without either extensive energy-dependent polarization data or a better theory of how to construct $M_{\rm eff}$; given the rising σ_T there is basically no choice for us.

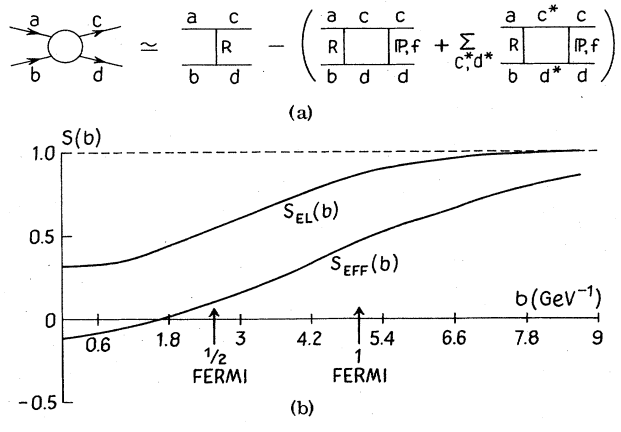

FIG. 4. Part (a) illustrates the contribution of one Reggeon R to the process $a+b\to c+d$. There is the pole term, the elastic absorption with Pomeron rescattering and with f rescattering, and the sum over inelastic intermediate states. See Sec. IV.E for discussion. Figure 4(b) shows the effective absorbing s-matrix vs b, for pp scattering at 6 GeV/c. The contribution from the elastic and the full $S_{\rm eff}$ are shown. Note how $S_{\rm eff}$ absorbs almost completely below $\frac{1}{2}$ F ($|S_{\rm eff}|<0.1$ there).

The other contribution to $M_{\rm eff}$ is the sum of all inelastic intermediate states, as shown in Fig. 4. Here we need to know three things in practice: the size of the contribution, its energy dependence, and its shape in b. Fortunately the latter is probably known—it is peripheral—since the main contributions will be low-mass diffraction and Reggeon exchanges, both of which are known to give peripheral amplitudes. The size is also not too bad a problem. Assuming it is a parameter for one reaction, once it is determined there, its relative value in every other reaction can be guessed at from coupling constant values, at least crudely. We can even guess at its absolute value from knowing inelastic and two-body cross sections, and the results are reasonable, though too crude to take as more than a consistency check.

The energy dependence is a harder question. One can construct arguments giving everything from a falloff to a rise like σ_T. Again, the energy dependence implies a definite phase, and we know phenomenologically what phase the absorption should have. This suggests the inelastic intermediate state contribution varies more slowly with s than the elastic. Higher-mass intermediate states will come in at higher energy, and Reggeon contributions will have a falling power. When good polarization data is available at energies above 25 GeV/c for nonelastic two-body reactions it will be possible to directly test the energy dependence of $M_{\rm eff}$. For now, we have parameterized it as in Eq. (3.13).

We also need to consider the energy dependence of absorption as we go to low energies. At extremely low energies no particle production occurs, so there is no absorption into other channels. However, unitarity bounds exist at each impact parameter and are often approached or exceeded by Reggeon exchange contributions. A suppression of partial waves thus occurs which is very like absorption in that it is smooth and reduces the central partial waves the most. The presence of the π-exchange peak in $np\to pn$ and $\gamma p\to\pi^+ n$ down to low energies is evidence for this. Consequently we expect approximately a constant amount of absorption as the energy increases until at high energies shrinkage effects spread the Pomeron out in b and reduce the absorption. These arguments lead us to choose the connection between M and S to be

$$S_{\rm eff}(s,b)=1-i\tilde{M}_{\rm eff}(s,b)/4\pi s \qquad (4.12)$$

at all energies, with $\tilde{M}(b)=2q^2M(b)$. Since $\tilde{M}\sim s$, the energy dependence of $\tilde{M}_{\rm eff}(s,b)$ is due mainly to the logarithmic growth of R^2.

Here we have summarized our approach to choosing the amplitude that determines the hadronic rescattering, in the absence of a way to derive it. Perhaps someday a derivation will be possible but for now we have to be content with the above hybrid approach, where we mix conjectures, known theoretical constraints, and phenomenological requirements. We emphasize that, having settled on a procedure, we do not vary it. All of the results of Sections VI, VII, and VIII are obtained with this absorption procedure.

It is worth remarking that in principle, and maybe in practice, the question of how hadron rescattering behaves can be directly studied (Block *et al.*, 1973). This is because in several processes which proceed by photon exchange, such as $K_2 p \to K_1 p$, $pp \to \Delta\Delta$, $\Lambda p \to \Lambda p$, factors of $\sqrt{-t}$ come from mass or spin changes at the vertices to cancel the photon propagator. Then the t dependence comes from the form factors and is sharp, so that the interaction occurs in a small impact parameter region of order one fermi, and absorption will strongly affect the observables. Since the photon exchange poles are known, absorption models can be tested and perhaps the appropriate procedures deduced. This can be done at high energies where the photon exchange will dominate these processes; it is barely possible that it could be carried out at Fermilab and the ISR. It could certainly be done at Isabelle energies.

E. Why are s-channel helicity amplitudes useful?

In the absence of any physics apart from the Lorentz group, all sets of amplitudes are of course equally good. It is common to use s-channel helicity amplitudes (SCHA), t-channel helicity amplitudes (TCHA), invariant amplitudes, and transversity amplitudes. For various purposes one or another set of these will be most convenient.

If one's purpose is to look for useful and simple structure in HE two-body hadron reactions, it now seems clear that one should use SCHA for two basic reasons. This was first emphasized by Ross *et al.*, 1969.

The first reason is completely general, and is that angular momentum conservation gives constraints which must be satisfied and are only simply expressed for SCHA. From Eq. (A23), each SCHA must vanish as the scattering angle approaches zero as

$$[\sin(\theta/2)]^{|\lambda_a-\lambda_b-\lambda_c+\lambda_d|} = [\sin(\theta/2)]^n , \tag{4.13}$$

where n is the net helicity flip. Thus a peaking or vanishing in the forward direction is characteristic of SCHA for general reasons. Any other set of amplitudes mixes the SCHA so it is harder to interpret forward behavior. In addition, theoretical models for other sets of amplitudes must be made to satisfy the above constraint, which can make calculations complicated, and understanding parameter behavior difficult.

The second reason follows from the importance of absorptive rescattering effects. In practice we expect definite parity exchanges which are modified by absorptive rescattering of the external particles. The absorptive rescattering has the properties of diffractive elastic scattering and to a good approximation is known not to flip s-channel helicities. Thus, generally, the spin properties of the SCHA definite parity contributions are preserved by the absorption, while those of the TCHA definite parity contributions are completely mixed up and no simple properties hold for the full TCHA. This is the essential reason why SCHA are more useful than TCHA.

There are two different sorts of behavior that are simpler for SCHA; several examples will be given below. The first occurs when an amplitude is zero from the definite parity exchange. Then it stays zero for the SCHA, but not for the TCHA. For the latter one must rotate to the s channel, absorb, and rotate back; the effect of absorption is different on different amplitudes and the cancellation that gave zero for some TCHA no longer happens. The second occurs because absorption (whatever one's approach) removes low partial waves in a smooth way from SCHA, so momentum transfer distributions are sharpened and perhaps zeros introduced in a systematic way for SCHA. For other kinds of amplitudes the zeros are obscured by mixing together several amplitudes with different zero structure.

When resonance production is studied, it is thus most important for experimenters to present s-channel, helicity frame density matrices. Amplitude analyses can be done for any convenient set of amplitudes, but at the present time attempts at understanding the underlying physics should normally relate data to the SCHA.

In Sec. IV we have discussed why the model takes the form it does. In the next two sections we go on to develop an understanding of the properties of the model, first at a crude level in Sec. V, and then for the full model in Sec. VI.

V. HOW ABSORBED AMPLITUDES BEHAVE

The various forms of absorption models should be viewed as attempts to take unitarity effects into account. It should probably be emphasized that they are not viewed by their originators as attempts to fit data but as models for the behavior of strongly interacting particles. As we have remarked, although the approximate models constructed may not yet be good ones, it would seem quite remarkable if two-body hadron interactions were not strongly affected by s-channel unitarity.

We will not analyze the derivation of the absorption model carefully—there have been no new insights into that in several years. Rather, in this section we will give the most naive and physically transparent argument that gets one to the standard answer, and discuss in detail the interpretations and implications of that answer and how absorbed amplitudes behave.

The purpose of Sec. V is to provide a simple illustrative analytic example of the properties of absorbed amplitudes, for readers who have not previously encountered such questions. The results are not particularly realistic, but they do show how the basic effects arise. An understanding of the structure of the complete model is perhaps best achieved by seeing how the simple version is improved.

A. Approximate calculations for spinless amplitudes

Assume that in the absence of unitarity corrections for the external particles the high-energy amplitude for some reaction is $R(s,t)$, with partial-wave expansion

$$R(s,t) = \sum_l (2l+1) R_l(s) P_l(\cos\theta) . \tag{5.1}$$

We will refer to $R(s,t)$ as a *pole term*. The particle poles have definite naturality—poles of spin J and natural parity have parity $=(-1)^J$ and poles of spin J and unnatural parity have parity $=(-1)^{J+1}$.

Next we assume that the effect of the initial and final state interactions is to shift the phase in an amount given by the diffractive elastic scattering of the initial or final states, the Sopkovich result. We assume that the full amplitude M, including all effects, is given in each partial wave by

$$M_l(s) = e^{i\delta_l^f(s)} R_l(s) e^{i\delta_l^i(s)} \tag{5.2}$$

where the $\delta_l^{f,i}$ are the phase shifts of the elastic scattering in the final or initial states, respectively. Each δ_l is mainly imaginary because the scattering is diffractive; the δ_l are related to the elastic amplitude M^{el} at high energies by

$$S_l^{el} = e^{2i\delta_l} = 1 - iM_l^{el}/8\pi . \tag{5.3}$$

In practice, we also assume that M_l^{el} is the same for initial and final states, although one could carry out calculations using Eq. (5.2) if so desired. Then we can substitute $e^{2i\delta_l}$ from Eq. (5.3) into Eq. (5.2), giving

$$M_l(s) = R_l(s) - (i/8\pi) R_l(s) M_l^{el}(s) . \tag{5.4}$$

It is a little easier to see what happens if we switch to an impact parameter representation. Writing

$$l + \tfrac{1}{2} \approx qb , \quad \Delta l = 1 \approx q\,\Delta b ,$$

$$\sum_l \sim \int_0^\infty q\,db , \tag{5.5}$$

$$P_l(\cos\theta) \sim J_0(b\sqrt{-t}) ,$$

we have

$$R(s,t) = 2q^2 \int_0^\infty b\,db J_0(b\sqrt{-t}) R(s,b) , \tag{5.6}$$

$$R(s,b) = \frac{1}{2q^2} \int_0^\infty \sqrt{-t}\,d\sqrt{-t}\, J_0(b\sqrt{-t}) R(s,t) , \tag{5.7}$$

and Eq. (5.4) becomes

$$M(s,b) = R(s,b) - (i/8\pi) R(s,b) M^{el}(s,b) , \tag{5.8}$$

with $M(s,t)$ given by a transform as in Eq. (5.6). Note from Eq. (5.4) or (5.8) that the absorption correction adds to the pole (destructively) and is constructed by multiplying amplitudes in impact parameter or partial waves. If the correction did not have the opposite sign to the pole it could not be thought of as due to the physics of absorption.

The basic physical idea is apparent here—the absorptive rescattering occurs locally in impact parameter (angular momentum conservation, approximately). Thus, we calculate R at each b, multiply by M^{el} at the same b, and transform to t.

Next we want to see how this behaves by choosing very simple forms for R and M^{el}. If R is a Regge pole, it is proportional to

$$R \sim [(s/s_0) e^{-i\pi/2}]^{\alpha_0 + \alpha' t} = a e^{At} \tag{5.9}$$

$$a = [(s/s_0) e^{-i\pi/2}]^{\alpha_0} , \quad A = \alpha' (\ln(s/s_0) - i\pi/2) ,$$

where the t dependence is explicitly shown. Ignoring all other t dependence to see qualitative behavior, we can use this form:

For M^{el} we assume

$$M^{el} = -is\sigma_T e^{Bt} . \tag{5.10}$$

This form (with our normalization) satisfies the optical theorem, and assumes a purely imaginary Pomeron giving a diffraction peak of slope $2B$ in $d\sigma/dt$. Again, it should give us a reasonable indication of how the absorbed amplitude behaves (though it seriously misleads us about detailed questions, as we will see below).

Using the identity

$$\int_0^\infty J_\mu(\beta x) x^{1+\mu} e^{-\gamma x^2} dx = \beta^\mu e^{-\beta^2/4\gamma} / (2\gamma)^{1+\mu} , \tag{5.11}$$

we get

$$M^{el}(s,b) = \frac{-is\sigma_T}{4q^2 B} e^{-b^2/4B} \tag{5.12}$$

and

$$R(s,t) = \frac{a}{4q^2 A} e^{-b^2/4A} , \tag{5.13}$$

so

$$M(s,b) = R(s,b) - \frac{a\sigma_T}{32q^2 AB} e^{-(b^2/4)(1/A+1/B)} \tag{5.14}$$

and

$$M(s,t) = R(s,t) - \frac{a\sigma_T}{16\pi AB} \int b\,db J_0(b\sqrt{-t}) e^{-(b^2/4)(1/A+1/B)}$$

$$= a\left(e^{At} - \frac{\sigma_T}{8\pi B} \frac{B}{A+B} e^{ABt/(A+B)} \right) . \tag{5.15}$$

The first term is the pole $R(s,t)$. The second is the absorption correction. Note that the two terms interfere destructively.

Note also that

$$S^{el}(s,b) = 1 - \frac{\sigma_T}{8\pi B} e^{-b^2/4B} . \tag{5.16}$$

As soon as we put in some numbers we can see the structure. For πN scattering we have typically

$$\sigma_T \approx 25 \text{ mb} \approx 60 \text{ GeV}^{-2} , \quad |A| \approx |B| \approx 4 \text{ GeV}^{-2} \tag{5.17}$$

so

$$\sigma_T / 8\pi B \approx 0.6 , \quad B/(A+B) \approx 1/2 . \tag{5.18}$$

Thus

$$S^{el}(s,b) \approx 1 - 0.6 e^{-b^2/4B} \tag{5.19}$$

$$M(s,t) \approx a(e^{4t} - 0.3 e^{2t}) . \tag{5.20}$$

The s wave ($b = 0$) is 60% absorbed away and higher partial waves are less and less absorbed in a smooth way. The pole and absorption correction interfere destructively, introducing a zero in $M(s,t)$ at $-t = 0.6$ when the two terms cancel. Although a zero is introduced, this is a spinless amplitude ($n = 0$) so we suspect (from our experience with data, e.g., crossovers) that the zero really should be at about -0.2. The units for t are always GeV^2. At small t, the amplitude (and cross section) is reduced in size and is sharper in t.

When we think about the structure of Eq. (5.8) we see that we can think of the absorption correction as a double

scattering in an appropriate sense (Fig. 4); the amplitudes involved are always physical on-mass-shell ones. This is just the meaning of multiplying amplitudes in impact parameter space.

We can then ask why we did not include other intermediate states in addition to c and d. For example, the Reggeon could excite a state c^* which could make a diffractive transition to c. Since the total amount of diffractive production is at least $\frac{1}{2}$ of the elastic cross section, if we again take the most naive approach and assume (incorrectly) that both have the same shape in b, we could have a coefficient of 0.9 for the Gaussian in b in Eq. (5.19) rather than 0.6. Thus the s wave would be 90% absorbed away—this seems a more reasonable result for hadrons. Now the zero moves in as well, to about $-t=0.4$, also a more reasonable result.

The question of the strength of the absorption has long been a controversial subject. To some workers it has seemed clear that for hadron interactions with big cross sections the s wave had to be essentially absorbed away (strong absorption). To others it was desirable that only elastic intermediate states would contribute (weak absorption). From a different point of view, Russian theorists, beginning with Gribov, Pomeranchuk, and Ter-Marterosyan (1965), and followed by Kaidalov, Ter-Marterosyan, and collaborators, have used field theory and J-plane techniques to discuss and estimate the size of intermediate states in addition to the elastic one. They have generally found amounts giving fairly strong absorption.

We believe that the sum over intermediate states contributes significantly, but with a shape in impact parameter different from the elastic shape (peripheral versus central). It is peripheral in b because most inelastic contributions, diffractive or not, are peripheral in b. Then a much smaller size for the sum enters but in just such a way as to play an important role; it blackens the absorbing disk at larger b, increasing its radius [see Fig. 4(b)].

In the past (before 1972) the absorption was often strengthened by the approximation of a multiplicative factor λ. This procedure was reasonable for seeing the behavior of absorption models in the earliest applications, but for the past few years it has been only of historical interest and one should directly include the additional contributions, with their different behavior in impact parameter and perhaps in other variables. As often happens, the first efforts in a new direction had some validity but needed improvement. We emphasize this because some workers in recent years have apparently not been aware that the inelastic intermediate state contribution is better understood now, and they have compared the older approach with experiment, rather than the improved one.

We see then that absorption modifies considerably the t dependence of the pole. The absorbed amplitude also has a different energy dependence from the original pole. The basic s^{α_0} is in the factor a in front in Eq. (5.20). At small t the pole dominates and shrinks, while beyond the zero the cut dominates and shrinks differently while falling somewhat faster because of the $1/\ln s$. The intersection point, where the zero is, moves slowly with energy because both terms shrink and one falls with energy.

One subtlety we have ignored above is that M is complex. Its real and imaginary parts will really have separate zeros because they always have a different zero structure in the pole, but the final zeros will be nearby. They are all complex zeros in t. If the pole term had zeros to start with, the pole-absorption correction interference would move them in toward zero.

Finally, the size is affected in an important way; it is reduced by about a factor of 2 in amplitude at $t=0$, and more at larger t. Thus attempts to relate cross sections to coupling constants must take absorption into account.

Next we want to consider how data would look if some version of a naive absorption model were valid. Finally, still later below, we will add the effects embodied in the present form of the model and see where they matter.

B. Helicity structure

For understanding real data it is *essential* to take account of spin. Different helicity amplitudes behave in completely different ways as functions of both s and t.

A good deal of the apparent complexity of hadron data comes from the presence of several helicity amplitudes, each behaving differently. The structure of each amplitude is, in the model, rather simple and characteristic.

For the spinless case $P_l(\cos\theta)\to J_0(b\sqrt{-t})$ [Eq. (5.5)]. When spin is present we have the Jacob–Wick helicity amplitude expansion, Eq. (A23). The general case has

$$d^J_{\lambda\mu}(\theta)\to J_n(b\sqrt{-t})\,,$$

where $b\sqrt{-t}\approx(2J+1)\sin(\theta/2)$ and $n=|\mu-\lambda|$, giving Eq. (5.21) below. This is valid in the same approximation for the case of general spins as the form with J_0 is for the spinless case, except that in addition here we are neglecting any contributions in $S_{\rm eff}$ which flip helicities. The form of $M^{\rm el}$ is just the same. We are assuming that $M^{\rm el}$ does not flip s-channel helicities, which is certainly a good approximation at nucleon vertices, and presumably everywhere. Remember, the Reggeon term will have a factor $(-t)^{(n+x)/2}$ because of angular momentum conservation and definite t-channel parity, while the absorbed amplitude has only $(-t)^{n/2}$, as $t\to 0$, since it does not have a definite parity.

Thus for an arbitrary SCHA we have

$$M^{(n)}_{\lambda_c\lambda_d;\lambda_a\lambda_b}(s,t)=2q^2\int_0^\infty bdbR_{\lambda_c\lambda_d;\lambda_a\lambda_b}(s,b)\times S_{\rm eff}(s,b)J_n(b\sqrt{-t})\,. \qquad (5.21)$$

Since the absorption only depends on n as far as helicity dependence goes, *all amplitudes with the same n are absorbed the same way. This is an important and testable prediction of the absorption model.* It generates relations among density matrix elements, and certain aspects of universal impact parameter shapes and derivative relations among amplitudes.

C. Qualitative systematics—Bessel functions, range of forces

Amplitudes calculated from Eq. (5.21) have a number of rather general and characteristic features, some of

which we describe here.

Consider amplitudes with $x=0$. Suppose the Reggeon term, which decreases like a Gaussian in b, is negligible beyond some radius R_0. $S_{\rm eff}$ is very small at small b, absorbing away essentially all of the s-wave, and grows to one at large b. Thus

$$bR(S,b)S_{\rm eff}(S,b) \sim \delta(b-R_0)\,, \tag{5.22}$$

leading to (Ross *et al.*, 1969)

$$M_{\lambda_c\lambda_d;\lambda_a\lambda_b}(s,t) \sim \gamma_{\lambda_c\lambda_a}\gamma_{\lambda_d\lambda_b}J_n(R\sqrt{-t})\,. \tag{5.23}$$

The γ's are constants associated with the sizes of the pole vertices. In this naive form the systematics are very clear. *We expect zeros in the real and imaginary parts of the* SCHA near the zeros of J_n. If $R_0=1$ F, for $n=0$ the first zero is at $-t=0.23$ GeV^2, for $n=1$ it is at 0.6, and for $n=2$ it is at 1.06. Of course, even in the naive absorption model the real and imaginary parts of the amplitude will not have exactly coincident zeros because the integration over the phase separates them. An edge which is spread out instead of a delta function may multiply J_n by a smooth function such as e^{ct}; for a reasonable interpretation we must have $c \lesssim 3$ GeV^{-2}.

It should be emphasized that these systematics are only meaningful in a model which includes significant contributions from intermediate states in addition to the elastic ones—a strong absorption model. Otherwise important central contributions are present and the J_n behavior is *not* expected.

If we go back one step to see how the systematics arise we can get a feeling for how changes will occur. The four main amplitudes needed to understand two-body reactions are shown in Fig. 5, still for the naive model. The real amplitudes will not behave precisely in this way, but these pictures are very useful for understanding the basic ways in which the model amplitudes behave for different helicity flips.

In the following we abbreviate "absorption correction" by AC.

The $n=x=0$ amplitude behaves as in the spinless case above. The pole is approximately exponential, while the AC is approximately exponential with a smaller slope, so they intersect giving the amplitude a zero. For $n=1, x=0$, both pole and AC vanish as $\sqrt{-t}$ in the forward direction; then the AC slope is smaller so they intersect, but at a larger $-t$ than for the $n=x=0$ case, near 0.6. For $n=2$ the intersection is even further out. Even with the full absorption it can be seen that *for small t ($-t \lesssim 0.4$ GeV^2) only $n=0$ amplitudes are significantly affected;* this is because the other amplitudes all vanish for $b=0$ and thus feel much less the removal of low partial waves.

For amplitudes with $n>0$ and for $t \lesssim 0.4$ GeV^2 it is a detailed quantitative question to distinguish between models. For example, the $n=1$ amplitudes from the naive absorption model and from an exchange degenerate pole model are hardly different there. Since all models will have approximate exchange degeneracy near $t=0$ because the data do, it will be safe to assume that amplitudes with $n>0$ are approximately exchange degenerate at small t in any reasonable model, including a strong absorption model without exchange degenerate poles.

Finally, consider the $n=0, x=2$ amplitude which is (for example) responsible for the sharp π-exchange peaks. Such amplitudes, for all exchanges, are often important when several particles have spin. The pole has the extra so-called evasive factor of t, but the AC does not have to vanish since $n=0$. They interfere destructively. Thus the amplitude is given by the AC at $t=0$, while it is essentially zero when the pole reaches its peak. For π exchange the pole is of the form $te^{at}/(m_\pi^2-t)$ and its peak is at a t value near $-t \lesssim 0.05$ GeV^2; the sharp forward peak is just the one seen in $np \to pn$, $\gamma p \to \pi N$, $\pi N \to \rho N$. For other exchanges such as A_2 the pole peaks further out, at $-t \sim 0.15$ GeV^2, and the AC is smaller in magnitude because of the missing forward peak of the pole, so that one sees zeros at about $-t=0.1$ and $-t \sim 0.3$. An important point for actually understanding data is that in any process with an $n=0, x=2$ amplitude where π exchange is allowed an A_2 always accompanies the π. The two must be considered together; so the pole term peaks very early and is very broad; the AC is largely parallel to the pole over a sizeable range in t and the $n=0, x=2$ amplitude is negligible compared to its forward peak over a sizeable range. The wide zero region should show up in ρ_{1-1} in

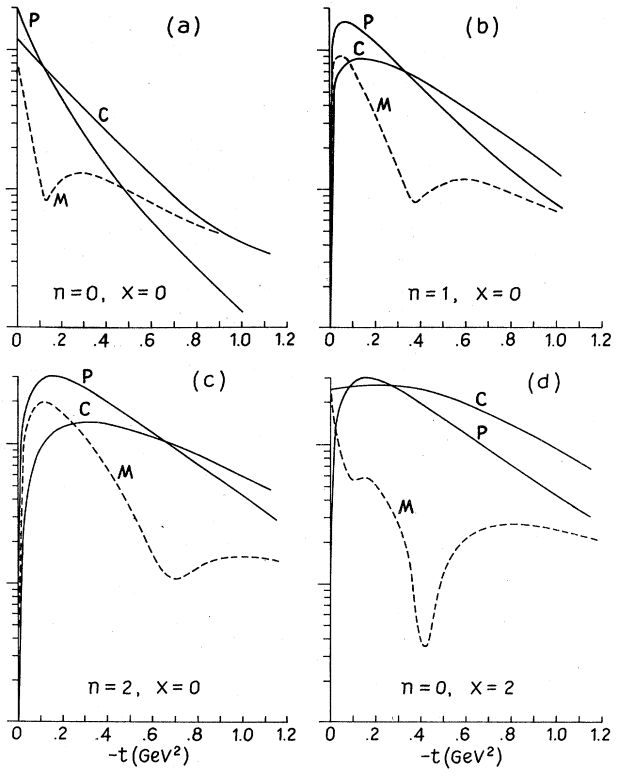

FIG. 5. This illustrates the behavior of the four most important s channel helicity amplitudes. The magnitudes of pole, absorption correction ("cut"), and full amplitude are shown. Real and imaginary parts of amplitudes usually are similar, except when the poles have zeros due to the $e^{-i\pi\alpha/2}$ signature factors. Essentially all experimentally accessible quantities are constructed of combinations of these four amplitudes, so a detailed understanding of them provides a simple way to visualize all data.

$\pi N \to \rho N$ as a broad zero near $-t \simeq 0.15$, for example. In $\mathrm{Re}\rho_{10}$ what appears is approximately twice the pole minus the AC, so the zeros are widely separated, one at very small $-t$ (0.01 GeV^2) and the other out beyond $-t = \frac{1}{2}$ GeV^2 where other contributions are big and it may be hard to see it.

By giving these four amplitudes their proper weights in a cross section or polarization, one can get a good qualitative picture of most data. Although $n=0$ and $n=1$ cross sections both have dips, an incoherent sum of both with about equal weights produces a monotonic cross section as in Fig. 6. Bearing in mind the identity

$$1 = J_0^2(Z) + 2\sum_{k=1} J_k^2(Z)\,, \tag{5.24}$$

one can see the general pattern.

At this stage the reader should have a picture of the ways various kinds of amplitudes can behave. In a gross sense the experimental data, particularly for cross sections, do resemble these amplitudes.

Now we turn to the slightly more subtle effects that are present in the full model. While the real or imaginary part of any given amplitude may only change a little, the changes have a big effect on observables and so it is essential to understand them if one wishes to confront actual data.

VI. PROPERTIES OF THE FULL MODEL

The amplitudes of the full model differ from naive amplitudes in two major (related) respects, both arising from the phase of M_{eff}. These are their phases and energy dependence. They affect most observables considerably, particularly polarizations and the shrinkage properties of cross sections. To understand real data it is essential to understand these effects.

In this section we isolate and examine four major aspects of the behavior of amplitudes absorbed by the procedure of Sec. III: (A) their phases, (B) shrinkage, (C) fixed-t s-dependence, and (D) fixed-s t-dependence. The purpose is to see, qualitatively and with physical arguments wherever possible, why the prescription of Sec. III produces amplitudes which behave in certain ways. When a particular aspect of the behavior is related to well known puzzles we try to show how the puzzle appears in the model and how the model deals with it when it can.

All the properties discussed below are consequences of the procedure of Sec. III.

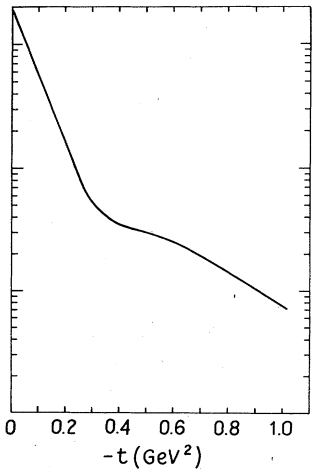

FIG. 6. This shows how combinations of the amplitudes of Fig. 5 (each with dips) can add to give featureless cross sections. Since the dip structure of amplitudes with $n=0$ or $n=1$ or $n=2$ is essentially orthogonal, it is fairly easy to pick out of a cross section how much of each is present. Here we only show $n=0$ and $n=1$ added, as for $0^-\frac{1}{2}^+ \to 0^-\frac{1}{2}^+$ reactions.

A. Understanding the phases of absorbed amplitudes

The phase behavior affects all helicity amplitudes, so we ignore spin in explaining it. Our amplitudes have the form

$$\mathrm{Re}M(s,t) = \mathrm{Re}R(s,t) + \int b\,db J_0(b\sqrt{-t})\{[\mathrm{Re}R(s,b)][\mathrm{Im}M_{\mathrm{eff}}(s,b)] + (\mathrm{Im}R)(\mathrm{Re}M_{\mathrm{eff}})\} \tag{6.1}$$

$$\mathrm{Im}M(s,t) = \mathrm{Im}R(s,t) + \int b\,db J_0(b\sqrt{-t})\{[\mathrm{Im}R(s,b)][\mathrm{Im}M_{\mathrm{eff}}(s,b)] - (\mathrm{Re}R)(\mathrm{Re}M_{\mathrm{eff}})\} \tag{6.2}$$

With our conventions, $\mathrm{Im}M_{\mathrm{eff}}(b) < 0$ for all b, while $\mathrm{Re}M_{\mathrm{eff}}(b)$ is mainly positive where absorption effects are most important (see Fig. 7), opposite to $\mathrm{Im}M_{\mathrm{eff}}$.

If $\mathrm{Re}M_{\mathrm{eff}} = 0$ as in old approaches which do not take account of the Pomeron phase, the second terms in each bracket are missing and we have the standard result, with destructive interference caused by absorption since $\mathrm{Im}M_{\mathrm{eff}} < 0$.

Let us first consider vector meson exchange for which $R \sim e^{-i(\pi/2)[\alpha(t)-1]}$. Then Re$R$ and ImR have the same

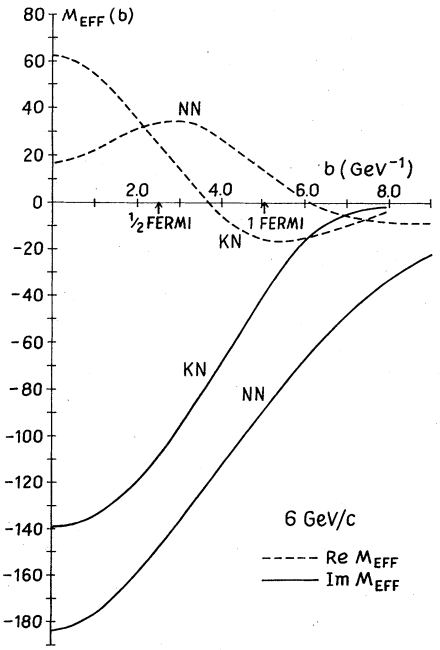

FIG. 7. The real and imaginary parts of M_{eff} (b) are shown for KN and NN scattering. The unitarity limit on M is $4\pi s$. Note that ReM_{eff} is opposite in sign to ImM_{eff} over the important b values for absorption.

sign, so the Reggeon is in the first or third quadrant; assume the first for definiteness. For ReM we have, showing relative signs

$$\mathrm{Re}M \sim \mathrm{Re}R + \int (\mathrm{Re}R\mathrm{Im}M_{\mathrm{eff}} + \mathrm{Im}R\mathrm{Re}M_{\mathrm{eff}})J_0(b\sqrt{-t})b\,db \qquad (6.3)$$
$$+ \quad - \quad + \quad +$$

so the added contribution due to $\mathrm{Re}M_{\mathrm{eff}}$ tends to cancel the conventional contribution and to reduce the absorption in ReM.

This has two important practical effects. First, in the real parts of $n=1$ vector exchange amplitudes, such as in $\pi^- p \to \pi^0 n$, this contribution rotates an amplitude which would have a single zero at $-t \simeq 0.5$ into one with a double zero structure (i.e., two nearby or coincident zeros), because the second term has an increasingly important positive contribution at larger t. This is what has been observed in analyses of πN scattering, and it is like the behavior of the real part of the pole itself in an exchange degenerate theory. A similar effect is present for $n=0$, with the double zero closer in because the absorption is stronger for $n=0$.

Second, in the $n=0, x=2$ amplitude which has the dramatic small t peaks in $np \to pn$, charged pion photoproduction, etc., the same effect operates. At $t=0$ we can conveniently write the integrals over t, so that

$$\mathrm{Re}M(s,t) \sim \int dt[\mathrm{Re}R(s,t)\mathrm{Im}M_{\mathrm{eff}}(s,t) + \mathrm{Im}R\mathrm{Re}M_{\mathrm{eff}})] .$$

Since $R(s,t) \sim t$ because $x=2$, the important contributions come from t away from zero, and $\mathrm{Re}R(s,t) \sim \sin\pi\alpha/2$ has a zero at $t \sim -0.5$. Thus the relative contribution of the second term is enhanced, and there is significant suppression near $-t=0$ for odd-signature exchange in the real part of the $n=0, x=2$ amplitude. (This is just the opposite of the even-signature case, with the π (and A_2) having sharper peaks, because the two contributions to the real parts add and the imaginary parts are suppressed.)

Experimentally this result helps solve a well known problem. It has long been known that $d\sigma/dt$ at $t=0$ was equal for $\gamma p \to \pi^+ n$ and for $\gamma n \to \pi^- p$, and for $np \to pn$ and $\bar{p}p \to \bar{n}n$. These reactions had the sharp "π-exchange" peak. The same mechanism that produces the peak in the π contribution would, it was thought, also produce a peak in the ρ contribution. The ρ would interfere oppositely for $\gamma p \to \pi^+ n$ and for $\gamma n \to \pi^- p$, and oppositely for $np \to pn$ and for $\bar{p}p \to \bar{n}n$.

Thus one would have found differences between these cross sections of perhaps 50% at $t \approx 0$, as well as away from $t \approx 0$, contrary to experiment. With the present mechanism, 10% differences can be obtained. This problem is solved here, automatically, by the same mechanism that gives the double zero to the real parts of the πN amplitudes, and that solves the shrinkage problem too (see below). In addition, the destructive interference for odd-signature real parts of amplitudes becomes a constructive one for even-signature real parts of amplitudes, enhancing the π and A_2 contributions and building up a large peak with reasonable numbers. In the imaginary parts of odd-signature amplitudes (such as ρ) the effect is automatically opposite, moving the zero closer to $t=0$ and producing a satisfactory cross over zero. This illustrates how one can obtain an imaginary part zero closer to $t=0$, and a real part zero further out, without introducing unsatisfactory analyticity properties for some amplitudes. To see this in detail, just put the signs from Eq. (6.3) into (6.2) and see that the two contributions add.

The phase structure has a number of other roles to play, especially in polarizations. Those discussed above are the main qualitative results of which we are aware.

B. The shrinkage properties of absorbed amplitudes

If two single contributions have exponential behavior in t with slopes B_1 and B_2, their double scattering has a slope

$$B_1 B_2/(B_1+B_2) ,$$

as illustrated in Eq. (5.15). Thus an absorbed Reggeon would have about half the slope of the Reggeon pole, and about half the shrinkage. This was the behavior of the absorption models studied before 1972.

In the model of HK and the present work the situation is quite different. The effect again arises from the energy dependence and phase of the Pomeron amplitude. The point is somewhat subtle, and some incorrect statements have appeared in the literature (including conference rapporteurs), so we discuss it in some detail here.

To understand what happens, consider the following typical calculation. This is not a modification of our general procedure, but a simplified example to see what happens more easily. Let the Reggeon pole be

$$R(s,t) \simeq s^{\alpha(t)} = s^{\alpha_0} e^{(\alpha' \ln s)t}$$

and, for example, consider the edge part of M_{eff},

$$M_{\mathrm{eff}} = -isAe^{Bt}J_0(R\sqrt{-t}) + \cdots . \qquad (6.4)$$

Then the absorption calculation can be done analytically and gives

$$M(s,t) = R(s,t) - \frac{As^{\alpha_0}}{8\pi(B+\alpha'\ln s)} \exp\left[\frac{B\alpha'\ln s}{B+\alpha'\ln s}t\right] \times J_0\left(\frac{\alpha'\ln s}{B+\alpha'\ln s}R\sqrt{-t}\right) e^{-R^2/4(B+\alpha'\ln s)} + \cdots \qquad (6.5)$$

and $R^2 = R_0^2 \ln s$. Numerically, say $B \approx \alpha' \ln s$. The pole has shrinkage characterized by α'. Thus the absorption correction has shrinkage with the coefficient of t ln$s$ given by

$$\frac{B}{B+\alpha'\ln s}\alpha' + \left(\frac{\alpha'\ln s}{B+\alpha'\ln s}\right)^2 \frac{R_0^2}{4} \qquad (6.6)$$

at small t. Numerically the two terms are comparable; the first is the usual slope and the second arises from the shrinking Bessel function. *At larger t the absorption term continues to get shrinkage both from the exponential and from the increasing radius of the Bessel function, so that the absorption correction has a shrinkage similar to that of the pole.*

This is a general property of the model. Basically, the full amplitude has a pole-like shrinkage. Further, the factor $\exp[-R^2/(4B+4\alpha'\ln s)]$ decreases with s signi-

ficantly at medium energies, so it lowers the effective absorption strength and simulates shrinkage. Experimentally, whenever a single amplitude has dominated, a pole-like shrinkage has been observed, and it is a strong point of our approach that it can have this behavior.

Assuming that at very high energy $B \simeq \beta' \ln s$, even then the amplitude has a slope

$$\left(\frac{\alpha'\beta'}{\alpha'+\beta'}+\frac{\alpha' R_0^2}{4\alpha'\beta'}\right)\ln s$$

from the absorption and $\alpha' \ln s$ from the pole. For $\alpha' = \beta' = R_0^2/4$ each piece has the same shrinkage.

Thus the shrinkage properties of the absorbed amplitude are complicated, but it will always have more or less pole-like shrinkage in a given amplitude, even at very high energies.

The shrinkage properties are illustrated in Fig. 8, drawn for the ρ exchange in $\pi N \to \pi N$. Figure 8(a) shows the nonflip pole vs t at $P_L = 2$, 6, 25, and 100 GeV/c. The shrinkage is obvious, and clearly $\alpha_{\text{eff}} \simeq 0$ at $-t = 0.65$ GeV^2. Figure 8(b) shows the same thing for the absorption correction, and it is apparent that the absorption correction has a shrinkage similar to that of the pole.

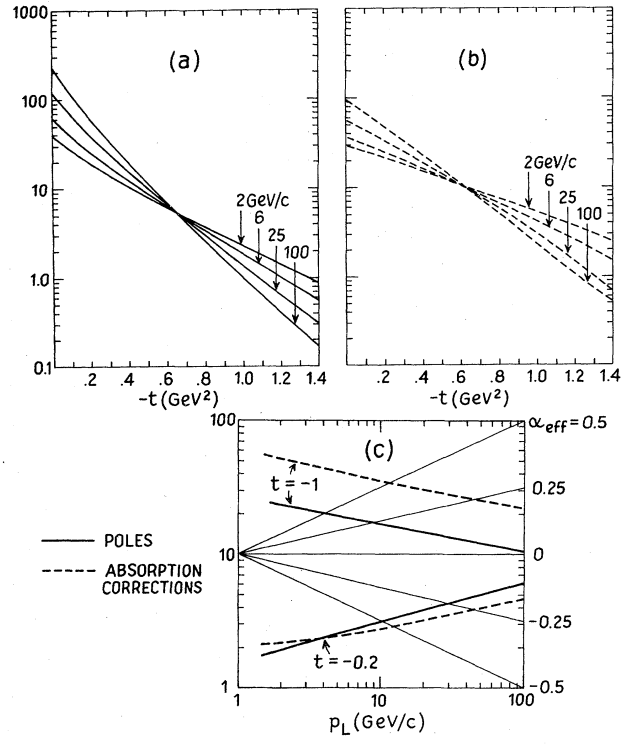

FIG. 8. This figure shows that in our model the absorption correction and the pole have about the same amount of shrinkage: (a) shows the pole vs t at four energies (2, 6, 25, 100 GeV/c); and (b) shows the absorption correction for the same s,t values. The lines cross in each case where the effective trajectory is zero, since the amplitude shown goes as s^{α}. It is apparent that the absorption correction shrinks approximately as the pole does; (c) shows the fixed t energy dependence at $-t = 0.2$ and 1.0 GeV^2, showing explicitly that pole and absorption correction have about the same effective trajectory.

The effective trajectory for the absorption correction also has $\alpha_{\text{eff}} \simeq 0$ at $-t = 0.65$ GeV^2. Figure 8(c) shows the fixed $-t$ energy dependence, so one can see that the pole and the absorption correction have about the same effective trajectory at $-t = 0.2$, 0.6, and 1.0 GeV^2.

Thus the old problem of too little shrinkage from absorption is not present in our approach, because of the Pomeron shrinkage. As we remarked, this was already qualitatively true for HK, but we have gone into some detail here because a number of people have had mistaken impressions.

When more than one amplitude is present for a given exchange somewhat less shrinkage will appear, as each amplitude will have regions of s and t where interferences are important and shrinkage is less. When several exchanges are present as well, different ones can dominate in different t regions and one can obtain a large variety of shrinkage patterns. In each case one can understand the result by noting which exchange is important in each region of t and what its effective energy dependence is there (see next section).

C. The effect of absorption on energy dependence

In certain regions of t for certain amplitudes the energy dependence of absorbed amplitudes can change dramatically from that of the pole. This often has rather direct implications for understanding experiment. Since energy dependence is one of the standard techniques used to identify exchanges, it is important to understand qualitatively what happens.

First consider $t = 0$, and the vector (ρ and ω) exchanges, relevant to total cross-section differences, etc. Relative to the pole, absorption is a destructive interference which decreases in strength with increasing energy, so it raises the effective intercept. Figure 9 shows how the effect depends on reactions, i.e., on the different absorption associated with different external particles. The ω contribution [$\alpha_\omega(0) = 0.3$] has an effective *phase* intercept of 0.38 in KN and of 0.44 in NN, at 10 GeV/c. (One could calculate an effective "energy" intercept from s^{α_0}, or an effective "phase" intercept from knowing ImM/ReM.) This figure and

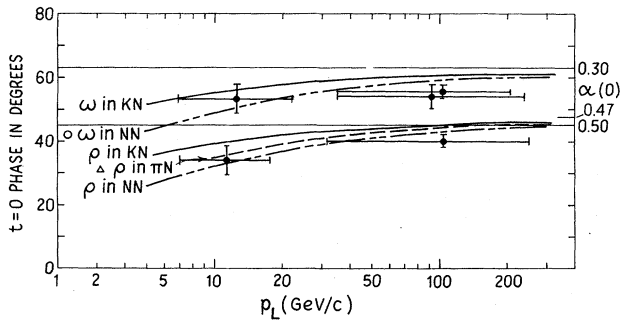

FIG. 9. The $t = 0$ energy dependence of ω,ρ exchanges in NN, KN, πN in the imaginary part of the nonflip amplitude is shown. The poles have an intercept $\alpha_\omega(0) = 0.3$, $\alpha_\rho(0) = 0.47$, and the associated phase. The absorbed amplitudes have an effective intercept which is higher and approaches the pole asymptotically. Data is from Carroll *et al.* (1975) plus B. Winstein (private communication) for KN.

the following ones are drawn for the actual amplitudes which give data fits.

At typical energies a given exchange will have real differences in energy dependence in different reactions. The effect will be different for different amplitudes and for the real and imaginary parts of each amplitude. Figure 10(a) shows the energy dependence of both $\mathrm{Im}\varphi_1$ and $|\varphi_1|$, the nonflip NN amplitude, for ρ exchange. Below 20 GeV/c or so $\mathrm{Im}\varphi_1$ clearly rises faster with s than $|\varphi_1|$. Asymptotically, of course, all energy dependence approaches that of the pole.

Each amplitude of different n or x is affected differently, in a way that varies with t. That is because the absorption has the same b dependence for all amplitudes, while for kinematic reasons the poles of different n,x have different b dependence and thus feel absorption differently. One effect is that the greater the n the faster the pole vanishes as $b\to 0$, and thus the less it feels the absorption (which removes at small b). Thus higher flip amplitudes at small t show mainly pole-like behavior.

Figures 10(a)–(c) show the energy dependence of different amplitudes for a given exchange, mainly for ρ exchange in NN reactions. In a pole model, all ρ exchange contributions would have the same s dependence, while here there are marked differences. The reader can

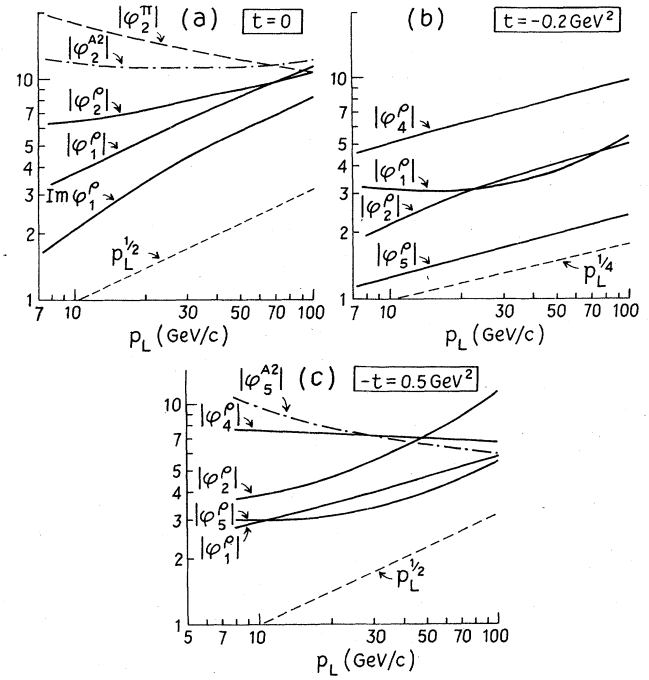

FIG. 10. The energy dependence at fixed $t=0$, -0.2, and -0.5 GeV^2 is shown for a number of exchanges and NN amplitudes. Here φ_5 is a single flip, $n=1$, analogous to M_{+-} for $0^-\frac{1}{2}^+$ reactions; φ_1 is nonflip, $n=0$, analogous to M_{++}; φ_2 has $n=0$, $x=2$ and φ_4 has $n=2$, $x=0$. The amplitudes are normalized to grow as s^α if the only contributions are poles. Many aspects of relative and absolute energy dependence can be read off. Note, for example, that $|\varphi_2^{A_2}|$ dominates over $|\varphi_2^\pi|$ beyond about 75 GeV/c; that will determine the high-energy forward structure in $\gamma p\to\pi^+ n$ and $np\to pn$. $\mathrm{Im}\varphi_1^\rho$ grows faster than $|\varphi_1^\rho|$ at low energies since the imaginary part of vector exchange feels absorption more and has a higher effective trajectory.

estimate the energy dependence of any reaction by seeing what amplitudes dominate and using the results for the analogous one here.

One could make many points about these figures. We will just note a few. At medium energies at $t=0$, $\mathrm{Im}\varphi_1^\rho$ increases most rapidly, then $|\varphi_1^\rho|$ which has $\mathrm{Re}\varphi_1^\rho$ too, and then $|\varphi_2^\rho|$. The latter is down by powers of const $+\ln s$ because it is wholly given by absorption. Similarly, $|\varphi_2^\pi|$ falls with s rather than going like s^0, and $np\to pn$ and $\gamma p\to\pi^+ n$ have π-like energy dependence only because some ρ and A_2 are mixed in.

In dip regions, one finds first a more rapid fall with s at fixed t, and then a rapid rise as the dip position moves by. Interpreting energy dependence in dip regions is subtle. Often $\alpha_{\rm eff}$ arguments are misleading.

[In general, one can see fairly simply how amplitudes with different n,x depend on energy. Carrying out a calculation like the one in Sec. V.A, where $M_{\rm eff}$ and the Reggeon are approximated by exponentials in t apart from the correct kinematic factors, and noting that poles with $x\neq 0$ have extra powers of t which can always be replaced by derivatives with respect to α', one can avoid more extensive numerical calculations and obtain an approximate expression for the absorption correction (Henyey and Kane, 1975)

$$M_{n,x}(s,t)-R_{n,x}(s,t)\simeq\frac{-\Sigma R_0}{4\pi}\left(\frac{s}{s_0}\right)^{\alpha_c(s,t)}[-K(s)t]^{n/2}P_{n,x}(s,t)Y^{1+n/2+x/2}, \tag{6.7}$$

where

$$\begin{aligned}
&R_{n,x}(s,t)\simeq R_0(-t)^{(n+x)/2}\left(\frac{s}{s_0}\right)^{\alpha_0}e^{\alpha_R' t\ln(s/s_0)},\\
&M_{\rm eff}(s,t)\simeq is\Sigma e^{Bt},\\
&B=B_0+\alpha_p'\ln(s/s_0),\\
&Y=B_0+(\alpha_p'+\alpha_R')\ln(s/s_0),\\
&K(s)=B^2/Y,\\
&\alpha_c(s,t)=\alpha_0+Bt/Y,
\end{aligned} \tag{6.8}$$

and $P_{n,x}$ is a polynomial in Kt with $P_{n,0}=1$, $P_{n,2}=n+1-K(s)t$. Using reasonable approximate values for the quantities involved, one can see what energy dependence is expected for absorption corrections and for absorbed amplitudes. For pp scattering, one might use $B_0=5$ GeV^2, $\alpha_p'=0.3$ GeV^{-2}, $s_0=\frac{1}{10}$ GeV^2, $\alpha_R'=1$ GeV^{-2}, $\Sigma\simeq 1.5\sigma_T$. Each Reggeon considered has its characteristic α_0. Details of the s dependence, especially shrinkage, will not be too good with such a simple form, but approximate trends will be right and one can see simply how much the energy dependence will deviate from the pole form.]

Additional energy dependence effects have been discussed by Kane (1973, 1974), and some will be mentioned in context below.

D. The t dependence of amplitudes

The real content of our approach, and the aspect which ideally will be tested against experiment, is the s and t

dependence of amplitudes. Comparison with experiment at present also requires specifying coupling strengths to combine amplitudes into observables, and often measures differences of large numbers when several contributions are involved, so much is being tested besides the direct individual amplitude behavior.

Here we show a number of amplitudes. One use of Figs. 11-13 is for the reader who is using our method to check that he is calculating correctly. Another is that he can visualize the behavior of the amplitudes which go into constructing different observables, and understand why the observables behave as they do.

It is important to remember that we expect the amplitudes to have a certain universality. Approximately, amplitudes with given n, x values and given pole characteristics (e g., all vector meson exchanges with similar intercept) will have the same amplitudes in all reactions. Small differences will occur, and are automatically part of the procedure of Sec. III, due to (i) exchange degeneracy breaking in the trajectory, as for $\alpha_\rho(0) - \alpha_\omega(0) \simeq 0.15$, (ii) differences in the Regge residue expected from different t-channel intermediate states (e.g., the ρ should have a steeper residue than the ω because it couples to a 2π t-channel state), and (iii) differences in the strength of absorption for different external particles.

Figures 11–13 show a number of amplitudes for KN and NN reactions. By comparison of different parts one can see the approximate universality.

We restrict ourselves to a few comments:

(1) The full amplitudes have approximately the behavior expected of exchange degenerate ones. This is in keeping with our view (Sec. IV.A) that the evidence and arguments for exchange degeneracy and for phenomenological duality should apply to the full amplitudes and not the poles. The K^+N amplitudes $(A_2+\rho)$ are mainly real at small t, the K^-N amplitudes $(A_2-\rho)$ rotate in phase, the real part of the ρ amplitude has a "double zero" structure near $-t = 0.5$ GeV^2, etc.

(2) Tensor exchange is $\pi/2$ out of phase with vector exchange due to signature, so qualitatively $\mathrm{Re}T \to \mathrm{Im}V$, $\mathrm{Im}T \to -\mathrm{Re}V$, except that tensor exchange is more central so its scale in t is expanded.

(3) The ω and ρ amplitudes are almost the same. They differ slightly as mentioned above, but clearly they represent the same underlying physics. Remarkably, however, they give rise to quite different polarizations! These are shown in Fig. 14. Fortunately, they are observable too, as the ρ exchange gives the $\pi^-p \to \pi^0 n$ polarization, while the ω exchange essentially gives the polarization in $\gamma p \to \pi^0 p$. It has been a puzzle why these two apparently identical reactions given exchange degenerate ρ, ω should behave differently experimentally (Worden, 1972), and we see here that a tiny difference in amplitudes can produce the observed effects. The reader can easily see what happens by drawing a few Argand diagrams at $-t$ near 0.3 GeV^2. It is all a question of whether the real part of the flip amplitude goes negative or not, i.e., whether its two zeros are a little separated or coincident.

(4) It has often been remarked that $n = 1$ (flip) amplitudes showed pure Regge pole behavior, or at least that one could assume that they did without violating data. In fact, there is strong circumstantial evidence to the contrary, and amplitudes with the absorption characteristics shown here are consistent with experiment. Some evidence is summarized by Worden (1974) for ω and K^*,

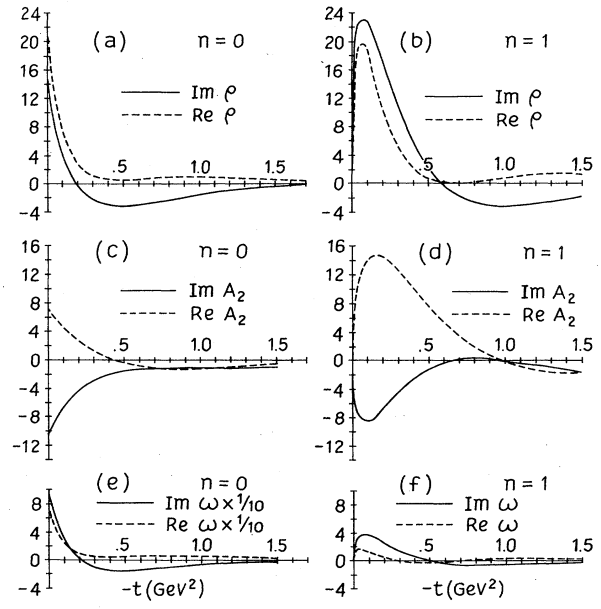

FIG. 11. Amplitudes are shown for ρ, ω, A_2 in KN at 6 GeV/c. They are normalized as in the text and dimensionless. Note that the real parts of the ρ amplitudes do not go negative, while the real parts of the ω flip amplitudes do go negative, which is a small effect in the amplitudes with a large effect in the observables. See discussion in the text, VI.D, and Fig. 14.

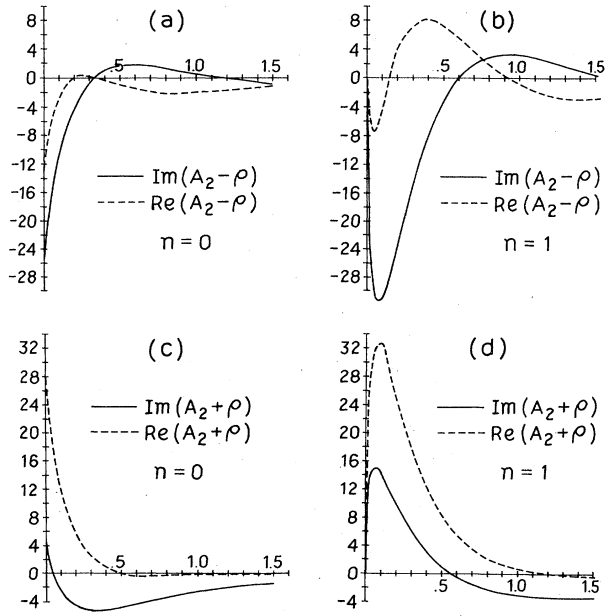

FIG. 12. Amplitudes for $A_2 \pm \rho$ in KN at 6 GeV/c. These correspond to the charge exchange reactions $K^+n \to K^0p$ and $K^-p \to \bar{K}^0 n$, and to "real" and "rotating" processes in general.

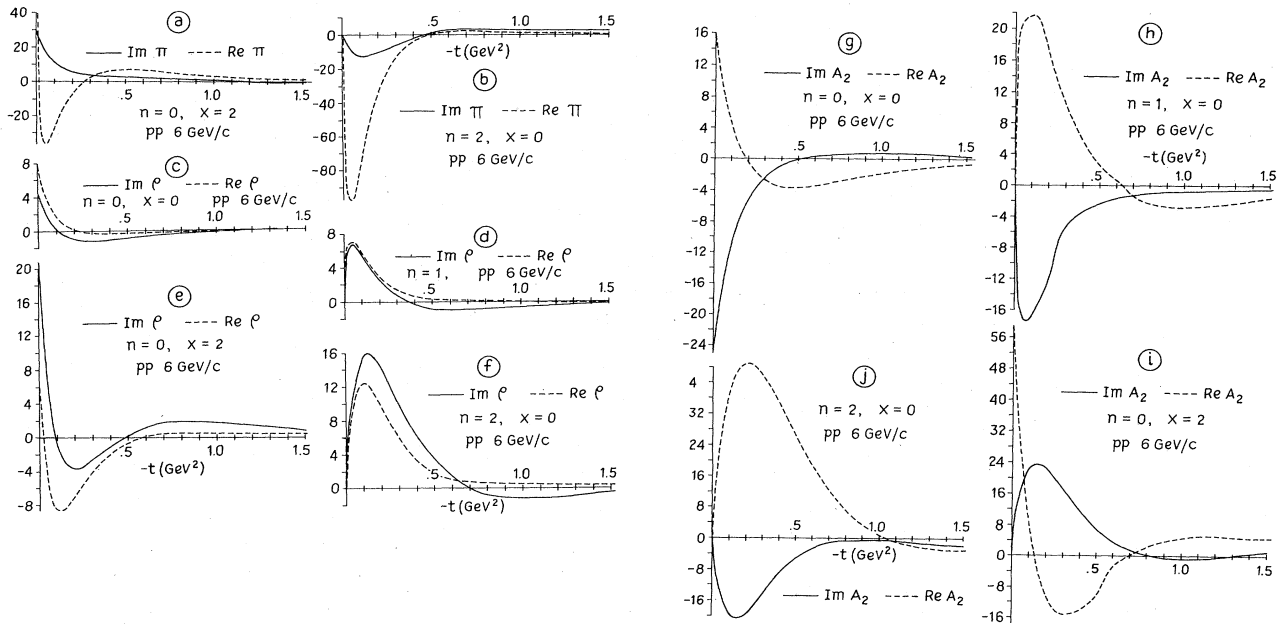

FIG. 13. Amplitudes in pp at 6 GeV/c, including π exchange. By comparing different exchanges and the same exchange in KN and NN, one can understand quite a lot of the variation and complexity of data.

K^{**} contributions. The size of $P(np \to pn)$ and the zero structure of $P(pp \to pp)$ and $P(np \to np)$ are further evidence, and the dip in the pure $n=1$ π exchange observable $\rho^s_{00} d\sigma/dt$ for $\pi N \to \rho N$ is still more. Hopefully, people will stop making the "pure Regge pole" assumption, which produces unfortunate biases in any subsequent analysis.

In Sec. VI we have tried to illustrate how individual absorbed amplitudes would behave. Now we turn to applications. First we consider in Sec. VII several kinds of properties, such as polarizations, line-reversed reactions, and various regularities. Then in Sec. VIII we treat specific reactions.

VII. GENERAL FEATURES OF DATA

In this section we try to describe how one can understand features of data in a way organized around the separate features, rather than reaction by reaction. In this way, one can to some extent obtain a unified view of the situation. In Sec. VIII specific reactions are emphasized.

A. Polarizations

Here we give in one place a brief description of why polarizations P for common reactions behave as they do. We cover $\pi^- p \to \pi^0 n$, $\pi^\pm p \to \pi^\pm p$, $K^\pm p \to K^\pm p$, $pp \to pp$, $\bar{p}p \to \bar{p}p$, $np \to np$, $np \to pn$ explicitly. For other reactions the arguments are usually direct transpositions of one of these.

First consider the forward elastic reactions. Then the polarization is essentially the interference between the imaginary part of the nonflip amplitude (call it N) and the real part of the flip (call it F). For $\pi^\pm p$, F is dominated by the ρ, so the polarizations have the mirror-symmetric double zero. N is dominated by the Pomeron, P. Both $\mathrm{Im}P \times \mathrm{Re}\rho$ and $\mathrm{Re}P \times \mathrm{Im}\rho$ are important, and both contain a "double zero." ImP is monotonic, while Reρ has a double zero from absorption (see Sec. VI.A). Imρ and ReP both have a single zero near -0.6 GeV^2. In both cases the double zero arises from the effect of ReP, once from its effect on the absorption and once from its zero. For K^+p, F is dominated by the real part of the Reggeon amplitude, so the polarization is large at small t, while for K^-p, F is mainly imaginary at small t and the polarization starts out

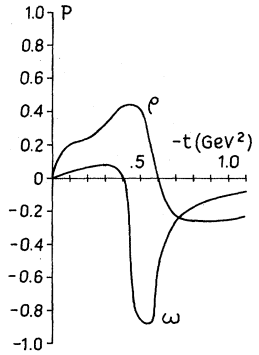

FIG. 14. This shows polarizations computed with the ω exchange amplitudes of Fig. 11(e), 11(f), and with the ρ exchange amplitudes of Fig. 11(a), 11(b) (with sizes adjusted to resemble flip dominance for the ω). The huge difference in polarizations arises mainly from the small difference between the real parts of the $n=1$ amplitudes. The ω polarization resembles that in $\gamma p \to \pi^0 p$, while the ρ resembles that in $\pi^- p \to \pi^0 n$, thus explaining why these two reactions can have very different behavior with exchanges that are very similar. The ρ polarization here can be compared with the $\pi^- p \to \pi^0 n$ polarization of Fig. 24, to see the differences caused by having different external particles. These points are discussed in the text in detail.

slowly. Since ReF has an absorption zero for $-t \lesssim 1$ GeV^2 for K^+p and ImN is nonzero to large t for K^+p, the polarization $P(K^+p)$ is expected to show a single zero near $-t=1$ GeV^2.

The $pp \to pp$ case is instructive. ReF is given by the Reggeons and has the expected absorption zero near $-t \sim 0.7$ GeV^2. Here, however, we know that σ_T decreases with s (as opposed to K^+p) and consequently that ImN has important Reggeon contributions. They can be thought of as an exchange degeneracy breaking effect if one likes. These contributions have the absorption zero at $-t \sim \frac{1}{4}$ GeV^2, so they interfere constructively with the Pomeron at $t=0$ and destructively for $-t \gtrsim \frac{1}{4}$ GeV^2. By itself, Im (Pomeron) would have a zero at $-t \simeq 1.4$ GeV^2. The Reggeon contributions interfere destructively and move the zero in ImN to $-t \sim 0.8$ GeV^2 at lower energies, giving the double zero structure in $P(pp)$ at that t. But as the energy increases the Reggeon contribution gets less important and the zero in ImN moves out toward -1.4 GeV^2. Then between the zero in ReF at $-t \sim 0.7$ GeV^2 and the zero in ImN, $P(pp)$ will go negative. This seems to be observed at 40 GeV/c. In contrast, for $K^+p \to K^+p$, ImN has no zero because the Reggeon contribution is smaller (σ_T is flatter) and the diffraction zero is much further out, so $p(K^+p)$ has only a single zero.

At high energies another effect (Pumplin and Kane, 1975) will be important. Essentially, diffraction (thought of as the shadow of inelastic production) will occur in helicity flip amplitudes too. These will be mainly peripheral. Higher helicity flip amplitudes will behave for net helicity flip n like

$$J_n\{R[-t(\ln s - i\pi/2]^{1/2}\} \tag{7.1}$$

and will generate polarization in NN (and ΛN, ΣN, πN, KN, etc.) at arbitrarily high energies. The results are shown for pp at several energies in Fig. 15. At 300 GeV/c, there is still a contribution from the Reggeon–Pomeron interference, which is about 20% of the diffractive one at $-t<1$ GeV^2, but gets large in the dip region where the Reggeon contribution (mainly real) and the Pomeron (mainly imaginary) became comparable in size as Im(Pomeron) approaches its zero. The large polarization in the dip region and the filling in of the dip in $d\sigma/dt$ as s decreases are related effects, both due to the real part of the amplitide, especially the Reggeon contributions.

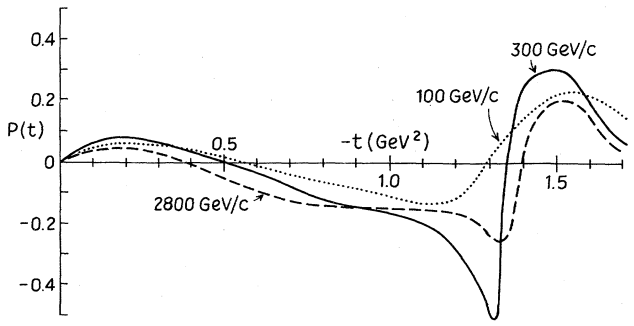

FIG. 15. Predictions for high-energy polarizations. These are for $pp \to pp$, and similar predictions hold with some changes in scale for $\Lambda p \to \Lambda p$, $\Sigma p \to \Sigma p$, etc. They are a sum of Reggeon contributions which decrease with energy, plus "Pomeron" helicity flip contribution (see text). The large polarization in the dip region is expected in general as the imaginary part of the nonflip amplitude has a zero. Its maximum size is sensitive to the size of the nonflip real part, but at some energy in the 100–400 GeV/c range, it will be quite large. Note that it is largest somewhat away from the dip, where the cross section is not too small, so it is probably measurable.

Next consider reactions where the polarization is generated by absorption of a single exchange and no Pomeron piece is present, such as $\pi^-p \to \pi^0n$. As is widely known, if only a single definite signature exchange were present (the ρ in this case) it would have the same phase in both N and F and would give $P=0$. When absorption is present, it affects N more than F (because F vanishes at $b=0$ from kinematics). Absorption also affects real and imaginary parts of amplitudes differently, since they have different impact parameter structure. Thus N is rotated more by absorption than F is, and polarization is generated proportional to the angle between N and F on an Argand diagram such as Fig. 16. These arguments apply at small t, before zeros occur, and require a definite sign of P there. As $-t$ increases the real and imaginary parts of the amplitudes are having zeros and one must trace the amplitudes out in order to understand the polarization. For example, in $\pi^-p \to \pi^0n$ if ReN and ReF both have a double zero structure and stay positive, then between the zero of ImN near -0.2 and that of ImF near $-t=0.6$ the amplitudes are in different quadrants and P could get sizeable. After ImF has its zero, beyond $-t$ near 0.6, both amplitudes will be in the fourth quadrant and P will be small. But if ReN also has a zero then N will go into the third quadrant while F is still in the first. Then at some t between 0.2 and 0.6 the two amplitudes will differ in phase by $\pi/2$ while F is decreasing in size toward a dip, and P will get quite large. If ReN has a zero before ImN then there is also a sign change and P gets large and negative. By such arguments one can understand each reaction with one or two similar exchanges.

It is instructive for pedagogical purposes to consider what kinds of information can be gained from the behavior of the polarization. One example was given in Sec. VI.D comparing $\gamma p \to \pi^0 p$ and $\pi^-p \to \pi^0 n$, and ω and ρ exchange. As another, suppose that the absorption were such that ReN had a zero at smaller t than ImN (as would happen with the naive absorption ignoring the

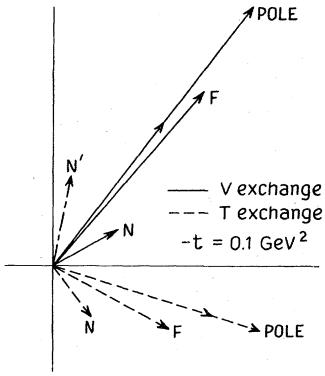

FIG. 16. Amplitude pictures, for the discussion of Sec. VII.A.

Pomeron phase). Then N would rotate into N' in Fig. 16. When N and F were parallel P would have a zero. Since ImN would have a zero soon afer ReN, N' would quickly rotate to point along the negative real axis. At some point in the second quadrant one would have N' and F perpendicular and P would get large and negative. This possibility is ruled out by both the Argonne and CERN–Saclay experiments, and we directly learn the important lesson that ImN has a zero at smaller $-t$ than ReN. It is much harder to learn more from the data. Once we know which way N, F rotate, it becomes a question of the detailed rate of rotation. Polarizations are very sensitive to details, and a theory which gives qualitatively correct amplitudes could give polarizations that are numerically quite wrong. Similarly, getting polarizations correct may not be a real indication of the validity of a theory. It may be that good polarization data help most to convert a qualitatively good theory into a precise one. To decide in a given situation whether polarization measurements are of general or of detailed significance is of course hard; if it can be done at all it is by carefully studying alternatives for amplitude behavior.

Finally we look at polarization in $np \to pn$ and $\bar{p}p \to \bar{n}n$. The situation will be analogous in $\gamma p \to \pi^+ n$ and $\gamma n \to \pi^- p$ and in many line-reversed pairs. In a sense these polarizations, especially $np \to pn$, are one of the major features that any model must explain if it is to be taken seriously, as they depend on the properties of ρ and A_2 exchanges (which we should understand) in a situation where both P and $d\sigma/dt$ are measured for a line-reversed pair. The cross-section behavior is discussed in Sec. VIII.C; here we concentrate on $P(np \to pn)$, which has a simple interpretation.

For $np \to pn$, P is given by Eq. (A37) with $\varphi_5 \equiv \varphi_5'$,

$$P d\sigma/dt \sim 2\mathrm{Im}(\varphi_1 + \varphi_2 + \varphi_3 - \varphi_4)\varphi_5^* . \tag{7.2}$$

The detailed properties of the NN amplitudes are given in the Appendix. Here we note that an unnatural parity π or B *pole* contribution always flips s-channel helicities so it does not contribute to φ_1 or φ_3 or φ_5, and it contributes equally to φ_2 and φ_4, so it does not contribute to P. Since absorption affects φ_2 and φ_4 differently, the absorption correction to $\varphi_2 - \varphi_4$ for π and B does not vanish and gives a small and slowly varying "background" contribution. It mainly affects whether P is a little positive or a little negative at small t. The important contributions to P come from ρ and A_2. Since pp is an exotic channel, some physicists would say that $\rho + A_2$ is mainly real in all amplitudes, and would remain so even with absorption by an imaginary Pomeron, so P would be expected to remain quite small. In fact, $P(np \to pn)$ is large over a long range in t; often $P \gtrsim 0.5$, making it one of the largest polarizations measured in hadron physics. Approaches which begin from exchange degenerate poles may have a difficult time in understanding $P(np \to pn)$; so far none have been able to do so.

From our point of view the explanation is as follows. First consider φ_5. It is a typical $n=1$ amplitude. At small t it is mainly real, say along the positive real axis. As $-t$ increases, Imρ decreases and goes negative after a while, ReA_2 behaves similarly, so φ_5 rotates slowly from the positive real axis down to the negative imaginary axis as $-t$ goes from 0 to 1 GeV^2.

Next consider φ_1 and $\varphi_2 - \varphi_4$. For any sum of definite parity contributions, e.g., natural parity poles $\varphi_3 = \varphi_1$ including full absorption. Since φ_1 is an $n=0$ amplitude and is mainly negative real at $t \sim 0$, Re φ_1 will have an absorption zero at $-t \sim 0.2$ GeV^2. Thus φ_1 has swung to negative imaginary and over to the third quadrant by $-t \sim 0.2$ GeV^2.

At small t for natural parity poles $\varphi_2 - \varphi_4 \approx 2$(pole) $-$(absorption correction to φ_2). The poles in φ_2 and φ_4 vanish at $t=0$, so Re$(\varphi_2 - \varphi_4)$ behaves as shown in Fig. 17, with a zero in the real part at $-t \approx 0.05$ GeV^2. Thus both $\varphi_1 + \varphi_3$ and $\varphi_2 - \varphi_4$ have real part zeros at small t, with the sum having a real part zero at $-t \approx 0.2$ GeV^2. At this point $\varphi_1 + \varphi_3 + \varphi_2 - \varphi_4$ is negative imaginary, while φ_5 is just below the real axis, so P can be quite large. As $-t$ increases, both pieces now slowly rotate clockwise, keeping about $\pi/2$ apart, and P stays large. Note that *one crucial ingredient of the argument is the small t absorption zeros in the real parts of* φ_1 *and* $\varphi_2 - \varphi_4$; without these P is very small. The other part of the argument is the sign of Im$(\varphi_1 + \varphi_2 + \varphi_3 - \varphi_4)$. It is dominated by the sign of φ_1 because ρ and A_2 add there (Imρ is strongly absorbed while ImA_2 is weakly absorbed, since they have opposite signature), giving a large negative imaginary part, while in φ_2 the imaginary parts cancel. The sign choices and convention implied in the above argument, which give the sign of P correctly, can be obtained from those in the Appendix.

A similar set of arguments can be traced through for $\bar{p}p \to \bar{n}n$, etc. While the arguments are subtle enough to require some effort to follow them, each step is simply a matter of combining our standard amplitudes in the manner required by the spins, and so it is basically simple. The argument above cannot be simplified much and retain its validity, although a qualitative argument just says that $\varphi_1 + \varphi_3 + \varphi_2 - \varphi_4$ is dominated by net flip zero and is expected to be mainly real at $t \approx 0$, so the standard systematics about $n=0$ amplitudes is what we use.

More sophisticated "polarization" experiments, such as spin–spin correlations in $pp \to pp$, are discussed in the sections on each reaction.

B. Line-reversed reactions

Considerable effort has been given to studying line-reversed reactions, both experimentally and theoretically.

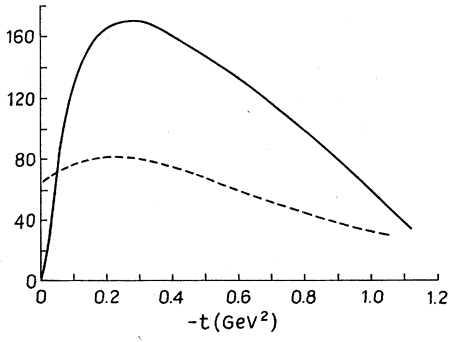

FIG. 17. Amplitude pictures, for the discussion of Sec. VII.A.

These are a pair of reactions where the particles at one vertex are just reversed so that a single exchange by itself will contribute equally to both, up to a sign. If two exchanges were incoherent, it would imply equal $d\sigma/dt$ for the pair; this is what would happen in an exchange degenerate pole model. Although the experimental situation is very confused by normalization problems, it appears in most cases that the line-reversed pairs are not behaving as the advocates of exchange degenerate poles would like, certainly not at a detailed level.

Here we want to see briefly how these reactions behave from our point of view, partially to understand better the implications of our approach, partially because one of the most unconventional predictions of our model appears here, and partially because line-reversed pairs of reactions such as $np \to pn$ and $\bar{p}p \to \bar{n}n$ give very strong constraints on any theory. For a detailed analysis of the predictions of models with exchange degenerate poles, see Fox and Quigg, 1973.

To understand what happens, examine Fig. 18, drawn for $np \to pn$ and for $\bar{p}p \to \bar{n}n$ so we can also see the role of the π below. A similar set of graphs shows what happens for any line-reversed pair. The graphs are all at $-t = 0.05$ GeV^2.

The particular amplitude shown is φ_4, which has $n = 2, x = 0$. The qualitative properties are the same for any SCHA. The magnitudes of some lines are shown in parentheses.

First draw the ρ and A_2 poles shown for NN. For $\bar{N}N$ the ρ pole changes sign. Since $\alpha_{A_2} < \alpha_\rho$ the A_2 is a little more real than the ρ is imaginary.

Next, form $A_2 \pm \rho$ to get the amplitudes for specific reaction; tensor + vector gives the amplitude for $K^+n \to K^0p$, $np \to pn$ (ignoring the π for the moment), and any exotic processes, while tensor-vector is for $K^-p \to \bar{K}^0n$, $\bar{p}p \to \bar{n}n$, etc. The angle between ρ and A_2 is $(1 + \alpha_{A_2} - \alpha_\rho)\pi/2$, which is less than $\pi/2$ since $\alpha_{A_2} < \alpha_\rho$, so it is always the case that $|A_2 + \rho| > |A_2 - \rho|$. Thus, for us, the pole for the "real" process is always greater in magnitude than the pole for the "rotating" process. Consequently, if absorption were not present, we would expect "real" cross sections to be larger than "rotating" ones.

The absorption correction to $A_2 \pm \rho$ is also shown in part (a); it is rotated somewhat more than π from the poles. Adding these contributions we get the full amplitudes. As shown here, the "real" amplitude is always absorbed more than the "rotating" one, so that the full amplitudes will always be closer in magnitude than were the poles. The magnitudes of poles and amplitudes (i.e., the lengths of the lines in the plot) are shown in parentheses in the figure. For our example, the absorbed amplitudes are about equal, so we would get equal line-reversed cross sections.

Next we have to consider the energy dependence because the effects of absorption change with s. Numerically, this is illustrated in the figure, with (a) showing the results at 8 GeV/c where the poles would give cross sections in a ratio of 1.55, while the full amplitude predicts a ratio of 0.94. Part (b) of the figure shows the results for 100 GeV/c, where the poles could give cross sections in a ratio of 1.46 while the amplitudes predict a ratio of 1.32. To understand what happens, next look at Fig. 19.

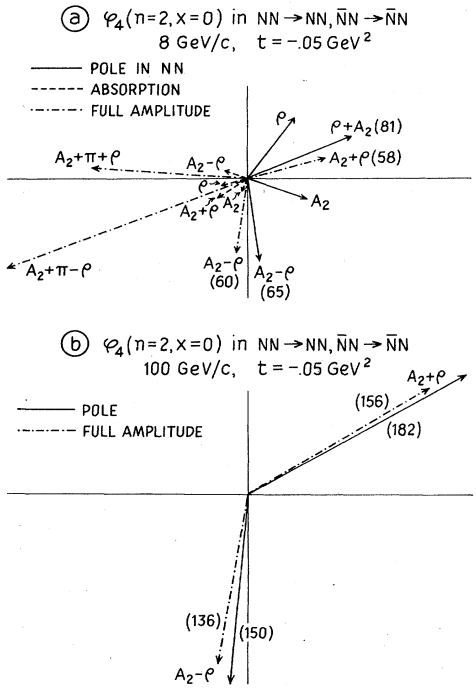

FIG. 18. Amplitude pictures, for the discussion of Sec. VII.D.

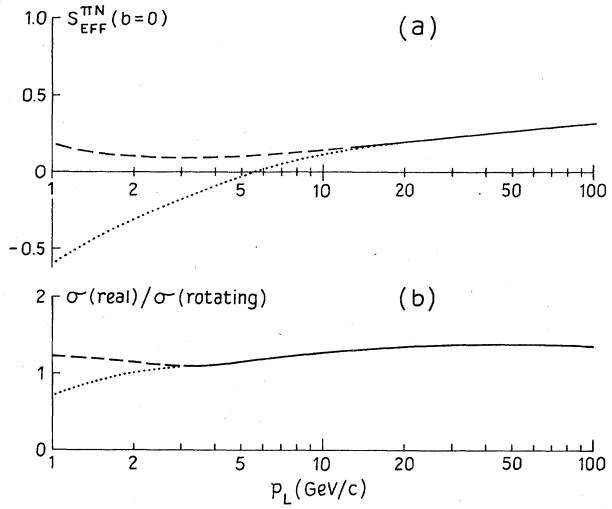

FIG. 19. $S_{\text{eff}}(b=0)$ is shown as a function of energy, for πN. Total absorption corresponds to $S=0$, and no absorption to $S=1$. The solid line, at higher energies, shows the behavior of our model, and the dotted line shows how it behaves at lower energies. The dashed line shows how it probably should behave at lower energies if the correct physics were present in the absorption down to threshold. In (b) the ratio of a "real" to a "rotating" cross section is shown [$\sigma(K^+n \to K^0p)/\sigma(K^-p \to K^0n)$ at $-t = 0.2$ GeV^2] vs energy, with curves interpreted as in part (a). That this ratio is significantly larger than unity is one of the most distinctive predictions we can make, and is one of the few places where different approaches to two-body reactions are completely different (see discussion in VII.B).

Starting at threshold, first unitarity limits suppress low partial waves. Then, as the energy increases, more inelastic channels open up and the amount of absorption increases. At higher energies the shrinkage of the Pomeron takes over and the effective strength of absorption decreases slowly. This is shown in Fig. 19(a), with the solid line giving the higher-energy behavior, the dashed line the low-energy behavior described above, and the dotted line the low-energy behavior of our model (which does not have in it the physics to make the absorption stop increasing near threshold.) The net result is that both reactions of a line-reversed pair are decreased in size by absorption, but the real one is decreased more, and the effect is maximal somewhere in the 5–10 GeV/c range. Consequently, at low energies the ratio of K^+n/K^-p cross sections has some value slightly larger than 1. As s increases the ratio decreases toward 1; whether it reaches 1 or stays somewhat above is model dependent. The ratio is a minimum somewhere in the 5–10 GeV/c range and then increases again perhaps to a value larger than 1.5. Finally, at very high energies, it decreases slowly. For typical numbers we get a result like that in Fig. 19(b).

This is one of our most important and distinctive predictions. It seems to clearly distinguish a model such as ours, with poles that are not exchange degenerate, from all models with exchange degenerate poles. For the latter case, the cross-section ratio observed at a given energy is necessarily closer to one than at a lower energy. For us, the ratio will behave as in Fig. 19b.

Currently, no high-energy measurements are available. The ratio for $K^+n \to K^0p$ and $K^-p \to \bar{K}^0n$ is observed to be about 1 at 5–10 GeV/c. If it should significantly exceed 1 at a higher energy, it will be very strong evidence for our viewpoint (and conversely). This is one of the few situations where qualitative experimental tests of different approaches are available, and it is feasible to carry out the experiments in the near future, for one of the pairs we have discussed or perhaps for $\pi^+p \to K^+\Sigma^+$ vs. $K^-p \to \pi^-\Sigma^+$.

Finally, look again at Fig. 18(a) and the dot-dashed lines which show the amplitudes when a pion contribution is added (e.g., for $np \to pn$ and $\bar{p}p \to \bar{n}n$, or for $K^+n \to K^{*0}p$ and $K^-p \to K^{-*0}n$). Because the π is mainly real, it just reverses the situation. Thus for reactions dominated by $T \pm V + \pi$ we expect the "rotating" reaction to have larger cross sections than the "real" one, as is indeed the case for $np \to pn$ vs $\bar{p}p \to \bar{n}n$ until the π contribution disappears with increasing energy.

Although the systematics of line-reversed processes are not trivial to understand, proceeding with Argand plots like the one in Fig. 18 allows one to see fairly simply what will happen. It is important to keep in mind, also, that the results discussed here are simply the implications of our model and the procedure of Sec. III spelled out in detail. This analysis illustrates how one can get an intuitive picture of the consequences of the model.

C. Relating reactions with different external particles

To work out the s and t dependence and size of each s-channel helicity amplitude, we have seen that we need to know the Reggeon pole for each t-channel exchange [its trajectory $\gamma(t)$ and its pole residue, including coupling strength], plus the absorption parameters (σ_T and the slope of B of the elastic scattering, the effective absorption radius, and the relative contribution of inelastic intermediate states).

Suppose we have obtained a full knowledge of one exchange in one reaction. If we change one external particle (e.g., go from the π or the A_2 exchange contribution in $\pi^-p \to \rho^0n$ to the π or the A_2 exchange contribution in $\pi^-p \to f^0n$) what can change? Some theoretical work has been done on this question [see the review of Hoyer (1974) on Finite Mass Sum Rules, and Michael (1973)] and it has been noted that phenomenologically there is indeed a change (Estabrooks and Martin, 1973; Ochs and Wagner, 1973; Irving, 1975).

The pole residue could change in two ways. The coupling strength could be different. For example $g_{\pi A_2 \rho}$ and $g_{\pi A_2 f}$ could be different; this probably accounts for part of the observed effect in ρ and f production (R. Worden, 1973b has also remarked on this).

In many cases a symmetry such as SU(3) can give at least approximate relations between coupling strengths. In general when this is done the results are satisfactory, though so far comparisons to accurate data have not been possible in situations that check results even to about the 25% level.

In addition, the t dependence of the pole residue could be different, giving different absorption. For example, if the pole is sharper in t the integrand to compute the absorption correction is cut off more sharply and there is less absorption even at $t=0$. We have seen that heavier exchanges have flatter residues [e.g., $\beta_{\pi\pi\rho}(t)$ for ρ exchange is steeper than $\beta_{\pi\pi f}(t)$ for f exchange], but we have no direct evidence about what happens for the same exchange and different external particles.

Michael (1973) has claimed that in dual resonance models there is a shrinkage effect with increasing m^2 of an external particle in s-channel helicity amplitudes, even though the expected $(s/m^2)^{\alpha(t)}$ gives an antishrinkage, the additional m^2 dependence arising from the crossing matrix. If that is a reliable indicator for real Reggeons, one would expect a steeper t dependence as an external particle mass increases, and a consequent decrease in absorption strength.

So far we have noted changes associated with the size or t dependence of the pole terms as external particles change. There are also changes associated with the absorption, and with the size of the inelastic intermediate state contribution.

First, the strength and shape of the elastic rescattering could differ—e.g., $\sigma_T(\rho N)$ and $\sigma_T(fN)$ might not be equal. In fact, recent experience with the new particles has suggested that for vector mesons one has $\sigma_T(aN) \sim 1/m_a^2$, and such a relation was predicted by Carlson and Freund (1973) and by vector dominance arguments (Sakurai, 1974; Greco, 1974). It would not be surprising if such a relation held in general. A possible argument is that for a reaction $a+b \to m^2+d$ we might expect a scaling relation so that $M(s,t) \sim (s/m^2)^{\alpha(t)}$. Then $\sigma_T \sim \mathrm{Im}M(0)/s$ with $\alpha(0)=1$ and so $\sigma_T \sim 1/m^2$. If such a result held, then the effect of absorption, which is proportion-

al to σ_T, would decrease for increasing m^2.

The effect of absorption also goes as $1/B$, where B is the slope of the elastic rescattering. One might argue that B and σ_T are proportional, as they would be in a conventional optical model. Then $B \sim 1/m^2$ would follow, and there is no net effect on absorption. For two, perhaps related, reasons, we think this argument is not correct. First, for $\psi p \to \psi p$ there is some evidence from photoproduction data that $\sigma_T(\psi p)/\sigma_T(\rho p) \sim m_\rho^2/m_\psi^2$, while $B_{\psi p}/B_{\rho p} \simeq 1/2$. Second, it has long been known (but not understood) for hadron elastic reactions that the best regularity was not that σ_T/B would be the same for all reactions, but that σ_T/B^2 was in fact the same for all processes. This suggests that $B^2 \sim 1/m^2$ or $B \sim 1/m$ so $\sigma_T/B \sim 1/m$ and the effective strength of absorption will decrease at least as $1/m$.

Finally, the inelastic intermediate state contribution will vary a little because the coupling of the intermediate states will be different for different external particles. For example, Fig. 20(a) shows a contribution to $\pi^- p \to \rho^0 n$ from ρ^* intermediate states; by isospin conservation in the Pomeron part this contribution cannot be present for f production. Similarly, an f^* intermediate is shown for f production which cannot be present for ρ. If the coupling products $g_{\rho^*\pi\pi} g_{\rho^* \rho P}$ and $g_{f^*\pi\pi} g_{f^* f P}$ are different, then the inelastic intermediate state contribution will be different. In general, it will only be a little different since (as here) one contribution replaces another.

While we can't do compelling numerical calculations here which indicate that the effect pointed out by Estabrooks and Martin, and Ochs and Wagner, may be understandable, we note the following arithmetic. We have for $\pi^- p \to \rho^0 n$ a net absorption strength (the size of the $n=0, x=2$ amplitude at $t=0$) of 1 in some units. We write this as $\frac{2}{3} + \frac{1}{3}$ where the first part is due to π exchange and the second due to A_2 (see Sec. VIII.D). As we go from ρ to f, suppose the A_2 coupling decreases by m_ρ/m_f relative to the π, and the net absorption strength decreases as $1/m$. Then the new absorption strength will be

$$\frac{m_\rho}{m_f}\left(\frac{2}{3} + \frac{m_\rho}{m_f}\frac{1}{3}\right) = 0.52\,, \tag{7.3}$$

which is consistent with what is observed. To establish that these arguments indeed explain the effect it will be necessary to check in a number of reactions and to find better theoretical arguments.

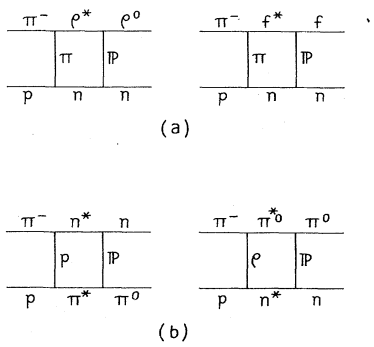

FIG. 20. Inelastic intermediate state contributions, to illustrate the discussion of Sec. VII.C.

In going from forward to backward reactions the inelastic intermediate state contribution should change somewhat. This is clear from Fig. 20(b), showing the two cases. In the forward direction the inelastic intermediate state contribution is proportional to $g_{\rho\pi\pi} g_{\rho NN^*}$, while in the backward case it is $g_{NN\pi} g_{NN^*\pi}$. Typically a meson vertex is described by a coupling about half as big as at a baryon–meson vertex, so we would expect that the inelastic intermediate state contribution in backward πN scattering *should* be about 50% larger than in the forward πN scattering, while the dominant elastic absorption is exactly the same. This is consistent with our analysis.

In this section we have discussed the ways in which pole terms and absorption effects might be expected to change when different external particles are considered. At the present time no systematic study has been done, but some theoretical and some phenomenological aspects are fairly clear. It has been observed for external pion pairs that the absorption strength decreases as $m_{\pi\pi}$ increases; that is probably understandable in terms of a combination of effects, particularly that we expect the effective strength of absorption to decrease about as $1/m_{\pi\pi}$. We have not done detailed calculations. If a generally applicable model of coupling strengths were available, it would probably be fairly easy to incorporate external particle changes into the systematics of the absorption model.

D. Regularities in the data

In recent years several systematic regularities have been noticed in the data. These include "geometrical scaling," universality of amplitude shape in impact parameter, derivative relations among amplitudes, and some aspects of duality. In this section we indicate how they appear from the point of view of the model. Some aspects were first predicted by the present approach, though that was not generally noticed at the time because they were a part of an explicit model. Seeing how the regularites arise in a general model also indicates how they will appear in new places (most of them have only been examined for a small number of the available reactions and exchanges) and clarities in what sense they are approximations.

1. Geometrical scaling

This is basically the notion that the energy dependence of hadron interactions can be put into an interaction radius which changes in a smooth way with energy. Its implications and phenomenology are discussed in detail by Barger, 1974, and some references given there. Since this is a property of our Pomeron amplitude, it is clear that we will have an approximate geometrical scaling, as is shown by the data.

In fact, one of the earliest proposals of geometrical scaling in this form was in the earliest form of the present Pomeron model (Kane, 1972). However, while it is useful to understand that much of the energy dependence of different properties of the data can arise from a common origin, it does not appear important to develop the idea much more or to worry in detail about how well it is satisfied, because it is inconsistent with the possi-

bility of fixed t singularities in the amplitude and thus with the possibility of t-channel unitarity. (This is because the geometrical scaling hypothesis requires the impact parameter distribution to depend only on $b/R(s)$, so the t distribution depends only on $R(s)\sqrt{-t}$. Consequently the amplitude cannot have any singularities at t values that are independent of s, such as $t=4m_\pi^2$, only 0.08 GeV^2 from the physical region.)

From a different direction we will violate geometrical scaling a little because we have a different rate of growth for the central and edge regions. Most of the obvious energy-dependent effects depend mainly on the edge, which gives the small t shrinkage, but the dip region behavior is mainly the central term and will show a somewhat slower variation than pure scaling would indicate.

In any case, "geometrical scaling" is a useful notion for organizing the data on very high energy elastic scattering, and is qualitatively consistent with our point of view.

2. Universality in impact parameter

Recently it has been suggested by several groups (for references and a discussion of the phenomenology, see Barger, 1974) that an s-channel approach to high-energy reactions would be fruitful. This has in turn suggested the idea (particularly emphasized by Ader *et al.*, 1974) that amplitudes have a "universal shape" in impact parameter b, often written as

$$M_n(s,b)\sim b^n M(s,b) \tag{7.4}$$

for an amplitude with net helicity flip n.

Such approaches must again for general reasons be only qualitative and approximate and of limited validity. For example, amplitudes with $n=0$, $x\neq 0$ will need a different form. Even more basic, the form must change at large b since the large b behavior reflects the nearest singularities in t. Explicitly, an amplitude of net helicity flip n, driven by a singularity at $t=m^2$, will have a contribution

$$m^{-n}\int \Delta^{n+1}d\Delta J_n\left(b(\Delta)/(\Delta^2+m^2)\right)=K_n(mb) \tag{7.5}$$

where $\Delta=\sqrt{-t}$, and asymptotically

$$K_n(mb)\sim\left(\frac{\pi}{2mb}\right)^{1/2}e^{-mb} \tag{7.6}$$

independent of n. The same results hold if the singularity in t is not a pole. Thus amplitude forms like $b^nM(s,b)$ can only be useful at small b.

The idea of an approximately universal form in b was one of the major predictions of the earlier work on the strong absorption model (Ross *et al.*, 1969). The general rule is [see Eq. (3.15)]

$$M_{n,x}(s,b)=R_{n,x}(s,b)S_{\rm eff}(s,b). \tag{7.7}$$

At the crudest level this is universal since $S_{\rm eff}$ removes amplitude at small b for all exchanges and all processes, while all Reggeons fall off at large b. A b^n is automatically in R for $b\to 0$. This gives a universal peripheral shape. According to the general prescription of Ross *et al.* (1969), $M_{n,x}(s,b)$ was universal at a much more detailed level too. The general form for a Reggeon was

$$R_{n,x}(s,t)\sim(-t)^{(n+x)/2}e^{-i\pi\alpha(t)/2}R(s,t), \tag{7.8}$$

where R was a real function that would be the same for any Reggeons with trajectory α. An overall constant that can depend on n, x and signature is left out. Consequently, separating off the kinematic $(-t)^{(n+x)/2}$ the prediction was for a completely universal shape in b, and one which could depend on n and x but not on individual helicities.

Although this prediction has generally been borne out, it seems to have one serious oversimplification, which was corrected in HK. Apparently exchanges retain a memory of the force range even when Reggeized, and the tensor mesons are more central than the vector mesons, the vector mesons more central than the pion. So $M(b)$ is more central for tensor exchange than for vector. There are also detailed differences due to exchange degeneracy breaking (see Sec. VII. E). So, altogether, we predict an approximate universality in impact parameter, with differences at a detailed level understandable in terms of the systematics of $R_{n,x}$ and $S_{\rm eff}$ which we have discussed in other sections.

3. Derivative relations

Various people have also suggested that various derivative relations should hold between different helicity amplitudes (Hogassen, 1971; see Schrempp and Schrempp, 1975, for an up to date exposition and tests).

For us the derivative relations are a necessary consequence of the peripherality of our amplitudes, as the derivative relations are just the relations holding between the Bessel Functions; the fact that we have approximately, when $x=0$, [see Eq. (5.23)]

$$M_n(s,t)\sim J_n(s,t) \tag{7.9}$$

means that we automatically satisfy the derivative relations to a good approximation. This is a prediction of any absorption approach where the absorption is strong enough so that $S_{\rm eff}\simeq 0$ at $b=0$, and was already true of the amplitudes of Ross *et al.*, 1969.

As with the previous regularities, because we can see their role in a definite model which satisfies general principles we can make several remarks. First, amplitudes with $x\neq 0$, such as the main one giving the π-exchange peak, will satisfy such relations when they are properly interpreted, but not in the usual simple form. The derivative relations will get less good at very high energies since $S_{\rm eff}(0)$ rises slowly with energy and the peripherality decreases a little.

Most important, on general grounds the derivative relations *cannot* apply to full amplitudes because the poles in t would be differentiated and give multiple poles, which is nonsense. They must be applied to data somewhat selectively (e.g., photon exchange near $t=0$ must also be avoided, and π exchange handled carefully).

Again, by having a general theoretical structure which incorporates the regularity we can automatically deal with all these situations and automatically generate

amplitudes which satisfy derivative relations in the appropriate way.

E. Exchange degeneracy breaking and trajectories

To a reasonable approximation data interpreted as due to ρ, ω, A_2 or f exchange are consistent with an effective trajectory for any of these particles with an intercept near 0.5 and a slope near 0.9 GeV^2. When one looks at the data in more detail, some differences appear.

Experimentally, it is clear that

$$\alpha_\rho(0) - \alpha_\omega(0) \simeq 0.15 \tag{7.10}$$

from comparison of many reactions, total cross sections, and regeneration phases. The analysis is given in detail by Davier, 1974.

It is also clear from the recent Fermilab experiment of the Caltech and Berkeley groups (Barnes *et al.*, 1974), which give $\sigma(\pi^- p \to \pi^0 n) \sim P_L^{-1.15}$ and $\sigma(\pi^- p \to \eta n) \sim P_L^{-1.47}$, that

$$\alpha_\rho(0) - \alpha_{A2}(0) \simeq 0.16. \tag{7.11}$$

The situation for the f is harder to establish, as there is no simple way to untangle it from the Pomeron. Our analysis of a number of reactions gives

$$\alpha_f - \alpha_{A2} \simeq 0.09, \tag{7.12}$$

but this must be considered as much less well established than $\alpha_\rho - \alpha_\omega$ and $\alpha_\rho - \alpha_{A2}$.

There is an argument which allows us to relate all these intercepts. Suppose that the basic pole trajectories all have equal intercepts $\bar{\alpha}$ in some bare theory without unitarity corrections. Then when we consider unitarity effects the resonances get widths, and trajectories get imaginary parts.

We can write the trajectories as

$$\alpha(t) = \bar{\alpha} + \alpha' t + \frac{1}{\pi}\int_{t_0}^{\infty} dt' \,\mathrm{Im}\alpha(t')/(t'-t), \tag{7.13}$$

so if $\mathrm{Im}\alpha \simeq 0$ then $\alpha(0) = \bar{\alpha}$.

For the ω this will have essentially no effect, as the low-lying resonances on the trajectory are narrow and the threshold is above $9m_\pi^2$, while for the ρ there will be a large effect since the threshold is at $4m_\pi^2$ and the low-lying resonances are wide.

For the ρ we expect

$$\mathrm{Im}\alpha \simeq \alpha'\sqrt{t_R}\,\Gamma_R \tag{7.14}$$

at resonances R along the trajectory. There is no particularly meaningful way to do the integral, but we can expect the extra contribution for the ρ to come from an estimate of the low-energy part,

$$\frac{1}{\pi}\int_{t_0}^{\infty} \frac{\mathrm{Im}\alpha(t')}{t'}\,dt' \gtrsim \frac{1}{\pi}\alpha'\sqrt{t_R}\,\Gamma_R \Delta t/t_R \approx \frac{\alpha'\Gamma_\rho \Delta t}{\pi m_\rho}. \tag{7.15}$$

Guessing $\Delta t = 1$ GeV^2, and using $\alpha = 1$ GeV^{-2}, $\Gamma_\rho = 0.15$ GeV, $m_\rho = .76$ GeV, we have

$$\alpha_\rho(0) \gtrsim \bar{\alpha}(0) + 0.063. \tag{7.16}$$

In addition, $m_\omega^2 - m_\rho^2 \simeq 0.03$. Thus we expect naively that $\alpha_\rho - \alpha_\omega \gtrsim 0.1$. The contribution of $\int \mathrm{Im}\alpha$ to $\alpha(0)$ for A_2 could be small, given the longer distance to the first wide resonance, with a small effect for the f since it is coupled to the 2π threshold.

Our best numbers are a little more separated than these, but given our lack of knowledge of how to take $\mathrm{Im}\alpha$ into account, perhaps it is consistent. We find

$$\begin{aligned} &\alpha_\rho(0) = 0.46, \\ &\alpha_f(0) = 0.39, \\ &\alpha_\omega(0) = 0.30, \\ &\alpha_{A2}(0) = 0.30. \end{aligned} \tag{7.17}$$

Possibly one can think of exchange degenerate bare pole trajectories with $\alpha(0) \simeq 0.3$, but shifted a little by mass splitting (the A_2 and ω are heavier than f and ρ), and with an extra shift for the ρ from its larger $\mathrm{Im}\alpha(t)$, to get the physical pole intercepts. The effective trajectories measured, of course, lie above these by amounts that depend on which amplitude dominates (see Sec. VI.C). For nonflip $t = 0$ amplitudes the effective trajectory is about 0.1 above the pole trajectory.

Additional evidence exists for the intercept separation given here and for exchange degeneracy breaking. For example, the discussion of hypercharge exchange reactions of HK requires $\alpha_\rho - \alpha_{A2} \simeq 0.15$. Worden (1974) has shown FESR results for amplitudes that have large exchange degeneracy breaking, especially away from $t \approx 0$.

F. Duality and FESR's

It is a remarkable fact that experimental data has the behavior that t distributions are approximately energy independent. Further, at small t exotic channels have approximately real amplitudes.

Technically, these regularities are expressed through finite energy sum rules (FESR's). Worden (1973, 1974) has remarked that high-energy models did not in general satisfy the FESR's and that was a fairly basic shortcoming. In particular he demonstrated that the model given in HK did not have the correct low-energy structure to satisfy FESR's.

There are two main ingredients that go into resolving this. The first we have already discussed briefly in Secs. VII.B and IV.D. It is the question of how the absorption behaves as one goes down to lower energies. Physically, we expect the absorption to increase slowly as the energy decreases, until an energy below which the inelastic cross section starts to decrease significantly. Then the absorption will stay constant or slowly decrease; even though there are fewer inelastic processes, unitarity bounds are still present and give an effective absorption. There has been no serious theoretical work on how to interpret absorption in this low-energy region. While we have kept the problem in mind, we have no particularly useful procedure to offer, and indeed our absorption does get somewhat too strong at low energies. Finding ways to connect low-energy unitarity with absorption due to increasing strength of inelastic production is an interesting theoretical problem.

The second important effect, noticed by Hartley

(1974), is the small t slope of the Reggeon pole term. The steeper the small t slope, the more spread out in impact parameter the Reggeon is, so the less is the effect of small b absorption. High-energy data (e.g., $P_L \gtrsim 4\text{GeV}/c$) is surprisingly insensitive to the small t Reggeon slope, because the t dependence of the amplitude is largely determined by absorption. But the continuation to low energies is strongly affected by the small t Reggeon slope. We probably take reasonable account of this effect now because we use Reggeon residue forms (Sec. IV.A) which take into account the t-channel thresholds (in particular the 2π branch point for the ρ) and allow for a sizable slope.

One good indication of how well we will agree with low-energy data is the position of the zero in the imaginary part of the nonflip amplitude for the ρ exchange (this is approximately the crossover zero). Our zero does not move too much, though it probably moves a little more than it should from the FESR's. It is shown in Fig. 21.

While we do not have any basic solution to the question of the low-energy extension of our model and the agreement with FESR's, it seems likely that in practice there is no problem in constructing the model to satisfy them. To do so, we need only to pay attention to maintaining a large enough pole slope at $t=0$, and to construct a reasonable way for the absorption to decrease a little at low energies. At the same time, as Hartley (1974) showed, the J-plane structure of the model will be satisfactory.

This viewpoint leads us to an interesting question of interpretation. First, obtaining a good description of the high-energy data is really very little dependent on the small t pole slope and the low-energy continuation of the absorption until the data is extremely accurate and over a wide range. This suggests that the connection with duality is very subtle. Second, it is likely that pole slopes at small t are not so large for other V, T exchanges as for the ρ. All others either have significantly more distant poles or are not coupled to the 2π t-channel cut. This suggests they will have a much less direct connection between the FESR's and the high-energy data, because of the dynamics of the Regge pole residue, and that the very good relation holding for the ρ exchange is partially an accident. There is some support for this view in the review of Worden (1974).

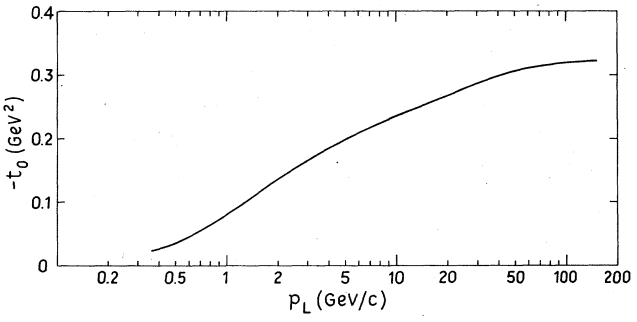

FIG. 21. The energy dependence of the first zero of the imaginary part of the ρ exchange in πN is shown, for the discussion of Sec. VII.F.

Altogether, while our results do not imply a total understanding of the meaning of duality, they allow an optimist to feel that duality could come as an output result in a theory which had Regge behavior and took unitarity constraints fully into account. We do find a surprising amount of the right kinds of behavior, which is not obviously input, in the final amplitudes.

Now we turn to detailed studies of specific reactions, and questions of fits to data.

VIII. STUDY OF SPECIFIC REACTIONS

A. General perspective on data fits in this model

For a given exchange and a given amplitude, the absorption model gives a fairly precise prediction for the s and t dependence. It is of course still necessary to specify the exchange trajectory and residue--this weakness is common to all of hadron physics at present, including the absorption model. If individual amplitudes with definite t-channel quantum numbers could be studied, the absorption model could be tested in many ways.

At present this is not possible, and instead we must study observables which often have several amplitudes, each with several exchanges. Most observables depend in subtle ways on interferences that make the results sensitive to some parameters. Even if the parameters are rather well known, it may not be enough.

Consider some examples:

(1) The polarization in $pp \to pp$ is given mainly by the interference of the imaginary Pomeron amplitude with the real part of the flip amplitude. The latter is dominated by approximately equal amounts of f and A_2 exchange, which add constructively. Thus their sum is largely insensitive to changes in either, and $P(pp \to pp)$ is almost totally insensitive to details of the model or to couplings. Next consider the polarization in $np \to np$. Now the isovector changes sign and one has a small result which is the difference of two large numbers. For example, at some t one might have $M_f = 15$ and $M_{A_2} = 10$, so $\varphi_5(pp) = 25$ and $\varphi_5(np) \simeq 5$. Twenty-percent changes in M_{A_2} and M_f give 20% or less changes in pp but could give $\varphi_5(np)$ from 0 to 8. Thus we could usefully say we predict the amplitudes and the pp polarization, but not the np polarization. On the other hand, the np polarization is more useful for fixing the couplings just because it is more sensitive.

(2) Even worse, the correlation polarization C_{NN} for $pp \to pp$ at $t=0$ is given by a difference of differences of large numbers. It is given by

$$C_{NN}(0) \sim \mathrm{Re}\varphi_1(0)\mathrm{Re}\varphi_2(0) - \mathrm{Im}\varphi_1(0)\mathrm{Im}\varphi_2(0). \qquad (8.1)$$

$\mathrm{Im}\varphi_1(0)$ is given by σ_T. $\mathrm{Im}\varphi_2(0)$ is measured by the difference $\sigma_T(\uparrow\downarrow) - \sigma_T(\uparrow\uparrow)$; theoretically it is mainly given at low energies by a π contribution minus a B contribution and is typically $\frac{1}{2}$ to $\frac{1}{3}$ of the π contribution. $\mathrm{Re}\varphi_2(0)$ is not so bad, with all the big contributions interfering constructively, and is measured by $d\sigma/dt$ for $np \to pn$. $\mathrm{Re}\varphi_1(0)$ is measured by Coulomb interference and is given mainly by a cancellation between the Pomeron real part and the Reggeon real parts; it is about $\frac{1}{2}$ of the Reggeon contribution. Thus

each of the two terms above involves a difference of two numbers and C_{NN} is their difference. The first term generally dominates; since $\mathrm{Re}\varphi_1(0)$ has a low-energy zero so will $C_{NN}(0)$. Above a few GeV/c where $\mathrm{Re}\varphi_1(0)/\mathrm{Im}\varphi_1(0)<0$, the above two terms have opposite signs so C_{NN} is a cancellation of two comparable numbers. Thus, while we can understand each part rather well, to say we have an accurate calculation of $C_{NN}(0)$ is not possible. Again, the redeeming feature is that a measurement of $C_{NN}(0)$ provides very useful information for pinning down the details of a model.

With these considerations in mind, one should proceed as follows. Look at the quantity which one wishes to predict or explain. See what interferences occur and how sensitive the result is likely to be. If important destructive interferences do not occur, the result should be rather reliable. If they do occur, additional constraints must be imposed to give a unique situation. In a situation with strong interferences often one can initially calculate the observables, find qualitative but mediocre agreement with data, and then obtain an excellent fit with no "parameter" changed by more than 5%. Until either a theory can accurately calculate the parameters, or experiments can determine individual amplitudes with definite quantum numbers, this situation is unavoidable.

We emphasize, however, that by simultaneously considering many reactions we constrain things as well as possible. Anyone who fits data from one or two reactions should have no difficulty doing so with many models. Only by both restricting the models to have good physics and by using constraints from data in many reactions can one eliminate inadequate approaches.

In the following we discuss specific features of a number of reactions. These are treated as just discussed. They all correspond to a standard set of parameters, but if variations of a few percent give "significant" improvements they are included. The resulting parameters are given in Tables I-III. They should be interpreted as rather accurate values that are averages or medians of ranges where applicable.

Most two-body hadron reactions can be studied with very few additional parameters by using those we have determined. Often only a small number of coupling constants plus some changes in Pomeron and absorption parameters for final states whose elastic scattering cannot be studied will be all that is needed.

TABLE I. The sign conventions are as in Fig. 4, with the Reggeon directed up toward the ac vertex. The amplitudes obtained will multiply a factor $\pm\exp(-i\pi(\alpha-J)/2)$ with the overall sign determined by phenomenological arguments such as duality, whether σ_T rises or falls, etc. The relation of the couplings which go at an SCHA vertex to those which enter in a Feynman diagram vertex are given by the vertex factors $ig_{\rho\pi\pi}(p_a+p_c)\cdot\epsilon_\rho^{(\lambda)}$ for ρ, $f_{A\eta\pi}A_{\mu\nu}^{(\lambda)}(p_{a\mu}p_{c\nu}+p_{a\nu}p_{c\mu})$ with $g_{A\eta\pi}=f_{A\eta\pi}\sqrt{s_0/2}$ for A_2 with an analogous form for f, $\epsilon_\mu^{(\lambda)}(G_v^\omega\gamma_\mu+G_T^\omega\sigma_{\mu\nu}r_\mu/2m)$ for ωNN with an analogous form for ρ, and $A_{\mu\nu}^{(\lambda)}(AP_\mu P_\nu/m_N^2+iB(P_\mu\gamma_\nu+P_\nu\gamma_\mu)/m_N)$ with $P=p_b+p_d$, $G_T^A=2\sqrt{2}A\sqrt{s_0/m_N^2}$, $G_v^A=2\sqrt{2}(A+B)\sqrt{s_0/m_N^2}$ for A_2NN, and an analogous form for f_{NN}. The numerical values given are determined by the whole set of reactions, sometimes rather uniquely but usually as appropriately weighted averages. The π coupling is known, the ω, ρ, and A_2NN couplings are probably known to 20% or better, the fNN 20% or a bit worse, and BNN to a factor of 2. The widths give $g_{\rho\pi\pi}\simeq 6$, $g_{f\pi\pi}\simeq 7$, $g_{A\eta\pi}\simeq 3.8$. The $t=0$ values presumably should be somewhat less than these numbers.

Vertex		SCHA	
rac	rbd	factor	Values
$\rho^0p(\frac{1}{2})p(\frac{1}{2})$		$\sqrt{2}G_v^\rho$	$G_v^\rho\simeq 2$
$\rho^0p(\frac{1}{2})p(-\frac{1}{2})$		$\sqrt{2}G_T^\rho/2m_N$	$G_T^\rho\simeq 15$
$\rho^0p(-\frac{1}{2})p(\frac{1}{2})$		$-\sqrt{2}G_T^\rho/2m_N$	
$\rho^0p(-\frac{1}{2})p(-\frac{1}{2})$		$\sqrt{2}G_v^\rho$	
	$\rho^0p(\frac{1}{2})p(\frac{1}{2})$	$\sqrt{2}G_v^\rho$	
	$\rho^0p(\frac{1}{2})p(-\frac{1}{2})$	$-\sqrt{2}G_T^\rho/2m_N$	
	$\rho^0p(-\frac{1}{2})p(\frac{1}{2})$	$\sqrt{2}G_T^\rho/2m_N$	
	$\rho^0p(-\frac{1}{2})p(-\frac{1}{2})$	$\sqrt{2}G_v^\rho$	
ω, f, A_2^0 couplings have the same form as ρ couplings			$G_v^\omega\simeq 12$
			$G_T^\omega\simeq 2$
			$G_v^f\simeq 25$
			$G_T^f\simeq 6$
			$G_v^{A2}\simeq 7$
			$G_T^{A2}\simeq 43$
$f\pi^+\pi^-$	$f\pi^+\pi^-$	$\sqrt{2}g_{f\pi^+\pi^-}$	$g_{f\pi^+\pi^-}\simeq 6.9$
$\rho^0\pi^+\pi^-$	$\rho^0\pi^+\pi^-$	$\sqrt{2}g_{\rho^0\pi^+\pi^-}$	$g_{\rho^0\pi^+\pi^-}\simeq 6$
$A_2^+\pi^-\eta$	$A_2^+\pi^-\eta$	$\sqrt{2}g_{A\eta\pi}$	$g_{A\eta\pi}\simeq 3.8$
$\pi^0p(\frac{1}{2})p(-\frac{1}{2})$	same	$g_{\pi NN}$	$g_{\pi NN}^2/4\pi=14.6$
$\pi^0p(\frac{1}{2})p(\frac{1}{2})$	same	0	
$B^0p(\frac{1}{2})p(-\frac{1}{2})$	same	g_{BNN}	$g_{BNN}^2/4\pi\simeq 41.4$
$B^0p(\frac{1}{2})p(\frac{1}{2})$	same	0	

While space and time considerations have limited us to considering only some reactions, we have included examples of almost every major kind of amplitude (i.e., n and x values and type of exchange) likely to be used. Thus the reader can usually obtain immediate deductions about his favorite reaction from the combined behavior of similar amplitudes for other processes.

In other words, the prediction is that if you have seen an $n=0$, $x=2$ amplitude for a given exchange in one reaction, you have seen it for that amplitude and exchange in all reactions. The forward peak in $np\to pn$, $\gamma p\to\pi^+ n$, $\pi N\to\rho N$ for transverse ρ's etc. are all the same basic amplitude structure. Nontrivial differences occur because different contributions add up in different ways in the different reactions (e.g., the ρ exchange is absent in $\pi N\to\rho N$) and because the absorption is a little different for different external particles, but basically they are the same. Similar remarks hold for each kind of amplitude.

Further, since the observables for reactions we do not consider here are generally constructed from amplitudes which do describe experiment for the ones we consider, there is a reasonable likelihood that we will not encounter a significant disagreement. Such a disagreement would therefore have serious implications for our point of view.

TABLE II. These are typical parameters needed to give the behavior of Reggeon trajectories and residues. The residues are given factorized so they can be used in any reaction. A fit to data for any reaction including these exchanges gives values near those listed, although not necessarily precisely these; they are a weighted choice from several nearby values. The relation between $\alpha(0)$ and $\alpha'(0)$ and α_1, α_2 of Eq. (3.5) is $\alpha_1 = [J-\alpha(0)^2]/\{2\alpha'(0)m^4-[J-\alpha(0)]m^2\}$, $\alpha_2=2[J-\alpha(0)-\alpha'(0)m^2]/[2\alpha'(0)m^2-J+\alpha_0]$.

Parameter	Particle	Value
s_0	all	1 GeV^2
$\alpha'(0)$	ρ	0.8
	ω	1.1
	A_2	0.8
	f	0.85
	π	0.85
	B	0.55
$\alpha(0)$	ρ	0.46
	ω	0.30
	A_2	0.30
	f	0.39
	π	−0.015
	B	0.21
C [Eq. (3.4)]	ρNN	1.2
	$\rho\pi\pi$	0.8
	ρKK	0.8
	ωNN	2.35
	ωKK	0.75
	fNN	1.0
	$f\pi\pi$	small
	fKK	small
	A_2NN	0
	$A_2\pi\eta$	0
	A_2KK	0
	πNN	0.4
	BNN	1.5

Our fits to data are generally easy and excellent for KN reactions, but somewhat strained for some NN data at low energies. We interpret this as evidence that when the results are not sensitively dependent on almost total absorption near $b=0$ we have things about right, while when results depend in detail on small b for reactions with the strongest absorption, considerable caution is advisable.

In the next sections we show some descriptions of data, both to illustrate how typical observables behave and to point out interesting aspects of the data. Since much of the explanation of the data has been given in earlier sections, we will be brief here. We also give a number of predictions.

B. πN and KN

Figures 22–27 show cross sections and polarizations for πN and KN reactions. There is little difference from the treatment of HK. The high-energy $d\sigma/dt$ are discussed in Sec. IV.B, and polarizations in Sec. VII.A. The total cross-section differences are shown in Fig. 28. Various high-energy predictions are shown.

The elastic πN polarizations are mirror symmetric because of a pair of almost coincident zeros in the ρ flip amplitude. The origin of these zeros was discussed in Sec. VI.A. A significant amount of helicity flip f exchange is present, as required by the $np\to np$ polarization, without altering the mirror symmetry much.

The differential cross sections will show an increasing curvature as energy increases from the mechanism described in Sec. IV.B. The imaginary part of the Pomeron amplitude has a zero at $-t\simeq 2.1$ GeV^2 for πN and $-t\simeq 2.5$ GeV^2 for KN; at Fermilab energy dips should occur in the πN and KN $d\sigma/dt$ near these t values.

The $\pi^- p\to\pi^0 n$ polarization is discussed in Secs. VII.A and VI.D.

Note that $d\sigma(\pi^- p\to\pi^0 n)/dt$ at small t from Fermilab data and the $\pi^\pm p$ total cross-section differences are both adequately described. People have questioned whether

TABLE III. Parameters for Pomeron and absorption [see Eqs. (3.6)–(3.13)]. When used for the Pomeron, these give fairly good descriptions of data, as shown. They obviously satisfy certain simple regularities, and one could abstract the expected largely geometrical conclusions. Because of the interest in the high-energy elastic data we have left these as precise values.

Pomeron	NN	πN	KN
A_c	11.93	13.78	10.75
B_c	2.36	2.05	1.64
A_e	1.08	0.88	0.78
B_e	4.40	3.32	2.78
R_{c0}	2.92	2.23	2.23
R'_c	0.58	0.47	0.59
R_{e0}	3.81	0	0
R'_e	1.70	1.950	2.08
Inelastic Intermediate States			
d	1.21	0.52	0.76
D	6.82	3.01	2.26
R''_0	3.12	2.35	2.42
K	83.97	119.75	65.30

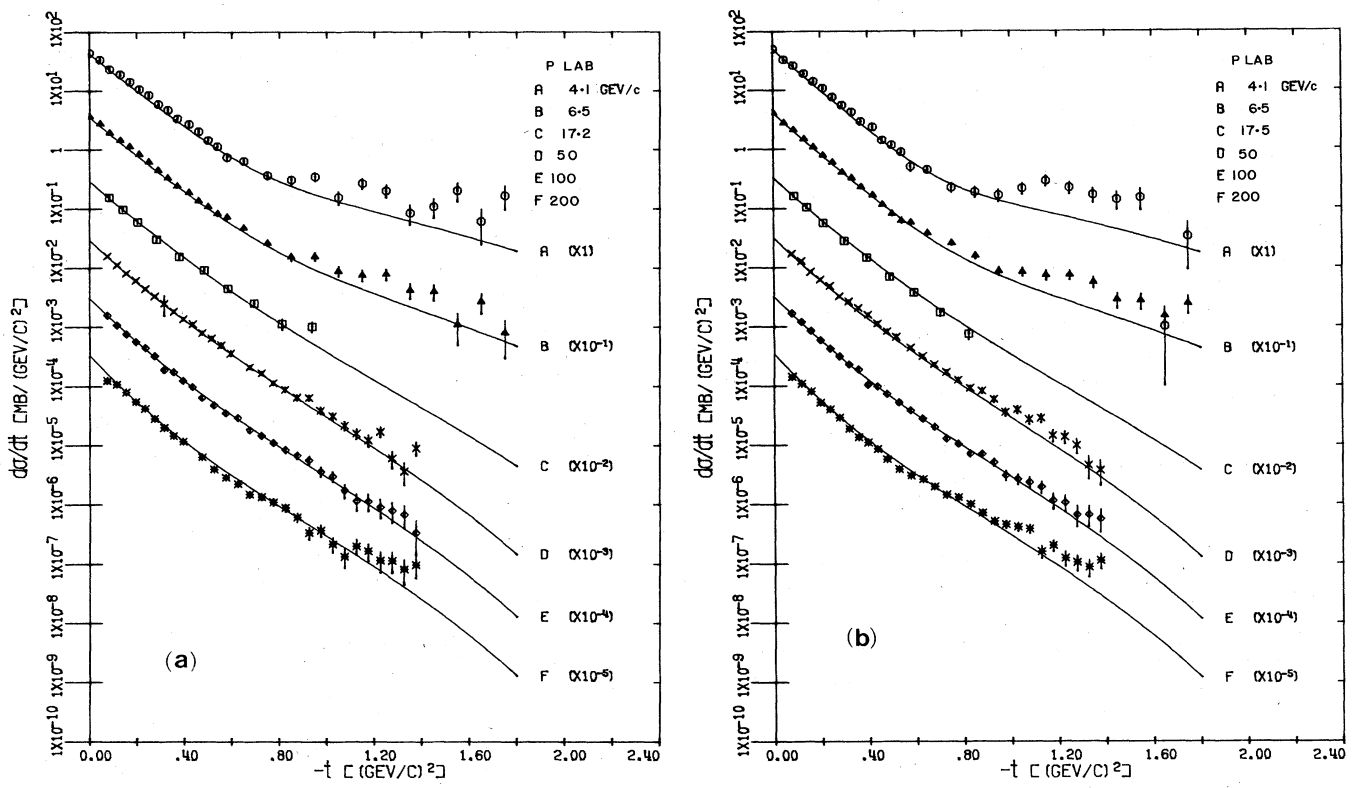

FIG. 22. Some fits to elastic scattering for $\pi^{\pm}p$. See discussion of Sec. VIII. Data shown are from Ambats *et al.* (1973), Foley *et al.* (1963), and Akerlof *et al.* (1975).

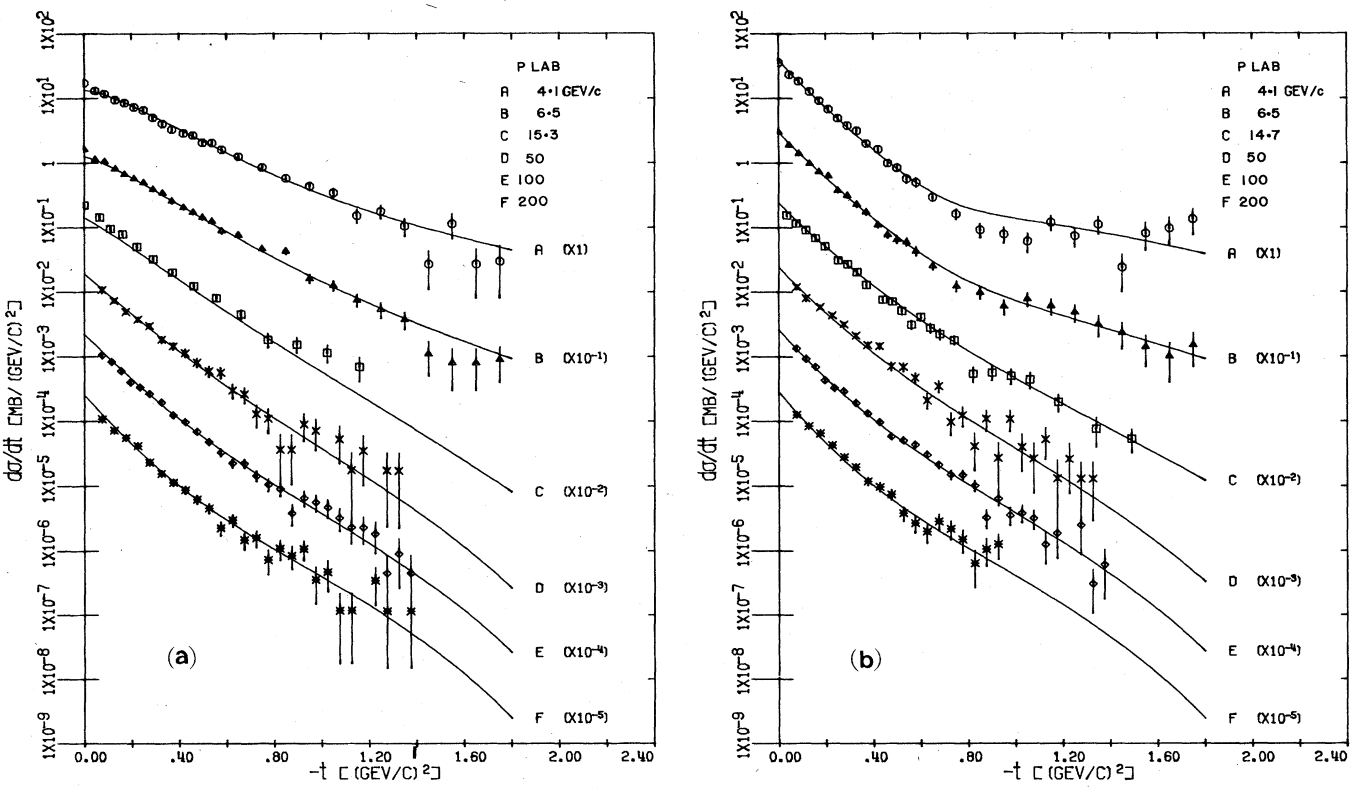

FIG. 23. Some fits to elastic scattering for $K^{\pm}p$. Data shown are from Ambats *et al.* (1973), Foley *et al.* (1963), and Akerlof *et al.* (1975).

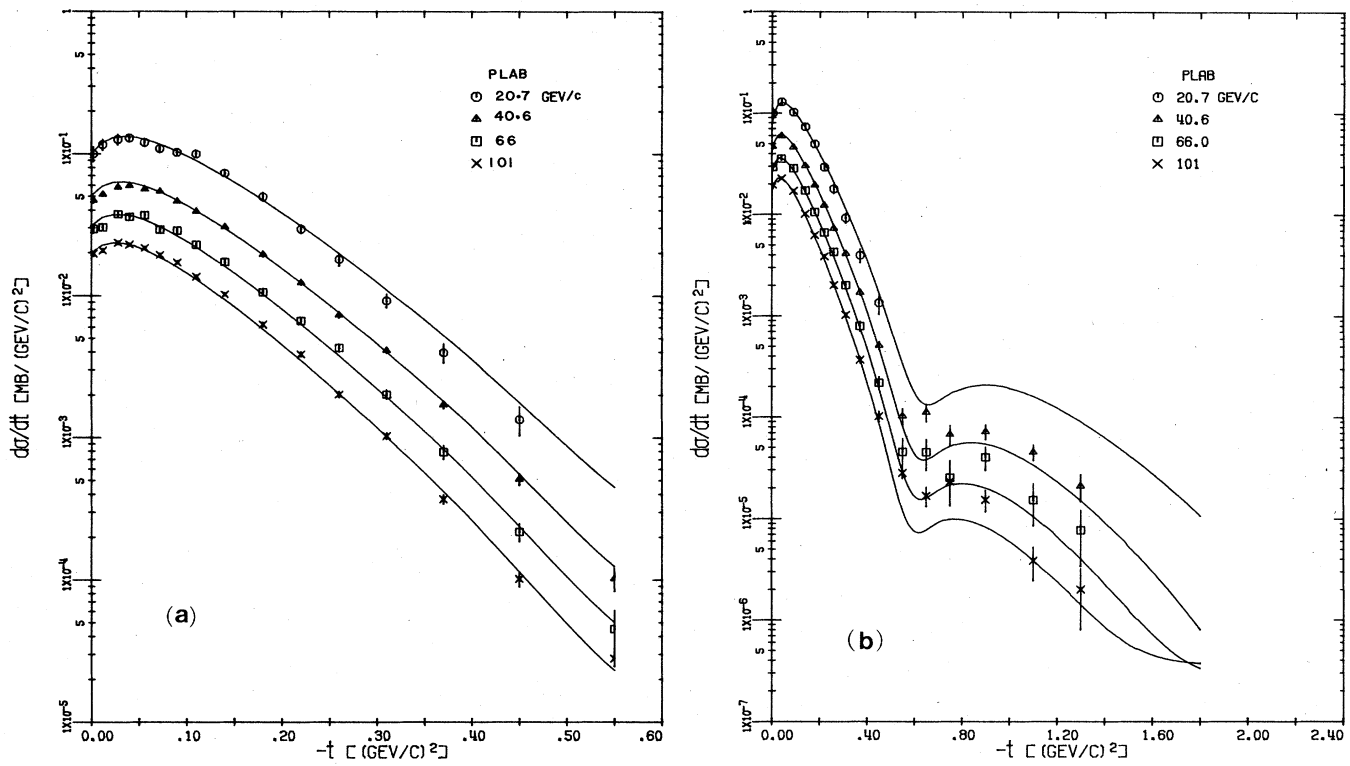

FIG. 24. Fits to high-energy $\pi^- p \to \pi^0 n$; data from Barnes *et al.* (1974). See discussion of Sec. VIII.

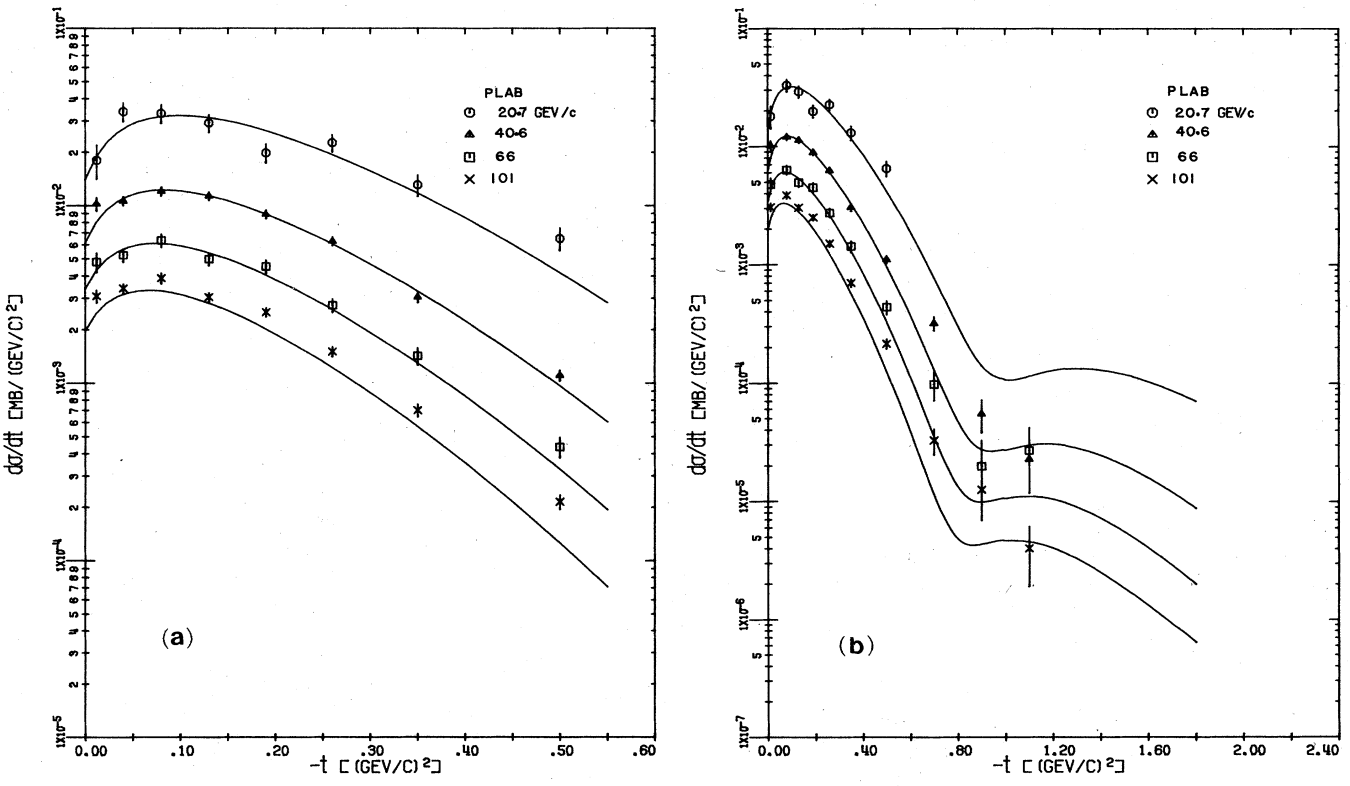

FIG. 25. Fits to high-energy $\pi^- p \to \eta n$; data from Barnes *et al.* (1974).

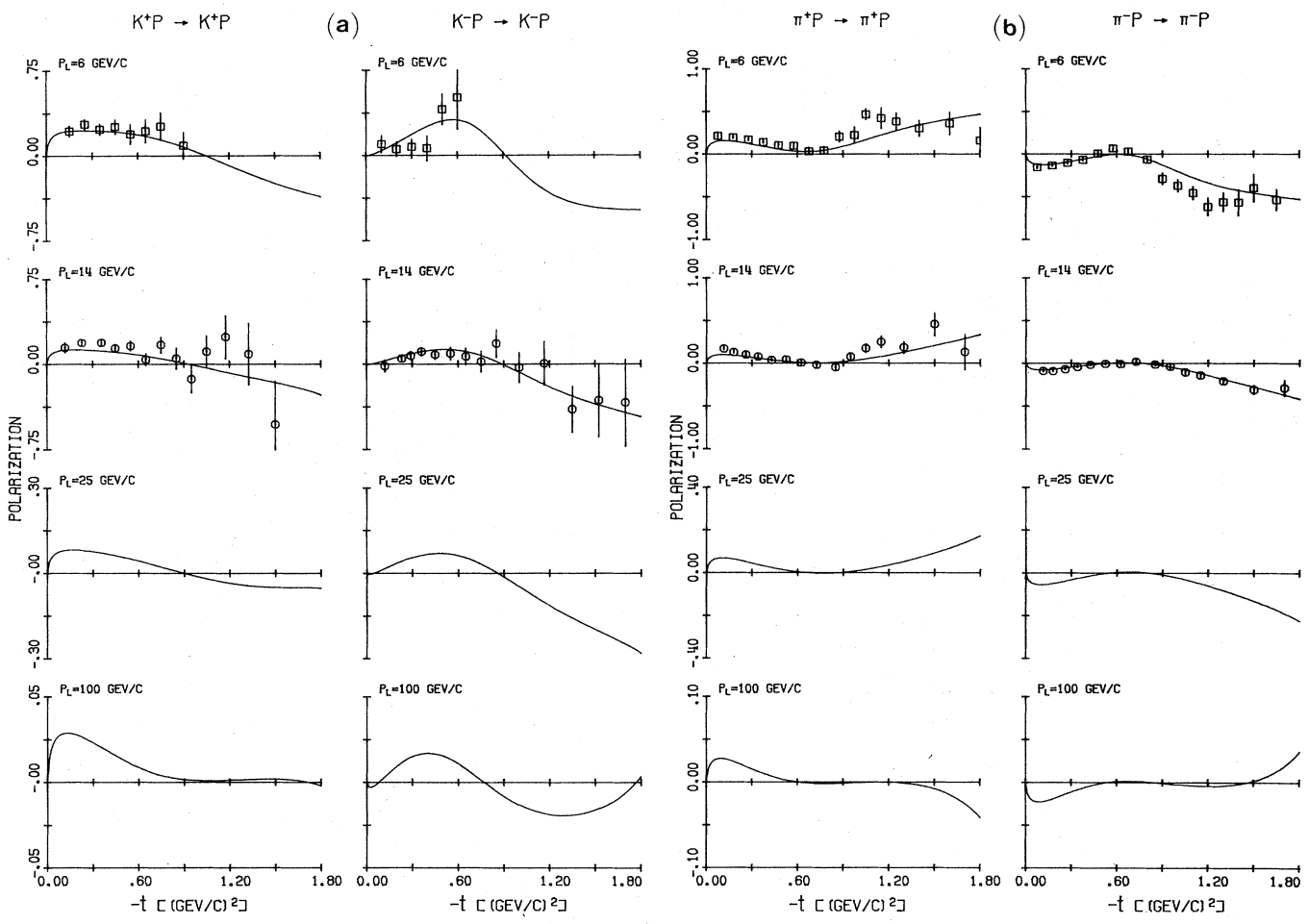

FIG. 26. Elastic polarization fits and predictions for $K^{\pm}p$ and $\pi^{\pm}p$. See discussion of Sec. VIII. Data from Borghini *et al.* (1970; 1971).

these data were consistent, but that was based on the assumption of a pure pole amplitude, without the phase rotation caused by absorption. The effects of absorption (Sec. VI) are to lower ImM relative to ReM in size, and to raise the effective intercept of ImM above that of ReM. We see no reason to question the consistency of any of the data. Note also, as discussed in Sec. VI.B and as often misrepresented in the literature, that there is no inconsistency in the shrinkage properties of the model and the data.

As discussed in Sec. VII.E, the KN and NN total cross-section differences, dominated by the ω, fall faster than πN. This seems to imply that ω and ρ intercepts are separated by about 0.16. This may be due mainly to the extra real part generated by the area under the imaginary part of the trajectory.

Crossover zeros for all elastic reactions are given approximately correctly by this model; they were one of its original major successes. They will move out in $-t$ slowly with increasing energy up to about 50 GeV/c and then back in, first because the absorption strength decreases and then from pole shrinkage. For KN and NN the crossover position is largely determined by the zero in Imω (Ross *et al.*, 1969). Since KN is absorbed less, the zero in Imω is further out in KN. The correction term due to ReωRe (Pomeron $+f$) goes opposite ways for the two reactions because f is also absorbed more for pp, moving the KN crossover about 10% closer to $t=0$ and the pp crossover about 10% further out. The KN crossover should be about 0.05 further out in t.

The $K_2p \to K_1p$ $d\sigma/dt$ is shown in Fig. 29, and the associated regeneration phase from the ω and ρ at $t=0$ in Fig. 9. The regeneration phase for $K_2p \to K_1p$ is given by $\omega+\rho$, with contributions proportional to $G_v^{\omega}=12$ and $G_v^{\rho}=2$ from Table I. Adding the phases from Fig. 9 vectorially gives a phase of 56° (or $-124°$) at 50 GeV/c, for example. A slow variation with energy will occur, as shown. The dip in $d\sigma/dt$ comes about because the ω exchange large nonflip contribution is the dominant one, so it has our standard dip near $-t=0.25$ GeV^2 for KN, filled in by the flip amplitude mainly generated by the ρ.

The KN charge exchange reactions of Fig. 29 constitute one of the most powerful tests of the model, as discussed in Sec. VII.B and shown in Fig. 19.

C. *NN* reactions and polarized beam data

Figs. 30–34 show various observables for NN reactions. Figure 30b shows $pp \to pp$ $d\sigma/dt$ at FNAL and ISR energies. Note the filling in of the dip as energy de-

creases, caused by the real part of the Reggeon amplitude, the slow motion of the dip minimum toward $t=0$, the curvature that develops from the small t shrinkage and medium t lack of shrinkage, and the slow rise of the secondary maximum. Curve E is for Isabelle energies.

In the dip region the polarization will be large because ImM has a zero; this is shown in Fig. 15 with diffractive flip amplitudes included.

The polarization in $pp \to pp$ is mainly Imφ_1 interfering with Reφ_5. As shown in Sec. VI.D and Fig. 13, Reφ_5 will have an absorption zero for $-t \sim 0.6$ GeV^2. At low and medium energies (say 5-20 GeV/c) Imφ_1 also has a zero near $-t = 0.8$ GeV^2, due to the zero in Im Pomeron at $-t \simeq 1.4$ GeV^2, and shifted in toward zero by a cancellation with the Reggeons, so the polarization has a "double" zero near -0.8. As the energy increases the Reggeon part of φ_1 drops away, so the zero in Imφ_1 moves out toward -1.4 and the two zeros separate, allowing P to go negative between them. A contribution of quite similar shape is obtained (Pumplin and Kane, 1975) with "helicity flip Pomeron" amplitudes so the polarization should persist to quite high energies with largely constant shape and size beyond 100 GeV/c.

When we go to $np \to np$ the isovector exchanges change sign. Since φ_5 is proportional to $G_v G_T$ and G_v is large for ω and f exchange, while G_v is quite small for ρ and A_2, a moderate G_T for the isoscalars will allow them to dominate φ_5. There is reason to expect such a G_T

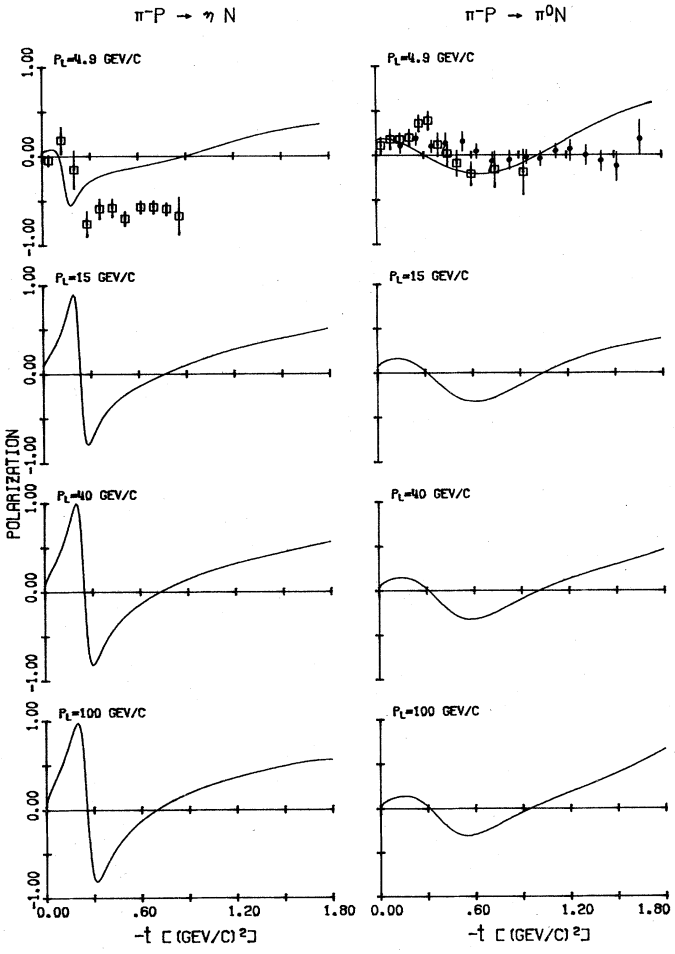

FIG. 27. Polarization for $\pi^- p \to \pi^0 n$ and $\pi^- p \to \eta n$. See discussion of Sec. VIII. Data from Bonary *et al.* (1973) and Hill *et al.* (1973).

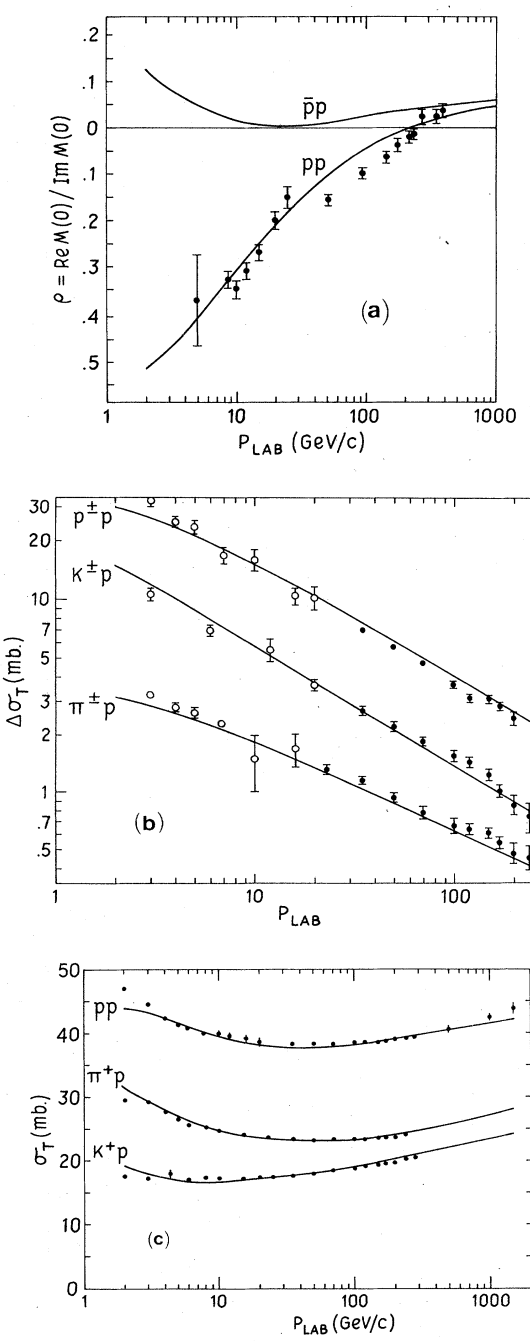

FIG. 28. Total cross-section differences, the pp ratio of real to imaginary parts of $\varphi_1(t=0)$, and total cross sections are shown vs energy. See discussion of Sec. VIII. Data from Benay *et al.* (1970), Enstrom *et al.* (1972), Bracci *et al.* (1972), and Carroll *et al.* (1975) for $\Delta\sigma_T$; from Bartenov *et al.* (1973) and Foley *et al.* (1967) for the real to imaginary ratio; and from Carroll (1975) for σ_T.

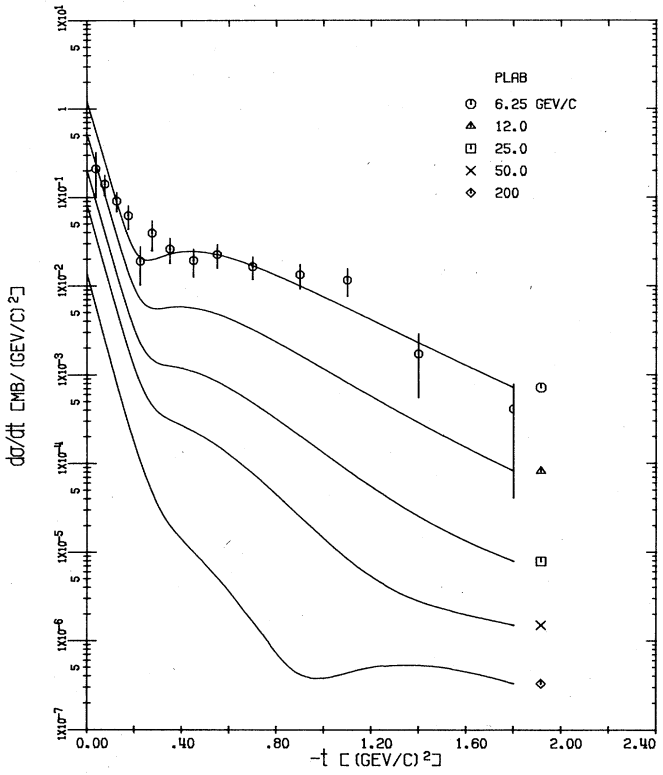

FIG. 29. Fits to $K_2 p \to K_1 p$ and high-energy predictions. See discussion of Sec. VIII. Data from Brandenburg *et al.*

(Gault *et al.*, 1973). If, on the other hand, G_T were zero for the isoscalars, as has often been claimed, then φ_5 would change sign and the $np \to np$ polarization would be mirror symmetric to $pp \to pp$. Thus the experiment basically measures the size of the isoscalar helicity flip couplings. The experimental results (Diebold, *et al.*, 1975) indeed confirm that the isoscalars dominate φ_5.

The observed $np \to np$ polarization also shows a rapid energy dependence from 2–6 GeV/c, which we do not reproduce. Our energy dependence will be quite similar to that for pp. We then predict that the rapid energy dependence at lower energies stops beyond about 6 GeV/c and that the dependence at low energies can be explained either in terms of specific particle production or a low-lying exchange.

It is amusing to note that the lower energy $np \to np$ polarization looks very much like the high-energy $pp \to pp$ polarization. While the analogy is valid for the zeros with the near zero in $\mathrm{Re}\varphi_5$ and the far zero in $\mathrm{Im}\varphi_1$ in both cases, it is misleading for the sizes, with the small size being basically $((f + A_2)/\text{Pomeron})$ for high energy pp, but $((f - A_2)/\text{Pomeron})$ for the low energy np, with f and A_2 similar in size.

Figure 35 gives results for some two-spin correlations. The difference $\Delta\tilde{\sigma}_T = \sigma_T(\uparrow\downarrow) - \sigma_T(\uparrow\uparrow)$ is given by $\mathrm{Im}\varphi_2(t=0)$. It vanishes identically for any definite parity exchange since a $\sqrt{-t}$ goes with the helicity flip at each vertex. Nonzero values are naturally generated by absorption in the familiar way which gives the sharp peak

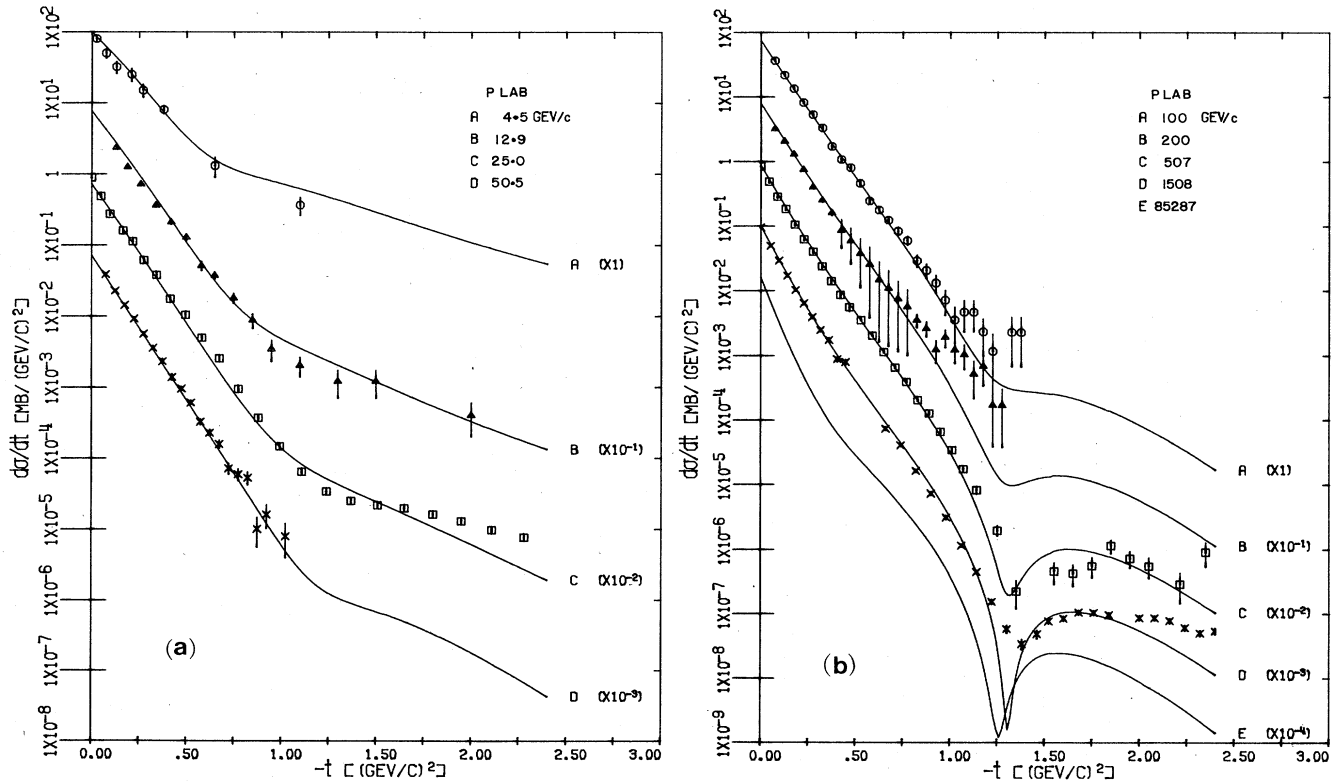

FIG. 30. Some fits to pp elastic scattering. See discussion of Sec. VIII. Data shown for pp are from Coletti *et al.* (1967), Hartung *et al.* (1965), Beznozikh *et al.* (1973), and Akerlof *et al.* (1975).

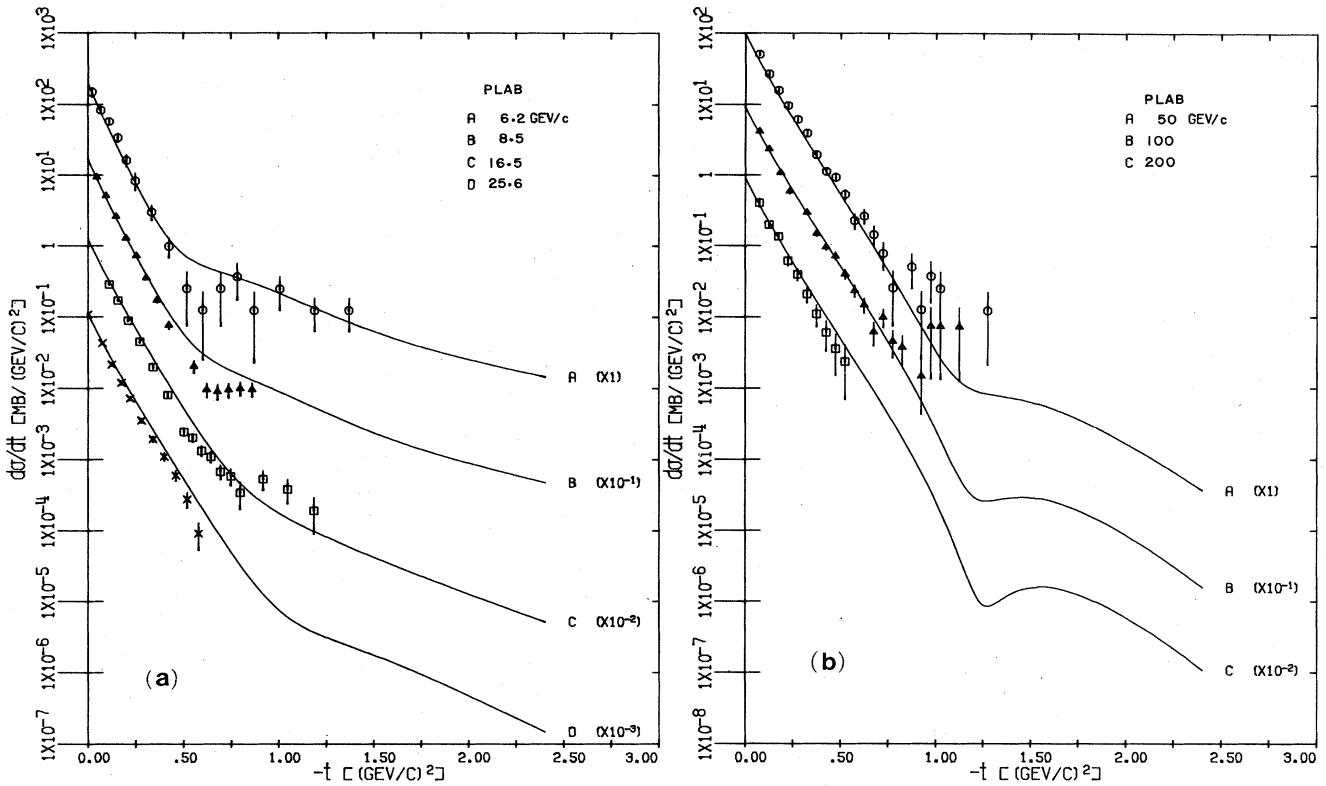

FIG. 31. Some fits to $\bar{p}p$ elastic scattering. See discussion of Sec. VIII. Data are from Boeckmann *et al.* (1966), Birnbaum *et al.* (1969), Antipov *et al.* (1972), and Akerlof *et al.* (1975).

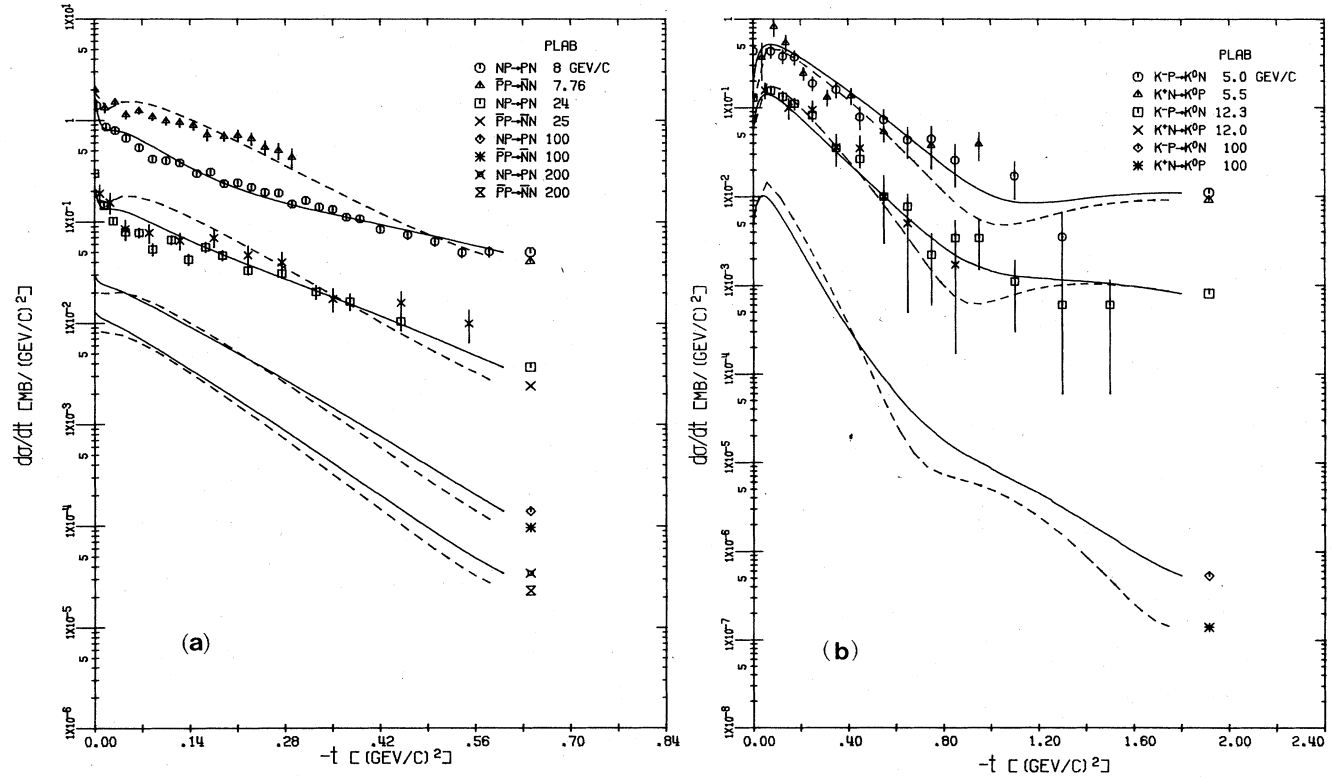

FIG. 32. Fits to $np \to pn$, $\bar{p}p \to \bar{n}n$, $K^-p \to \bar{K}^0 n$, and $K^+n \to K^0 p$, and high-energy predictions. See discussion of Sec. VIII. Data from Miller *et al.* (1971), and Engler *et al.* (1971) for $np \to pn$; Lee *et al.* (1973) and Bolotov *et al.* (1973) for $\bar{p}p \to \bar{n}n$; Astbury *et al.* (1966) for $K^-p \to \bar{K}^0 n$; and Cline *et al.* (1969) and Firestone *et al.* (1970) for $K^+n \to K^0 p$.

in $np \to pn$ or $\gamma p \to \pi^+ n$. Generating a nonzero imaginary part is harder, and tests the model more stringently; its size for us is largely determined by the phase of absorption and the way in which the absorption requires exchange degeneracy to be broken. The sign of $\Delta\vec{\sigma}_T$ was correctly predicted by this approach. At low energies the π contribution dominates our result for $\Delta\vec{\sigma}_T$ with significant cancellation from the B; at high energies the ρ exchange will dominate, with a transition in the 20–30 GeV range.

A subtle constraint on t-channel approaches from s-channel unitarity can be seen here. Since $\sigma_T(\uparrow\downarrow)$ has $J_y = 0$ while $\sigma_T(\uparrow\uparrow)$ has $J_y = 1$, presumably more s-channel intermediate states are available to the former and so it is larger, giving $\Delta\vec{\sigma}_T$ positive from an s-channel view. This then constrains the phase rotation due to absorption and the relative signs of π, ρ contributions to have at any high energy (where such an argument is valid) the correct sign to give $\Delta\vec{\sigma}_T$ positive, as indeed was the case. Such relations between s and t channel may give much insight into how unitarity and absorption are related.

Next consider the two-spin differential cross sections $d\sigma_{\uparrow\uparrow}/dt$, $d\sigma_{\uparrow\downarrow}/dt = d\sigma_{\downarrow\uparrow}/dt$, $d\sigma_{\downarrow\downarrow}/dt$. Expressions for these are given in Eqs. (A.47)–(A.50). They are a sensitive probe of any spin dependence, each being given by a dominant nonflip amplitude φ_1 plus its interferences with the other amplitudes. Note that it is not necessary to have amplitudes out of phase to obtain an effect; models with all amplitudes in phase could still have different polarized differential cross sections. The dominance of $\varphi_1 = \varphi_3$ leads to a break in each of these cross sections near the t-value where $\mathrm{Im}\varphi_1$ has a zero. Since the zero of $\mathrm{Im}\varphi_1$ is due to the Pomeron zero at $-t \simeq 1.4$ GeV^2 and is shifted in to $-t \simeq 0.8$ at ANL energies by a cancellation with the Reggeon contribution, the zero in $\mathrm{Im}\varphi_1$ and consequently the breaks in these cross sections are expected to move outward with increasing energy until the Reggeon contributions are negligible (say around 200 GeV/c).

The difference of these polarized $d\sigma/dt$ which eliminates the dominant $|\varphi_1|^2$ term is proportional to the Wolfenstein parameter C_{NN}. Since it is proportional to at least one small amplitude, it is small, of order 10%. This is a case where we can fit the data and we can explain its behavior in terms of the amplitudes, but it involves several cancellations of numbers of similar size and we cannot say that we predict it to better than a factor of 2. A comment on its value at $t = 0$ was used as an example in Sec. VIII.A. The energy dependence of C_{NN} will be interesting and complicated both at lower energies and at higher energies. At lower energies it can probably be understood in terms of the effect of a few dominant production channels. At higher energies it must decrease in some average sense at least as $1/s$ because it is of order Reggeon/Pomeron. However, its energy dependence in a given t region need not show this because the way the cancellations change with energy can dominate the energy dependence. An example is shown in Fig. 35.

The depolarization parameter D_{NN} is also measured; it basically measures how much unnatural parity exchange is present, but quadratically. It is predicted to be essentially unity with a few percent decrease below one near where $\mathrm{Im}\varphi_1 = 0$, and a noticeable decrease below one at larger t.

Finally we mention the nucleon charge exchange reactions $np \to pn$ and $\bar{p}p \to \bar{n}n$. Similar remarks hold for $\gamma p \to \pi^+ n$ and $\gamma n \to \pi^- p$ and for ρ production. The polarizations are discussed in detail in Sec. VII.A. The cross-section normalizations are worth noting for several reasons. First, that there is a peak at all at small t requires the absorption, and brings us full circle with our introductory remarks in Sec. II. To get the size correct requires both an absorbed π and an absorbed A_2. That is satisfactory, since by factorization the A_2 must be present. Models which attempt to get the correct size from the π alone, here or for $\gamma p \to \pi^+ n$ or for $\pi N \to \rho N$, must then somehow explain the mysterious absence of the A_2. Second, still at $t = 0$, if the real part of the ρ contribution in φ_2 is sizeable, it will separate the line-reversed cross sections, contrary to observation. This is also satisfactory with $\mathrm{Re}\varphi_2^\rho$ suppressed by the absorption phase, as explained in Sec. VI.A. Third,

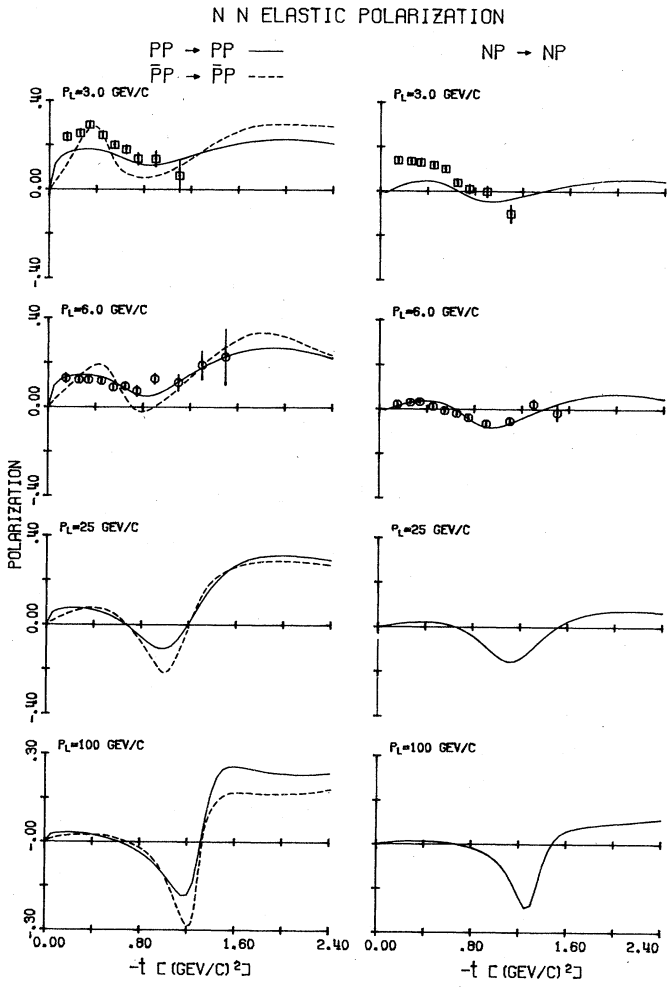

FIG. 33. Polarization for NN reactions. See discussion of Sec. VIII. Data from Diebold *et al.* (1975).

the interference as $-t$ goes away from zero generates a dip in $\bar{p}p \to \bar{n}n$ and a monotonic decrease in $np \to pn$, as shown in Fig. 32. Fourth, the difference in size at larger $-t$ of the line-reversed $np \to pn$ and $\bar{p}p \to \bar{n}n$ cross sections, and the direction of the difference, demonstrates that very large exchange degeneracy breaking occurs, and in a definite way. This is explained in Sec. VII.B. Note that the direction of the breaking changes with energy as the π contributions goes away, as shown in Fig. 18.

The line-reversed pair $np \to pn$ and $\bar{p}p \to \bar{n}n$, especially the polarizations, probably constitute the most difficult obstacle that any approach toward understanding two-body hadron reactions has to overcome. That the present model can give an explanation for the data in a way not inconsistent with other constraints is one of its major practical successes.

ACKNOWLEDGMENT

The authors are indebted to F. Henyey for many discussions, over several years, which have benefitted this review and the work on which it is based.

APPENDIX: CONSTRUCTING AMPLITUDES AND OBSERVABLES

With the techniques and reactions summarized in this appendix the reader can relate our SCHA couplings to Lagrangian forms and those of other approaches, apply the model immediately to processes involving the most common spins, and work out the relations between observables and amplitudes for any process. We have tried to give a self-contained treatment. As discussed in the text, we work in terms of s-channel helicity amplitudes (SCHA).

Although we try to give a self-contained summary, the reader may wish to consult other sources. Some useful general treatments are those of Jackson (1965), Berman and Jacob (1965), Jacob and Wick (1959). For NN reactions some useful treatments are Wolfenstein (1956), MacGregor *et al.* (1960), Goldberger *et al.* (1960), Phillips (1963), Scotti and Wang (1965), and Leader and Slansky (1966). For spin rotation parameters see, for example, Berger and Fox (1970).

Consider a process

$$a + b \to c + d$$

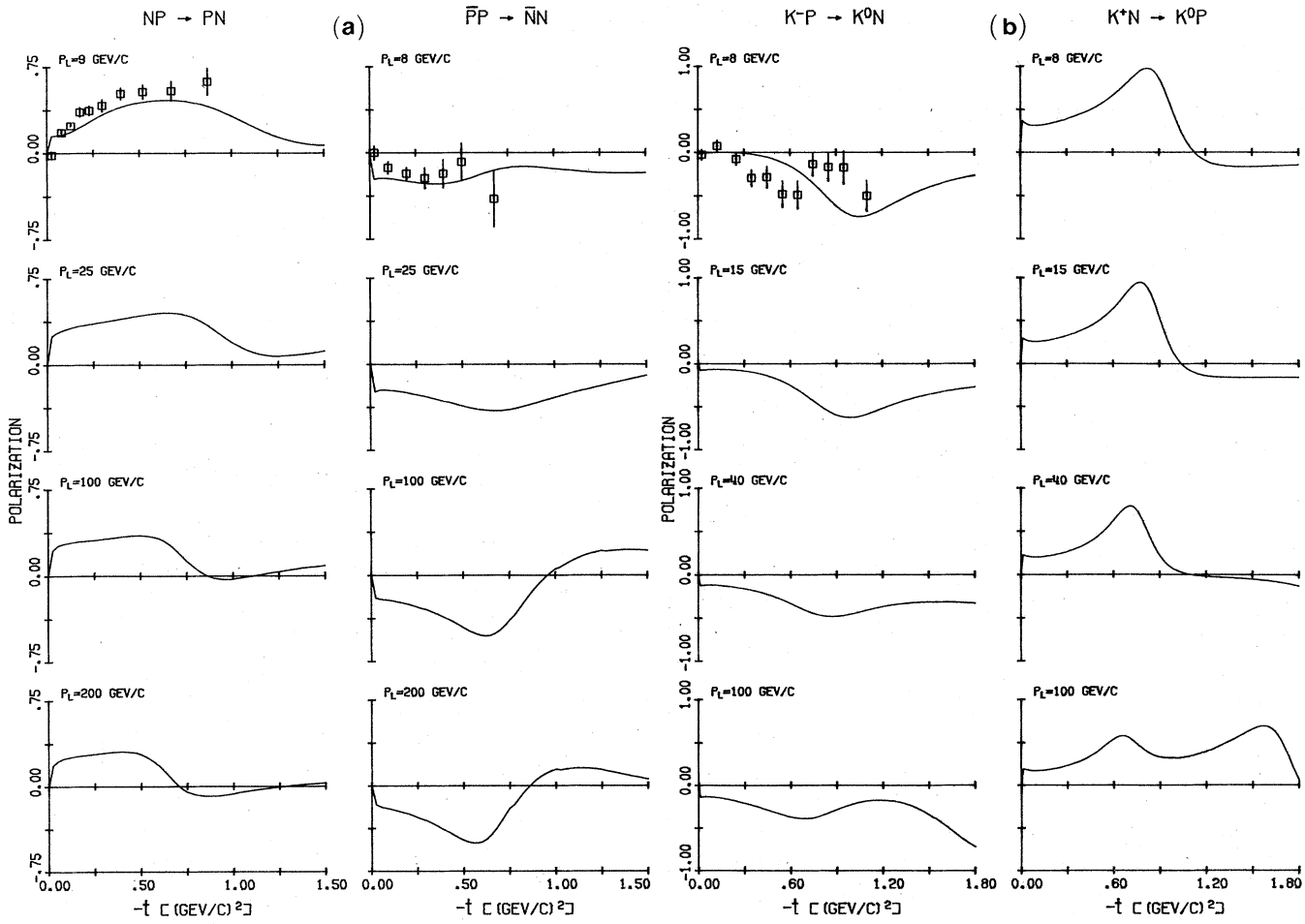

FIG. 34. Polarizations for NN and KN charge exchange. See discussion of Sec. VIII. Data from Abolins *et al.* (1973) and LeDu *et al.* (1973) for NN, and Beusch *et al.* (1973) for $\bar{K}N$.

with associated helicities λ_a, λ_b, λ_c, λ_d. There are $(2\lambda_a+1)\cdots(2\lambda_d+1)$ independent amplitudes ($2\lambda+1\to 2$ for a zero mass particle). We assume scattering in the x–z plane, with $\vec{a}$ along $+z$, in the c.m. system, and a scattering into c via an angle θ.

Parity conservation requires

$$M_{-\lambda_c-\lambda_d;-\lambda_a-\lambda_b}=\eta_a\eta_b\eta_c\eta_d(-1)^{S_a+S_b-S_c-S_d}\times(-1)^{(\lambda_c-\lambda_a)-(\lambda_d-\lambda_b)}M_{\lambda_c\lambda_d;\lambda_a\lambda_b}(s,t) \tag{A1}$$

and reduces approximately in half the number of independent amplitudes. Time reversal invariance gives

$$M_{\lambda_c\lambda_d;\lambda_a\lambda_b}(s,t)=(-1)^{\lambda_c-\lambda_d-\lambda_a+\lambda_b}M_{\lambda_a\lambda_b;\lambda_c\lambda_d}(s,t). \tag{A2}$$

If the particles scattering are identical or related by isospin or G parity, further restrictions can follow; the NN case is the main one of practical interest and we discuss it explicitly below.

To write the SCHA for exchange of any states of definite naturality ($P(-1)^J$) proceed as follows; these are the Reggeon poles in our case.

The Reggeon pole amplitude is given by

$$R^r_{\lambda_c\lambda_d;\lambda_a\lambda_b}(s,t)=\pm(-t)^{(n+x)/2}\gamma_{car}(t)\gamma_{dbr}(t)2\Gamma\left(\frac{J-\alpha_r(t)}{2}\right)\times e^{-i\pi(\alpha-J)/2}s^{\alpha_r(t)}. \tag{A3}$$

In Eq. (A3) R is the Reggeon pole amplitude, $\alpha(t)$ the Reggeon trajectory, J the spin of the lowest physical state on the trajectory ($J=0$ for π, $J=1$ for ρ, $J=\frac{1}{2}$ for N, etc.), n is the net helicity flip and x the extra flip to guarantee extra powers of t required by parity arguments; $n=|(\lambda_c-\lambda_a)-(\lambda_d-\lambda_b)|$ and $x+n=|\lambda_c-\lambda_a|+|\lambda_d-\lambda_b|$. Amplitudes with definite parity exchange must vanish as $(-t)^{(n+x)/2}$, while a general SCHA only need vanish as $(-t)^{n/2}$. The gamma function gives particle poles at every other integer along the trajectory. The factorizable residues $\gamma(t)$ (and the trajectory) are the main objects not yet calculated by theory, and we have to parametrize them (see text); they depend on helicities. The overall ± sign of a Reggeon needs to be fixed by additional physics.

When several exchanges contribute they are added together

$$R_{\lambda_c\lambda_d;\lambda_a\lambda_b}(s,t)=\sum_r R^r_{\lambda_c\lambda_d;\lambda_a\lambda_b}. \tag{A4}$$

Next one carries out the absorption procedure. Then the observables are constructed.

A. Pole residues and coupling constants

Before we do that we summarize our measured residues. Once we have determined a form for $\gamma_{car}(t)$, etc.,

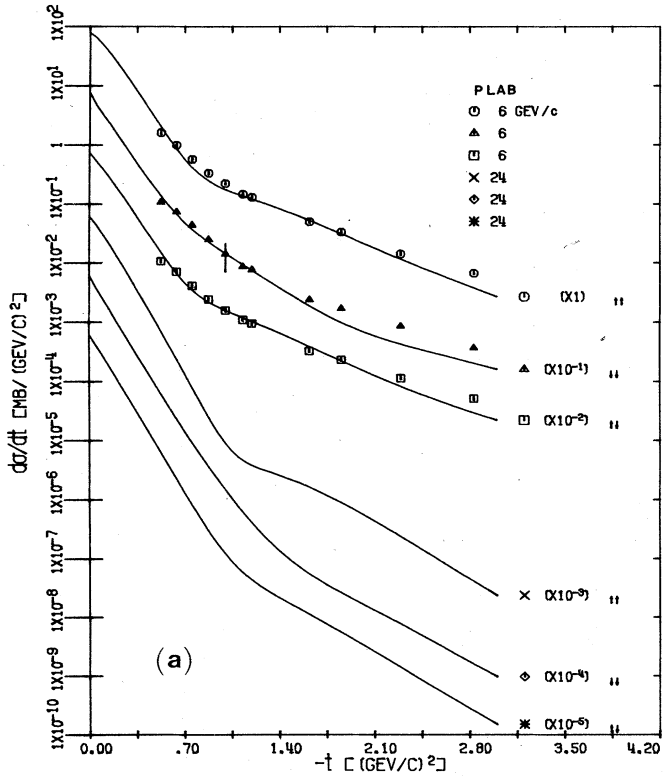

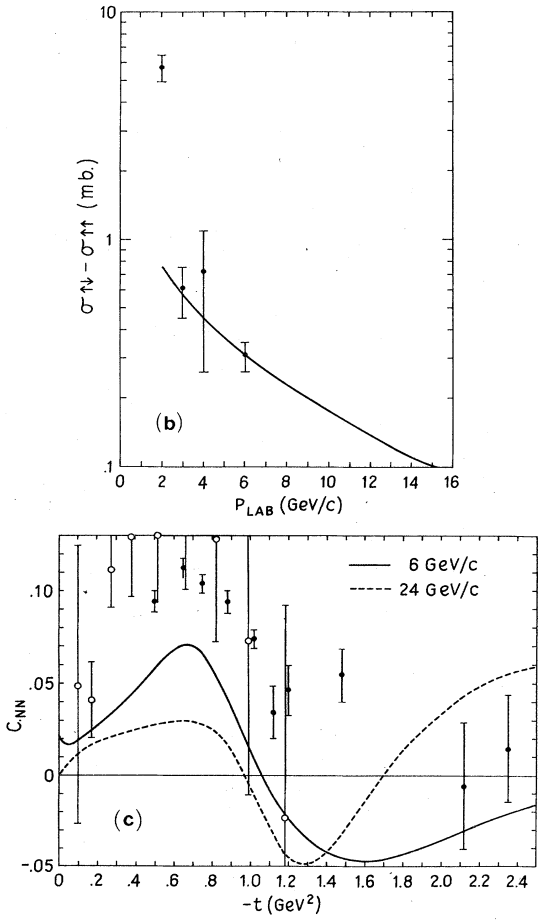

FIG. 35. Two spin observables from ANL experiments and predictions. See discussion of Sec. VIII. Data from Miettinen, to be published.

it can be used repeatedly in any process in which the *car* vertex appears. The form of the residues is discussed in Sec. IV.A. The $t=0$ value of γ is its main property and is a measure of the coupling strengths at $t=0$. Someone not wishing to use our full amplitudes can still use our $t\sim 0$ results profitably.

$$R^{r}_{\lambda_c\lambda_d;\lambda_a\lambda_b}(s,t\sim 0)=(-t)^{(n+x)/2}g_{car}g_{dbr}\frac{1}{m_r^2-t}\times e^{-i\pi(\alpha-J)/2}s^{\alpha} \tag{A5}$$

or near the pole,

$$R^{r}_{\lambda_c\lambda_d;\lambda_a\lambda_b}/(-t)^{(n+x)/2}\simeq g_{car}g_{dbr}s^{J}/(m_2^{r}-t)\,. \tag{A6}$$

We have written 2Γ as $1/(m^2-t)$ and expressed this in Feynman diagram form to facilitate comparisons.

The results for the g's are summarized in Table I.

Derivation

To avoid any confusion, we illustrate the relations between these SCHA and the Feynman diagrams for a few cases, and the technique for obtaining them. Extensive use is made of factorization and the high-energy approximation. To obtain an exchange contribution to leading order in s it is only necessary to retain the $\delta_{\mu\nu}$ propagator terms; the other parts of any propagator give daughter corrections. This section can be ignored by anyone not interested in obtaining our results or others for himself. Its purpose is to allow our couplings to be easily related to Lagrangian couplings, etc. Normalization conventions are given below.

For spinless particle σ exchange, the Feynman amplitude for $\pi\pi$ scattering is

$$M=g^2_{\pi\pi\sigma}/(m_\sigma^2-t) \tag{A7}$$

which gives a result in the form of Eq. (A.5) with $g_{car}=g_{dbr}=g_{\pi\pi\sigma}$. Similarly, for ρ exchange in $\pi\pi$ scattering

$$M=-\frac{g^2_{\pi\pi\rho}}{m_\rho^2-t}(P_c+P_a)\cdot(P_b+P_d)=\frac{g^2_{\pi\pi\rho}}{m_\rho^2-t}(s-u)\simeq\frac{2g^2_{\pi\pi\rho}}{m_\rho^2-t}s. \tag{A8}$$

Thus at a $\pi\pi\sigma$ vertex one uses $g_{\pi\pi\sigma}$ to get the SCHA, while at a $\pi\pi\rho$ vertex one uses $\sqrt{2}\ g_{\pi\pi\rho}$ to get the ρ exchange SCHA. Note that the signs are not determined here. With this normalization $\Gamma_\rho=q^3g^2_{\rho\pi\pi}/6\pi m_\rho^2$ so $g_{\rho\pi\pi}\simeq 6$ at the pole. Presumably then we expect $g_{\rho\pi\pi}$ somewhat less than 6 at $t=0$.

Next consider $\pi^-p\to\pi^0n$, with ρ exchange

$$M=-ig_{\rho\pi\pi}(P_c+P_a)_\mu\frac{\delta_{\mu\nu}}{m_\rho^2-t}\bar{u}(d)\times\left(\sqrt{2}\,G_V^\rho\gamma_\nu+\frac{\sqrt{2}\,G_T^\rho}{m_p+m_n}\sigma_{\nu\alpha}r_\alpha(b)\right)u(b). \tag{A9}$$

Note a $\sqrt{2}$ is inserted for the charged ρNN coupling so G_V^ρ is the $pp\rho^0$ coupling, etc. From this one obtains helicity amplitudes

$$M_{++}(s,t)=2\sqrt{2}\,g_{\rho\pi\pi}G_V^\rho\,s/(m_\rho^2-t), \tag{A10}$$

$$M_{+-}(s,t)=-\sqrt{-t}\,2\sqrt{2}\,g_{\rho\pi\pi}(G_T^\rho/2m_N)s/(m_\rho^2-t). \tag{A11}$$

Thus, apart from sign questions, one uses $2G_V^\rho$ at a $pn\rho^+$ nonflip vertex and $2G_T^\rho/2M_N$ at a $pn\rho^+$ helicity flip vertex. A consistent set of sign conventions is recorded in Table I.

The power of factorization now appears if one wishes to do $np\to pn$, for example. It is not necessary to calculate any further but only to put $2G_V^\rho$ or $2G_T^\rho/2M_N$ at each vertex. Thus one can immediately write the appropriate form of Eq. (A.5)

$$\varphi_1(s,t)=\langle++|M|++\rangle=4(G_V^\rho)^2s/(m_\rho^2-t) \tag{A12}$$

$$\varphi_2(s,t)=\langle--|M|++\rangle=(G_T^\rho)^2st/m_N^2(m_\rho^2-t)\ \text{etc.} \tag{A13}$$

Again, considerable care is needed to get signs correct (see Table I).

In Table I, we have given the SCHA vertices for a number of common vertices. From these, one can build most experimentally accessible reactions. The forms of the vertices for Feynman–Born diagrams are summarized in the table caption; note that these forms are only of interest to someone wishing to relate couplings to a different application (for example to determine their value), and can be ignored by anyone who wishes to deal only with two-body reactions by our method.

The above analysis shows how to write the pole terms for an arbitrary reaction. To summarize, list the independent helicity amplitudes, using parity and other symmetry operations to give relations among amplitudes where appropriate. Determine n and x. Obtain SCHA couplings from our Table I, Columns one or two, or simply use an expression for the couplings which you measure and later someone interprets. This gives a set of Reggeon poles in the form of Eq. (A.5). The general form is then obtained from Eqs. (3.3) and (3.4) in the text.

Having a set of Reggeon poles, one now constructs the complete amplitudes as described in the text (or one could use the poles directly as amplitudes in the following). Then, one wants to compute the observables. We give expressions for the standard ones here.

B. Observables

For unpolarized particles, the observables (and our normalization) are given by

$$\sigma_T=-\frac{1}{2qW}\frac{1}{(2s_a+1)(2s_b+1)}\sum_{\substack{\lambda_a\\\lambda_b}}\mathrm{Im}\langle\lambda_a\lambda_b|M(t=0)|\lambda_a\lambda_b\rangle \tag{A14}$$

$$d\sigma/dt=\sum_{\lambda_a\lambda_b\lambda_c\lambda_d}|\langle\lambda_c\lambda_d|M|\lambda_a\lambda_b\rangle|^2/64\pi q^2s(2s_a+1)(2s_b+1), \tag{A15}$$

where $2s+1=2$ for a massless particle, and

$$\rho_{\lambda_c'\lambda_c}=\frac{\sum_{\lambda_a\lambda_b\lambda_d}\langle\lambda_c\lambda_d|M|\lambda_a\lambda_b\rangle\langle\lambda_c'\lambda_d|M|\lambda_a\lambda_b\rangle^*}{\sum_{\lambda_a\lambda_b\lambda_c\lambda_d}|\langle\lambda_c\lambda_d|M|\lambda_a\lambda_b\rangle|^2} \tag{A16}$$

is the helicity density matrix. For clarity in this appendix, we have written $M_{\lambda_c\lambda_d;\lambda_a\lambda_b}\equiv\langle\lambda_c\lambda_d|M|\lambda_a\lambda_b\rangle$. If

information is obtained about two or more helicities, one forms correlation density matrices by summing over whatever helicities are unobserved.

When transverse polarizations of spin $\frac{1}{2}$ particles are observed, we proceed as follows. Whenever conventions matter, we will choose the scattering to be in the x–z plane, with a incident along the $+z$ direction, b thus incident along the $-z$ direction. Let $|\uparrow\rangle$ and $|\downarrow\rangle$ be eigenstates of σ_y. Then expressing these in terms of helicity states we have

$$\left.\begin{aligned} |a^{\uparrow}_{\downarrow}\rangle &= \frac{|+\rangle \pm i|-\rangle}{\sqrt{2}} \\ |b^{\uparrow}_{\downarrow}\rangle &= \frac{|-\rangle \pm |+\rangle}{\sqrt{2}} \\ \langle c^{\uparrow}_{\downarrow}| &= \frac{\langle + | \mp i \langle - |}{\sqrt{2}} \\ \langle d^{\uparrow}_{\downarrow}| &= \frac{\langle - | \mp i \langle + |}{\sqrt{2}} \end{aligned}\right\}. \tag{A17}$$

With these expressions one can express observables in terms of helicity amplitudes and compute them in the model. For example,

$$\sigma_T(\uparrow\uparrow) = -\,\mathrm{Im}\langle\uparrow\uparrow|M|\uparrow\uparrow\rangle_{t=0}/2qW \tag{A18}$$

which, for NN scattering, becomes

$$\sigma_T(\uparrow\uparrow) = -(\varphi_1(0)+\varphi_2(0)+\varphi_3(0))/4qW. \tag{A19}$$

Similarly, for a transversely polarized target,

$$\begin{aligned} \frac{d\sigma_{\uparrow,\downarrow}(\theta)}{dt} &= \frac{1}{64\pi q^2 s}\frac{1}{2s_a+1}\sum_{\lambda_a\lambda_c\lambda_d}|\langle\lambda_c\lambda_d|M|\lambda_a\uparrow,\downarrow\rangle|^2 \\ &= \frac{1}{128\pi q^2 s}\frac{1}{2s_a+1} \\ &\quad\times\sum_{\lambda_a\lambda_c\lambda_d}|\langle\lambda_c\lambda_d|M|\lambda_a -\rangle \pm i\langle\lambda_c\lambda_d|M|\lambda_a +\rangle|^2. \end{aligned} \tag{A20}$$

Normally, either

$$P^{\mathrm{LR}} \equiv \frac{d\sigma_{\uparrow}(\theta)/dt - d\sigma_{\uparrow}(-\theta)/dt}{d\sigma_{\uparrow}(\theta)/dt + d\sigma_{\uparrow}(-\theta)/dt} \tag{A21}$$

or

$$P^{\mathrm{UD}} \equiv \frac{d\sigma_{\uparrow}(\theta)/dt - d\sigma_{\downarrow}(\theta)/dt}{d\sigma_{\uparrow}(\theta)/dt + d\sigma_{\downarrow}(\theta)/dt} \tag{A22}$$

are measured and both are referred to as "the polarization." To find the behavior of a given amplitude under $\theta\to-\theta$, one can use the Jacob–Wick expansion

$$\langle\lambda_c\lambda_d|M|\lambda_a\lambda_b\rangle = \sum_J (2J+1)d^J_{\lambda\mu}(\theta)M^J_{\lambda_c\lambda_d;\lambda_a\lambda_b}, \tag{A23}$$

$$\lambda = \lambda_a - \lambda_b, \quad \mu = \lambda_c - \lambda_d,$$

and the known property

$$d^J_{\lambda\mu}(\theta) = (-1)^{\lambda-\mu}d^J_{\lambda\mu}(-\theta). \tag{A24}$$

The two polarizations P^{LR} and P^{UD} will generally be identical if only one independent amplitude exists with odd net helicity flip, and they will be different if there is more than one way to get odd net helicity flip.

Proceeding along these lines one can express any observable in terms of the amplitudes and thus calculate the predictions of any model for the amplitudes. [Additional observables are obtained when spins are polarized in the scattering plane (one then also uses eigenstates of σ_x as above); for $0^{-}\frac{1}{2}^{+}\to 0^{-}\frac{1}{2}^{+}$ reactions the additional observables are called R and A.]

For example, for $0^{-}\frac{1}{2}^{+}$ we get

$$\begin{aligned} d\sigma_{\uparrow,\downarrow}/dt &= [|M_{+-} \pm iM_{++}|^2 + |M_{--} \pm iM_{-+}|^2]/128\pi q^2 s \\ &= [|M_{++}|^2 + |M_{+-}|^2 \mp 2\mathrm{Im}M_{++}M^*_{+-}]/64\pi q^2 s, \end{aligned}$$

so

$$P^{\mathrm{LR}} = -2\mathrm{Im}M_{++}M^*_{+-}/[|M_{++}|^2 + |M_{+-}|^2] = P^{\mathrm{UD}}. \tag{A25}$$

We list here the results for several common reactions:

1. $0^{-}\frac{1}{2}\to 0^{-}\frac{1}{2}^{+}$

$$d\sigma/dt = 0.389(|M_{++}|^2 + |M_{+-}|^2)/64\pi q^2 s \ \mathrm{mb/GeV^2}, \tag{A26}$$

$$\sigma_T = -\,0.389\mathrm{Im}M_{++}(t=0)/2qW \ \mathrm{mb}, \tag{A27}$$

$$P = -\,2\mathrm{Im}(M_{++}M^*_{+-})/(|M_{++}|^2 + |M_{+-}|^2). \tag{A28}$$

Parity conservation gives $M_{--} = M_{++}, M_{+-} = -M_{-+}$.

$$r = (|M_{++}|^2 - |M_{+-}|^2)/(|M_{++}|^2 + |M_{+-}|^2), \tag{A29}$$

$$a = 2\mathrm{Re}M_{++}M^*_{+-}/(|M_{++}|^2 + |M_{+-}|^2), \tag{A30}$$

$$R = -r\cos\theta_R - a\sin\theta_R, \tag{A31}$$

$$A = r\sin\theta_R - a\cos\theta_R, \tag{A32}$$

where θ_R is the $\frac{1}{2}^{+}$ recoil lab angle

$$\tan\theta_R = (1-\cos^2\theta)^{1/2}/(E_b/m_b)[1-(m_b/E_b)^2/(1-(m_d/E_d)^2) - \cos\theta]^{1/2} \tag{A33}$$

with b and d the target and recoil $\frac{1}{2}^{+}$ particles. R and A are the conventionally reported observables, while r and a are the natural ones to calculate.

2. $NN\to NN$ *and* $\frac{1}{2}^{+}\frac{1}{2}^{+}\to\frac{1}{2}^{+}\frac{1}{2}^{+}$

Here we give some observables for nucleon–nucleon scattering. At first we treat the general case and then specialize to $NN\to NN$ by imposing the identical particle constraint. There are six independent helicity amplitudes

$$\left.\begin{aligned} &\langle++|M|++\rangle = \varphi_1 = \langle--|M|--\rangle \\ &\langle++|M|+-\rangle = \varphi_5 = -\langle--|M|-+\rangle \\ &-\langle+-|M|++\rangle = \varphi_5 = \langle-+|M|--\rangle \\ &\langle++|M|--\rangle = \varphi_2 = \langle--|M|++\rangle \\ &\langle+-|M|+-\rangle = \varphi_3 = \langle-+|M|-+\rangle \\ &\langle+-|M|-+\rangle = \varphi_4 = \langle-+|M|+-\rangle \\ &-\langle++|M|-+\rangle = \varphi'_5 = \langle--|M|+-\rangle \\ &-\langle+-|M|--\rangle = \varphi'_5 = \langle-+|M|++\rangle \end{aligned}\right\}. \tag{A34}$$

For $NN\to NN$, time reversal invariance and identical particle antisymmetrization give $\varphi'_5 = \varphi_5$. For a more general reaction such as $\Lambda p\to\Lambda P$, $\Sigma p\to\Sigma p$, etc., it is in principle possible to have $\varphi'_5 \neq \varphi_5$. This would happen, for example, if in addition to the natural parity exchanges (ρ, A_2, ω, f) one had a significant contribution

from an unnatural parity exchange with the quantum numbers of B or A_1; natural and unnatural parity would interfere with opposite sign in φ_5 and in φ_5'.

The cross section is

$$\frac{d\sigma}{dt} = \frac{1}{2}\frac{0.389}{64\pi q^2 s}\left[|\varphi_1|^2 + |\varphi_2|^2 + |\varphi_3|^2 + |\varphi_4|^2 + 2|\varphi_5|^2 + 2|\varphi_5'|^2\right] \text{ mb/GeV}^2 \tag{A35}$$

$$\sigma_T = -\frac{0.389}{4qW}\,\mathrm{Im}(\varphi_1(0) + \varphi_3(0)) \text{ mb} \tag{A36}$$

where the φ_i are labeled as in Eq. (A34).

For transverse polarizations, some precision is necessary. We distinguish by a subscript the particle whose spin is measured; and we distinguish between a left-right asymmetry with a fixed "target" spin (denoted by LR) and an up-down variation of spin with scattering detected at a fixed angle (denoted by UD). Then defining

$$P \equiv \frac{-2\mathrm{Im}[(\varphi_1+\varphi_3)\varphi_5^* + (\varphi_2-\varphi_4)\varphi_5'^*]}{|\varphi_1|^2|\varphi_2|^2|\varphi_3|^2 + |\varphi_4|^2 + 2|\varphi_5|^2 + 2|\varphi_5'|^2}, \tag{A37}$$

$$P' \equiv \frac{-2\mathrm{Im}[(\varphi_1+\varphi_3)\varphi_5'^* + (\varphi_2-\varphi_4)\varphi_5^*]}{|\varphi_1|^2 + |\varphi_2|^2 + |\varphi_3|^2 + |\varphi_4|^2 + 2|\varphi_5|^2 + 2|\varphi_5'|^2} \tag{A38}$$

we get

$$P_b^{\mathrm{LR}} = P = P_b^{\mathrm{UD}} \tag{A39}$$

(this is the conventional left-right asymmetry on a polarized target);

$$P_C^{\mathrm{UD}} = P' \tag{A40}$$

(this is, say, what is measured by the polarization of scattered Λ's at an angle θ in $\Lambda p \to \Lambda p$);

$$P_a^{\mathrm{UD}} = P' = P_a^{\mathrm{LR}} \tag{A41}$$

(this is the case with a polarized beam), etc.

[For completeness, we sketch one derivation. The reader can carry out any others of interest. For a target b transversely polarized we have

$$d\sigma_\uparrow(\theta)/dt = \sum_{\lambda_a\lambda_c\lambda_d} |\langle\lambda_c\lambda_d|M|\lambda_a\uparrow\rangle|^2 = \sum_{\lambda_a\lambda_c\lambda_d} |\langle\lambda_c\lambda_d|M|\lambda_a -\rangle + i\langle\lambda_c\lambda_d|M|\lambda_a +\rangle|^2$$

$$= \sum_{\lambda_c\lambda_d}\{|\langle\lambda_c\lambda_d|M|++\rangle|^2 + |\langle\lambda_c\lambda_d|M|-+\rangle|^2 + |\langle\lambda_c\lambda_d|M|+-\rangle|^2 + |\langle\lambda_c\lambda_d|M|--\rangle|^2$$

$$-2\,\mathrm{Im}(\langle\lambda_c\lambda_d|M|++\rangle\langle\lambda_c\lambda_d|M|+-\rangle^* + \langle\lambda_c\lambda_d|M|-+\rangle\langle\lambda_c\lambda_d|M|--\rangle^*)\}$$

$$= 2(|\varphi_1|^2 + |\varphi_2|^2 + |\varphi_3|^2 + |\varphi_4|^2 + 2|\varphi_5|^2 + 2|\varphi_5'|) - 4\,\mathrm{Im}(\varphi_1+\varphi_3)\varphi_5^* - 4\,\mathrm{Im}(\varphi_2-\varphi_4)\varphi_5'^*.$$

$d\sigma_\downarrow(-\theta)/dt$ is obtained by $\varphi_5 \to -\varphi_5$, $\varphi_5' \to -\varphi_5'$, from Eqs. (A.23)–(A.24). Thus

$$P_b^{\mathrm{LR}} \equiv \frac{d\sigma_\uparrow(\theta)/dt - d\sigma_\downarrow(-\theta)/dt}{d\sigma_\uparrow(\theta)/dt + d\sigma_\downarrow(-\theta)/dt} = P, \tag{A42}$$

as stated above.]

Remember, for $NN \to NN$ (i.e., $pp \to pp$, $np \to pn$, $\bar{p}p \to \bar{p}p$, $\bar{p}p \to \bar{n}n$, etc.) $\varphi_5 \equiv \varphi_5'$ and these reduce to the standard formulas.

Because of the availability of the polarized beam facility at Argonne National Laboratory, we list here a few formulas for NN experiments with both beam and target polarized, from Kane and Sukhatme, 1974; some results for $pp \to \Delta N$ are given there too. Further results can be obtained in that reference and by the techniques outlined above. For the connection with traditional names for observables, see Halzen and Thomas, 1974.

$$\sigma_T(\uparrow\uparrow) = -\frac{1}{2qW}\,\mathrm{Im}\langle\uparrow\uparrow|M|\uparrow\uparrow\rangle_{t=0}$$

$$= -\frac{1}{4qW}\,\mathrm{Im}(\varphi_1(0) + \varphi_2(0) + \varphi_3(0)) = \sigma_T(\downarrow\downarrow), \tag{A43}$$

$$\sigma_T(\uparrow\downarrow) = \sigma_T(\downarrow\uparrow) = -\frac{1}{4qW}\,\mathrm{Im}(\varphi_1(0) + \varphi_3(0) - \varphi_2(0)), \tag{A44}$$

$$\sigma_T(\uparrow\uparrow) + \sigma_T(\uparrow\downarrow) = 2\sigma_T, \tag{A45}$$

$$\sigma_T(\uparrow\downarrow) - \sigma_T(\uparrow\uparrow) = \frac{1}{2qW}\,\mathrm{Im}\varphi_2(0), \tag{A46}$$

$$\frac{d\sigma(\uparrow\downarrow)}{dt} = \frac{d\sigma(\downarrow\uparrow)}{dt}, \tag{A47}$$

$$\frac{d\sigma(\uparrow\downarrow)}{dt} = \frac{1}{128\pi q^2 s}\left[|\varphi_1 - \varphi_2|^2 + |\varphi_3 + \varphi_4|^2\right], \tag{A48}$$

$$\frac{d\sigma(\uparrow\uparrow)}{dt} = \frac{1}{128\pi q^2 s}\left[|\varphi_1 + \varphi_2 - 2i\varphi_5|^2 + |\varphi_3 - \varphi_4 - 2i\varphi_5|^2\right], \tag{A49}$$

$$\frac{d\sigma(\downarrow\downarrow)}{dt} = \frac{1}{128\pi q^2 s}\left[|\varphi_1 + \varphi_2 + 2i\varphi_5|^2 + |\varphi_3 - \varphi_4 + 2i\varphi_5|^2\right], \tag{A50}$$

$$\Delta(d\sigma/dt) \equiv d\sigma(\uparrow\uparrow)/dt + d\sigma(\downarrow\downarrow)/dt - d\sigma(\uparrow\downarrow)/dt - d\sigma(\downarrow\uparrow)/dt$$

$$= 4C_{NN} = \frac{1}{16\pi q^2 s}\left[2|\varphi_5|^2 + \mathrm{Re}(\varphi_1\varphi_2^* - \varphi_3\varphi_4^*)\right]. \tag{A51}$$

3. $0^-\frac{1}{2}^+ \to 1^-\frac{1}{2}^+$

For vector meson production there are six independent helicity amplitudes if parity is conserved. For reactions like $\pi N \to \rho N$ one is of course measuring $\pi N \to \pi\pi N$. The $\pi\pi$ pair can be in other partial waves than 1^-, so to be complete we should give the full formalism for the coherent production of several partial waves. We will content ourselves with just the 1^- partial waves, however, as the full case is well known to the small set of experts who use it.

We label our amplitudes $M^{\lambda_c}_{\lambda_d\lambda_b}$ with $\lambda_c = 1, 0, -1$ and $\lambda_b, \lambda_d = \frac{1}{2}, -\frac{1}{2}$. Parity gives

$$M^{-\lambda_c}_{-\lambda_d-\lambda_b} = (-1)^{1+\lambda_c-\lambda_d+\lambda_b} M^{\lambda_c}_{\lambda_d\lambda_b}. \tag{A52}$$

For definite parity exchanges, one can revserse signs at each vertex. We give the results for R to emphasize that they hold only for the definite parity poles and not for the full amplitudes in general; and in general they only hold to leading order in s,

$$\left\{\begin{matrix}\text{Natural}\\ \text{Unnatural}\end{matrix}\right\}\ \text{Parity Exchange}$$

$$\rightarrow \begin{cases} R^{-\lambda_c}_{\lambda_d\lambda_b} = \pm(-1)^{1+\lambda_c} R^{\lambda_c}_{\lambda_d\lambda_b} \\ R^{\lambda_c}_{-\lambda_d-\lambda_b} = \pm(-1)^{\lambda_d-\lambda_b} R^{\lambda_c}_{\lambda_d\lambda_b}. \end{cases} \tag{A53}$$

Remember the full amplitudes vanish at $t=0$, by angular momentum conservation, as $(-t)^{n/2}$, while the poles vanish as $(-t)^{(n+x)/2}$.

From these parity relations for the poles, some quite general and testable predictions follow:

(a) for Natural Parity Exchange (NPE) one has from Eq. (A53)

$$R^0_{\lambda_d\lambda_b} = -R^0_{\lambda_d\lambda_b} = 0\,. \tag{A54}$$

Consequently $M^0_{\lambda_d\lambda_b}=0$, and to leading order in s no resonances with s-channel helicity $\lambda_c=0$ are produced by NPE (the statement holds for particle c being a natural parity resonance of any spin).

(b) NPE gives $R^1_{1/2\,1/2} = R^1_{-1/2\,-1/2}$. Since both have $n=1$ they undergo the same absorption and thus, independent of details of form, we predict for NPE (M is for full amplitudes, R for definite parity poles)

$$M^1_{1/2\,1/2}(s,t) = M^1_{-1/2\,-1/2}(s,t)\,. \tag{A55}$$

(c) Similarly, UPE gives

$$-M^1_{1/2\,1/2}(s,t) = M^1_{-1/2\,-1/2}(s,t)\,. \tag{A56}$$

Next we summarize the observables. Define

$$N = |M^1_{1/2\,1/2}|^2 + |M^{-1}_{1/2\,1/2}|^2 + |M^1_{-1/2\,1/2}|^2 + |M^{-1}_{-1/2\,1/2}|^2 + |M^0_{1/2\,1/2}|^2 + |M^0_{-1/2\,1/2}|^2\,. \tag{A57}$$

Then,

$$d\sigma/dt = 0.389 N/64\pi q^2 s \text{ mb/GeV}^2\,, \tag{A58}$$

$$NP_b^{\mathrm{UD}} = -2\,\mathrm{Im}[M^{1*}_{1/2\,1/2}M^1_{1/2\,1/2} - M^{1*}_{-1/2\,-1/2}M^1_{-1/2\,1/2} + M^{0*}_{1/2\,1/2}M^0_{1/2\,-1/2}]\,, \tag{A59}$$

$$NP_d^{\mathrm{UD}} = -2\,\mathrm{Im}[M^{1*}_{1/2\,1/2}M^1_{-1/2\,1/2} - M^{1*}_{-1/2\,-1/2}M^1_{1/2\,-1/2} + M^{0*}_{1/2\,1/2}M^0_{-1/2\,1/2}]\,. \tag{A60}$$

Note that for NPE even with absorption we get

$$P_b^{\mathrm{UD}} = P_d^{\mathrm{UD}} \tag{A61}$$

from (a) and (b) above.

The s-channel density matrix is given by

$$2N\rho_{\lambda_c\lambda_c'} = \sum_{\lambda_d\lambda_b} M^{\lambda_c}_{\lambda_d\lambda_b} M^{\lambda_c'*}_{\lambda_d\lambda_b} \tag{A62}$$

and, using the parity relations and hermiticity, we get

$$N\rho_{00} = |M^0_{1/2\,1/2}|^2 + |M^0_{1/2\,-1/2}|^2\,, \tag{A63}$$

$$2N\rho_{10} = (M^1_{1/2\,1/2} - M^1_{-1/2\,-1/2})M^{0*}_{1/2\,1/2} + (M^1_{1/2\,-1/2} - M^1_{-1/2\,1/2})M^{0*}_{1/2\,-1/2}\,, \tag{A64}$$

$$N\rho_{1\,-1} = \mathrm{Re}(M^1_{1/2\,1/2}M^{1*}_{-1/2\,-1/2} - M^1_{1/2\,-1/2}M^{1*}_{-1/2\,1/2})\,. \tag{A65}$$

REFERENCES

Abolins, M. A., M. T. Lin, R. C. Ruchti, J. G. Horowitz, R. C. Kammerud, N. W. Reay, K. Reibel, N. R. Stanton, K. W. Edwards, D. G. Crabb, and J. R. O'Fallon, 1973, Phys. Rev. Lett. **30**, 1183.

Akerlof, C. W., *et al.*, 1975, Phys. Rev. Lett. **35**, 1406.

Ader, J. P., R. Peschanski, R. Lacaze, G. Cohen-Tannoudji, and G. Gilain, 1974, CERN preprint TH1903.

Arnold, R. C., 1967, Phys. Rev. **153**, 1523.

Amabts, I., D. S. Ayres, R. Diebold, A. F. Greene, S. L. Kramer, A. Lesnik, D. R. Rust, C. E. W. Ward, A. B. Wicklund, and D. D. Jovanovitch, 1973, ANL/HEP 7329.

Antipov, Yu. M., 1972, in *Proceedings of the Fourth International Conference on High Energy Collisions*, Oxford, 1972 (Rutherford Laboratory, Chilton, Didcot, Berks, UK), Vol. 2, p. 230.

Astbury, P., *et al.*, 1966 Phys. Lett. **23**, 396.

Barger, V., 1974, in *Proceedings of the XVII International Conference on High Energy Physics*, London, 1974 (Science Research Council, Rutherford, Chilton, Didcot, Oxon, UK), p. I-193.

Barger, V., and A. D. Martin, 1972, Phys. Lett. B **39**, 379.

Barnes, A. V., D. J. Mellema, A. V. Tollestrup, R. L. Walker, O. L. Dahl, R. A. Johnson, R. W. Kenney, and M. Pripstein, 1974, preprint CALT-68-465.

Bartenev, V., 1973, NAL-PUB 73/73 Exp.

Benary, O., L. R. Price, and G. Alexander, 1970, UCRL-20000 NN.

Berman, S., and M. Jacob, 1965, Phys. Rev. **139B**, 1023.

Berger, E. L., and G. C. Fox, 1970, Phys. Rev. Lett. **25**, 1783.

Beusch, W., *et al.*, 1973, Phys. Lett. B **46**, 477.

Beznozikh, G., *et al.*, 1973, Nucl. Phys. B **54**, 78.

Birnbaum, D., *et al.*, 1969, Phys. Rev. Lett. **23**, 663.

Blankenbecler, R., J. R. Fulco, and R. Suger, 1974, Phys. Rev. D **9**, 736.

Block, M., I. Drummond, and G. L. Kane, 1973, University of Michigan preprint UM HE 73-17.

Bockmann, K., *et al.*, 1966, Nuovo Cimento A **42**, 954.

Bolotov, V. N., *et al.*, 1973, IHEP 73-58.

Bonamy, P., P. Borgeaud, M. Crozon, J. P. Guillaud, O. Guisan, P. Le Du, P. Sonderegger, J. K. Bienlein, S. Mango, L. Paul, and H. Dinter, 1973, Nucl. Phys. B **52**, 392.

Borghini, M., *et al.*, 1970, Phys. Lett. B **31**, 405.

Borghini, M., *et al.*, 1971a, Phys. Lett. B **36**, 493.

Borghini, M., *et al.*, 1971b, Phys. Lett. B **36**. 497.

Bracci, E., J. P. Droulez, E. Flaminio, J. D. Hansen, and D. R. O. Morrison, 1972, CERN/HERA 72-2.

Brandenburg, G. W., W. B. Johnson, D. W. G. S. Leith, J. S. Loos, G. J. Luste, J. A. J. Matthews, K. Moriyasu, W. M. Smart, F. C. Winkelmann, and R. J. Yamartino, 1974, Phys. Rev. D **9**, 1939.

Bronzan, J., G. L. Kane, and U. Sukhatme, 1974, Phys. Lett. B **49**, 272.

Carrol, A. S., *et al.*, 1975, Fermilab-Pub-75/51-Exp. 7100.104.

Carlson, C. E., and P. G. O. Freund, 1972, Phys. Lett. B **39**, 349.

Chase, R. C., E. Coleman, H. W. J. Courant, E. Marquit, E. W. Petraske, H. Romer, and K. Ruddick, 1969, Phys. Rev. Lett. **22**, 1137.

Cheng, H., and T. T. Wu, 1971, Phys. Rev. Lett. **24**, 1456.

Ciafaloni, M., and G. Marchesini, 1974, Nucl. Phys. B **71**, 493.

Cohen-Tannoudji, G., A. Morel, and H. Navelet, 1967, Nuovo Cimento, A **48**, 1075.

Cohen-Tannoudji, G., A. Morel, and Ph. Salin, 1968, Nuovo Cimento A **55**, 412.

Cohen-Tannoudji, G., C. Quigg, and G. L. Kane, 1972, Nucl. Phys. B **37**, 77.
Coletti, S., *et al.*, 1967, Nuovo Cimento A **49**, 479.
Collins, P. D. B., and R. A. Swetman, 1972, Lett. al Nuovo Cimento **5**, 793.
Collins, P. D. B., and A. Fitton, 1974, Nucl. Phys. B **68**, 125.
Dar, A., T. Watts, and V. Weisskopf, 1969, Nucl. Phys. B **13**, 477.
Davier, M., 1974, "Lectures on Amplitude Structure in Two and Quasi-Two-Body Processes," in Proceedings of SLAC 1974 Summer Institute on Particle Physics, SLAC–179, Vol. 1.
De Boer, W., R. C. Fernow, A. D. Krisch, H. E. Miettinen, T. A. Mulera, J. B. Roberts, K. M. Terwilliger, L. G. Ratner, and J. R. O'Fallon, 1975, Phys. Rev. Lett. **34**, 558.
Dick, L., *et al.*, 1972, Nucl. Phys. B **43**, 522.
Dick, L., *et al.*, 1973, Nucl. Phys. B **64**, 45.
Diebold, R., *et al.*, 1975, ANL–HEP–PR–75–25.
Durand, L., III, and T. Y. Chiu, 1965, Phys. Rev. **139B**, 646.
Engler, J., K. Horn, F. Monnig, P. Schludecker, W. Schmidt-Parzefall, H. Schopper, P. Sievers, and H. Ullrich, 1971, Phys. Lett. B **34**, 528.
Enstrom, J. E., T. Ferbel, P. F. Slattery, B. L. Werner, Z. G. T. Guiragossian, Y. Sumi, and T. Yoshida, 1972, LBL–58.
Estabrooks, P., and A. D. Martin, 1973, in *Proceedings of the Conference on $\pi\pi$ Scattering*, Tallahassee, 1973 (American Institute of Physics, New York), p. 357.
Fernow, R., S. W. Gray, A. D. Krisch, H. E. Miettinen, J. B. Roberts, K. M. Terwilliger, W. de Boer, E. F. Parker, L. G. Ratner, and J. R. O'Fallon, 1974, Phys. Lett. B **52**, 243.
Field, R., and D. P. Sidhu, 1974, Phys. Rev. D **10**, 89.
Finkelstein, J., 1969, Phys. Rev. Lett. **22**, 362.
Finkelstein, J., and F. Zachariasen, 1971, Phys. Lett. B **34**, 631.
Firestone, A., G. Goldhaber, A. Hirata, D. Lissauer, and G. Trilling, 1970, Phys. Rev. Lett. **25**, 958.
Foley, K. J., S. J. Lindenbaum, W. A. Love, S. Ozaki, J. J. Russel, and L. C. L. Yuan, 1963a, Phys. Rev. Lett. **11**, 503.
Foley, K. J., S. J. Lindenbaum, W. A. Love, S. Ozaki, J. J. Russel, and L. C. L. Yuan, 1963b, Phys. Rev. Lett. **11**, 425.
Foley, K. J., R. S. Jones, S. J. Lindenbaum, W. A. Love, S. Ozaki, E. D. Platner, C. A. Quarles, and E. H. Willen, 1967, Phys. Rev. Lett. **19**, 857.
Fox. G. F., and E. Leader, 1967, Phys. Rev. Lett. **18**, 628.
Fox, G. F., and C. Quigg, 1973, Annu. Rev. Nucl. Sci. **23**, 219.
Gault, F., A. D. Martin, and G. L. Kane, 1971, Nucl. Phys. B **32**, 429.
Goldberger, M. L., M. T. Grisaru, S. W. MacDowell, and D. Y. Wong, 1960, Phys. Rev. **120**, 2250.
Gottfried, K., and J. D. Jackson, 1964, Nuovo Cimento **33**, 309.
Greco, M., 1973, Nucl. Phys. B **63**, 398.
Gribov, V. N., I. Ya. Pomeranchuk, and K. A. Ter-Martirosyan, 1965, Phys. Rev. **139B**, 184.
Halzen, F., and C. Michael, 1971, Phys. Lett. B **36**, 367.
Halzen, F., and G. Thomas, 1974, Phys. Rev. D **10**, 344.
Halpern, M., M. Klein, and J. Shapiro, 1969, Phys. Rev. **188**, 2378.
Harari, H., 1971, Ann. Phys. (N.Y.) **63**, 432.
Harting, D., *et al.*, 1965, Nuovo Cimento **38**, 60.
Hartley, B. J., 1974, "Making the Absorption Model Dual," Niels Bohr Institute preprint (unpublished).
Hartley, B. J., and G. L. Kane, 1972, Phys. Lett. B **39**, 531.
Hartley, B. J., and G. L. Kane, 1973, Nucl. Phys. B **57**, 157. (This is referred to in the text as HK.)
Henyey, F. S., 1973, Nucl. Phys. B **73**, 429.
Henyey, F. S., G. L. Kane, J. Pumplin, and M. H. Ross, 1969, Phys. Rev. **182**, 1579.
Henyey, F. S., and G. L. Kane, 1975, "Spin, and the Energy Dependence and Parity of Absorbed Amplitudes," University of Michigan preprint UM HE 75–19.
Hill, D., 1973, Phys. Rev. Lett. **30**, 239.
Hoyer, P., 1974, "Finite Mass Sum Rules," invited talk at the Argonne Symposium on Resonance Production (unpublished).
Irving, A. C., 1975, Nucl. Phys. B **86**, 125.
Jacob, M., and G. C. Wick, 1959, Ann. Phys. (N.Y.) **7**, 404.
Jackson, J. D., 1965, in *High Energy Physics, Les Houches Lectures*, edited by C. DeWit and M. Jacob (Gordon and Breach, New York).
Jackson, J. D., 1970, Rev. Mod. Phys. **42**, 12.
Jackson, J. D., and C. Quigg, 1970, Nucl. Phys. B **22**, 301.
Kaidalov, A. B., and B. M. Karnakov, 1969, Phys. Lett. B **29**, 372, 376.
Kane, G. L., 1972a, Phys. Lett. B **40**, 363.
Kane, G. L., 1972b, "Phenomenology of Diffractive Reactions," Lectures at the XII Crakow School of Theoretical Physics, Zakopane, Acta Physica Polonica B **3**, 845.
Kane, G. L., 1973, "Phenomenology of High Energy Processes," Invited talk at the APS/DPF Berkeley Particles and Fields Meeting, AIP Conference Proceedings 14.
Kane, G. L., 1974, "The Importance of Absorption in Understanding Hadron Interactions," SLAC Summer Institute on Particle Physics, Vol. II.
Kane, G. L., and U. Sukhatme, 1974, Nucl. Phys. B **78**, 110.
Kelly, R. L., G. L. Kane, and F. S. Henyey, 1970, Phys. Rev. Lett. **24**, 1511.
LeDu, P., *et al.*, 1973, Phys. Lett. B **44**, 390.
Leader E., and R. C. Slansky, 1966, Phys. Rev. **148**, 1491.
Lee, J. G., *et al.*, 1973, Nucl. Phys. B **52**, 292.
Loos, J. S., and J. A. J. Matthews, 1972, Phys. Rev. D **6**, 2463.
MacGregor, M. H., *et al.*, 1960, Annu. Rev. Nucl. Sci. **10**, 291.
Martin, A., and P. Stevens, 1973, Phys. Rev. D **8**, 2086.
Martin, A., and P. Stevens, 1973, Lett. al Nuovo Cimento **7**, 821.
Michael, C., 1972, in *Proceedings of the Fourth International Conference on High Energy Collisions*, Oxford, 1972 (Rutherford Laboratory, Chilton, Didcot, Berks, UK), Vol. 1, p. 415.
Michael, C., 1973, Nucl. Phys. B **63**, 431.
Miettinen, H., 1976, Phys. Reports, to be published.
Miller, E. L., *et al.*, 1971, Phys. Rev. Lett. **26**, 984.
Ochs, W., and F. Wagner, 1973, Phys. Lett. B **44**, 271.
Owens, D. P., *et al.*, 1969, Phys. Rev. **181**, 1994.
Phillips, R. J. N., 1963, Nucl. Phys. **43**, 413.
Phillips, R. J. N., 1971, in *Proceedings of the Amsterdam International Conference on Elementary Particles*, Amsterdam, 1971 (North-Holland, Amsterdam), Vol. 1, p. 110.
Pumplin, J., and G. L. Kane, 1975, Phys. Rev. D **11**, 1183.
Ringland, G. A., R. G. Roberts, D. P. Roy, and J. Tran Thanh Van, 1972, Nucl. Phys. B **44**, 395.
Ringland, G. A., and D. P. Roy, 1972, Phys. Lett. B **39**, 531.
Ross, M., F. S. Henyey, and G. L. Kane, 1969, Nucl. Phys. B **23**, 269.
Sakurai, J. J., 1972, in McGill University of Summer School Proceedings, Toronto, 1972 (The Institute of Particle Physics, Montreal).
Schrempp, B., and F. Schrempp, 1975, CERN Preprint TH 2015.
Schwarz, J., 1974, Phys. Rep. **8**, No. 4.
Scotti, A., and D. Y. Wong, 1965, Phys. Rev. **138**, B145.
Sopkovich, N. J., 1962, Nuovo Cimento **26**, 186.
Stodolsky, L., 1970, SLAC preprint, (unpublished).
Ter-Martirosyan, K. A., and S. T. Sukhorokov, 1973, Nucl. Phys. B **54**, 522, and references therein.
Wolfenstein, L., 1956, Annu. Rev. Nucl. Sci. **6**, 43.
Worden, R., 1972, Nucl. Phys. B **37**, 253.
Worden, R., 1973a, Nucl. Phys. B **58**, 205.
Worden, R., 1973b, in *Proceedings of the Daresbury Pion Exchange Meeting*, Daresbury, 1973 (Science Research Council, Daresbury).
Worden, R., 1974, in *Proceedings of the XVII International Conference on High Energy Physics*, London, 1974 (Science Research Council, Chilton, Didcot, Oxon), p. I–152.